GOAL-ORIENTED ADAPTIVE MULTILEVEL STOCHASTIC GALERKIN FEM

ALEX BESPALOV, DIRK PRAETORIUS, AND MICHELE RUGGERI

Abstract. This paper is concerned with the numerical approximation of quantities of interest associated with solutions to parametric elliptic partial differential equations (PDEs). We consider a class of parametric elliptic PDEs where the underlying differential operator has affine dependence on a countably infinite number of uncertain parameters. We design a goal-oriented adaptive algorithm for approximating the functionals of solutions to this class of parametric PDEs. The algorithm applies to bounded linear goal functionals as well as to continuously Gâteaux differentiable nonlinear functionals. In the algorithm, the approximations of parametric solutions to the primal and dual problems are computed using the *multilevel* stochastic Galerkin finite element method (SGFEM) and the adaptive refinement process is guided by reliable spatial and parametric error indicators that identify the dominant sources of error. We prove that the proposed algorithm generates multilevel SGFEM approximations for which the error estimates in the goal functional converge to zero. Furthermore, in the case of bounded linear goal functionals, we show that, under an appropriate saturation assumption, our goal-oriented adaptive strategy yields optimal convergence rates with respect to the overall dimension of the underlying multilevel approximations spaces.

1. Introduction

Numerical approximation methods and efficient solution strategies for high-dimensional parametric partial differential equations (PDEs) have received a significant attention in the last two decades, particularly in the context of uncertainty quantification; see the review articles [SG11, GWZ14, CD15]. The focus of the work presented in this paper is on the design and analysis of adaptive algorithms that generate accurate approximations of (linear and nonlinear) quantities of interest (QoIs) derived from solutions to parametric elliptic PDEs. While the classical Monte Carlo sampling and its more efficient modern variants (such as Quasi-Monte Carlo and multilevel Monte Carlo) are effective in estimating the moments of solutions, the surrogate approximations that are *functions* of the stochastic parameters can be used to estimate a wide range of QoIs derived from solutions. Two variants of surrogate approximations, both based on spatial discretizations with the

Date: August 22, 2022.

2010 *Mathematics Subject Classification.* 35R60, 65C20, 65N30, 65N12, 65N15, 65N50.

Key words and phrases. goal-oriented adaptivity, nonlinear goal functionals, a posteriori error analysis, multilevel stochastic Galerkin method, finite element method, parametric PDEs.

Acknowledgments. The work of the first author was supported by the EPSRC under grant EP/P013791/1. The work of the second author was supported by the Austrian Science Fund (FWF) under grants F65 and P33216. All authors would like to thank the Erwin Schrödinger International Institute for Mathematics and Physics (ESI) at the University of Vienna for support and hospitality during the workshops on *Adaptivity, high dimensionality and randomness* (April 4–8, 2022) and *Approximation of high-dimensional parametric PDEs in forward UQ* (May 9–13, 2022), where part of the work on this paper was undertaken.

finite element method (FEM), have been extensively studied: *stochastic collocation FEMs* generate uncoupled discrete problems by sampling the PDE inputs at deterministically chosen points (typically, the nodes of a sparse grid) and build a multivariate interpolant from the sampled discrete solutions; in *stochastic Galerkin FEMs*, the approximations are defined via Galerkin projection and represented as finite (sparse) generalized polynomial chaos (gPC) expansions whose spatial coefficients are computed by solving a single fully coupled discrete system.

Numerical approximations of QoIs derived from solutions to parametric PDEs have been addressed in a number of works. The multilevel Monte Carlo (MLMC) algorithm for estimating bounded linear functionals and continuously Fréchet differentiable nonlinear functionals of the solution has been studied in [CST13] and [TSGU13] for a large class of elliptic PDEs with random coefficients. In particular, the convergence with optimal rates for MLMC approximations of nonlinear output functionals has been proved in [TSGU13] using the duality technique from [GS02]. In the same context of using the MLMC for estimating QoIs, an *adaptive algorithm* based on goal-oriented *a posteriori* error estimation has been developed in [EMN16]. The proposed algorithm performs a problem-dependent adaptive refinement of the MLMC mesh hierarchy aiming to control the error in the QoI and thus substantially reducing the complexity of MLMC computations.

Goal-oriented *a posteriori* error estimates for generic *surrogate approximations* of solutions to parametric PDEs have been proposed in [BPW15] and specifically for *stochastic collocation* approximations in [AO10]. In both these works, various goal-oriented adaptive refinement strategies guided by the error estimates are discussed and tested for model PDE problems with inputs that depend on a *finite* number of uncertain parameters. In the context of *stochastic Galerkin FEM* (SGFEM), the *a posteriori* error estimation of linear functionals of solutions was addressed in [MLM07, BPRR19b] and, for nonlinear problems, in [BDW11]. In particular, in our previous work [BPRR19b], we considered a class of parametric elliptic PDEs where the underlying differential operator had affine dependence on a *countably infinite* number of uncertain parameters. We used the duality technique (e.g., from [GS02]) to design a goal-oriented adaptive SGFEM algorithm for accurate approximation of moments of linear functionals of the solution to this class of PDE problems. In the algorithm, the solutions to the primal and dual problems were computed using the SGFEM in its simplest (so-called *single-level*) variant, where all spatial coefficients in the gPC expansion resided in the same finite element space. In each iteration, the dominant sources of error were identified using reliable spatial and parametric error indicators that guided the adaptive refinement process.

While, as evident from the above, there are many works addressing the design of goal-oriented adaptive algorithms, relatively little is known about their convergence and rate optimality properties, particularly for the algorithms based on surrogate approximations. With this paper we aim to bridge this gap in the theory. To that end, we employ the *multilevel* variant of SGFEM, where different spatial gPC-coefficients are allowed to reside in different finite element spaces; see [EGSZ14, CPB19, BPR21b]. Firstly, for bounded linear goal functionals, we design the multilevel version of the goal-oriented adaptive algorithm from [BPRR19b]; see Algorithm 6 below. Secondly, we prove the convergence result for the proposed algorithm and thus provide a theoretical guarantee that, given any positive error tolerance, the algorithm stops after a finite number of iterations (Theorem 8). Furthermore, under appropriate saturation assumptions, we prove that Algorithm 6 generates

multilevel SGFEM approximations such that the error estimates in the goal functional converge to zero with optimal rate (Theorem 19). Finally, we extend the goal-oriented *a posteriori* error analysis in [BPRR19b] as well as Algorithm 6 and the convergence result of Theorem 8 in the present paper to a class of continuously Gâteaux differentiable nonlinear goal functionals (see Proposition 25 and Theorem 26).

The paper is organized as follows. Section 2 introduces the parametric PDE problem that we consider in this work along with its weak formulation. In section 3, we follow [BPR21b, BPR21a] and recall the main ingredients of the multilevel SGFEM as well as the computable energy error estimates for multilevel SGFEM approximations. Section 4 addresses the goal-oriented error estimation for multilevel SGFEM approximations, the goal-oriented adaptive algorithm as well as the convergence and rate optimality analysis in the case of bounded linear goal functionals. In section 5, the goal-oriented error estimation strategy, the adaptive algorithm and the associated convergence analysis are extended to a class of nonlinear goal functionals. The results of numerical experiments that demonstrate the effectiveness of our goal-oriented error estimation strategy and illustrate the performance of the adaptive algorithm for linear and nonlinear goal functionals are reported in section 6.

2. Problem formulation

Let $D \subset \mathbb{R}^d$, $d \in \{2,3\}$, be a bounded Lipschitz domain with polytopal boundary ∂D, endowed with the standard Lebesgue measure. With $\Gamma := \prod_{m=1}^{\infty}[-1,1]$ denoting the infinitely-dimensional hypercube, we consider a probability space $(\Gamma, \mathcal{B}(\Gamma), \pi)$. Here, $\mathcal{B}(\Gamma)$ is the Borel σ-algebra on Γ and π is a probability measure, which we assume to be the product of symmetric Borel probability measures π_m on $[-1,1]$, i.e., $\pi(\mathbf{y}) = \prod_{m=1}^{\infty} \pi_m(y_m)$ for all $\mathbf{y} = (y_m)_{m\in\mathbb{N}} \in \Gamma$. We refer to D and Γ as the *physical domain* and the *parameter domain*, respectively.

We aim to approximate a functional value $\boldsymbol{g}(\boldsymbol{u}) \in \mathbb{R}$, where $\boldsymbol{u}\colon D \times \Gamma \to \mathbb{R}$ solves the stationary diffusion problem

$$\begin{aligned} -\nabla \cdot (\boldsymbol{a}(x,\mathbf{y})\nabla \boldsymbol{u}(x,\mathbf{y})) &= \boldsymbol{f}(x,\mathbf{y}) \qquad && x \in D,\, \mathbf{y} \in \Gamma, \\ \boldsymbol{u}(x,\mathbf{y}) &= 0 && x \in \partial D,\, \mathbf{y} \in \Gamma. \end{aligned} \tag{1}$$

In (1), the differential operators are taken with respect to the spatial variable $x \in D$. We assume that $\boldsymbol{f} \in L^2_\pi(\Gamma; H^{-1}(D))$ and that the diffusion coefficient $\boldsymbol{a}$ has affine dependence on the parameters, i.e., there holds

$$\boldsymbol{a}(x,\mathbf{y}) = a_0(x) + \sum_{m=1}^{\infty} y_m a_m(x) \quad \text{for all } x \in D \text{ and } \mathbf{y} = (y_m)_{m\in\mathbb{N}} \in \Gamma. \tag{2}$$

We suppose that the scalar functions $a_m \in L^\infty(D)$ in (2) satisfy the following inequalities (cf. [SG11, section 2.3]):

$$0 < a_0^{\min} \le a_0(x) \le a_0^{\max} < \infty \quad \text{for almost all } x \in D, \tag{3}$$

$$\tau := \frac{1}{a_0^{\min}} \left\| \sum_{m=1}^{\infty} |a_m| \right\|_{L^\infty(D)} < 1 \quad \text{and} \quad \sum_{m=1}^{\infty} \|a_m\|_{L^\infty(D)} < \infty. \tag{4}$$

Let $\mathbb{X} := H^1_0(D)$. We consider the Bochner space $\mathbb{V} := L^2_\pi(\Gamma;\mathbb{X})$ and define the following symmetric bilinear forms on $\mathbb{V}$:

$$B_0(\boldsymbol{u},\boldsymbol{v}) := \int_\Gamma \int_D a_0(x)\nabla\boldsymbol{u}(x,\mathbf{y})\cdot\nabla\boldsymbol{v}(x,\mathbf{y})\,\mathrm{d}x\,\mathrm{d}\pi(\mathbf{y}), \tag{5}$$

$$B(\boldsymbol{u},\boldsymbol{v}) := B_0(\boldsymbol{u},\boldsymbol{v}) + \sum_{m=1}^\infty \int_\Gamma \int_D y_m a_m(x)\nabla\boldsymbol{u}(x,\mathbf{y})\cdot\nabla\boldsymbol{v}(x,\mathbf{y})\,\mathrm{d}x\,\mathrm{d}\pi(\mathbf{y}). \tag{6}$$

Owing to (2)–(4), the bilinear forms $B(\cdot,\cdot)$ and $B_0(\cdot,\cdot)$ are continuous and elliptic on $\mathbb{V}$. Moreover, the norms they induce on $\mathbb{V}$, denoted by $|\!|\!| \cdot |\!|\!|$ and $|\!|\!| \cdot |\!|\!|_0$, respectively, are equivalent in the sense that

$$\lambda\,|\!|\!|\,\boldsymbol{v}\,|\!|\!|_0^2 \le |\!|\!|\,\boldsymbol{v}\,|\!|\!|^2 \le \Lambda\,|\!|\!|\,\boldsymbol{v}\,|\!|\!|_0^2 \quad \text{for all } \boldsymbol{v}\in\mathbb{V}, \tag{7}$$

where the constants $\lambda := 1-\tau$ and $\Lambda := 1+\tau$ satisfy $0<\lambda<1<\Lambda<2$.

The weak formulation of (1) reads as follows: Find $\boldsymbol{u}\in\mathbb{V}$ such that

$$B(\boldsymbol{u},\boldsymbol{v}) = F(\boldsymbol{v}) := \int_\Gamma\int_D \boldsymbol{f}(x,\mathbf{y})\boldsymbol{v}(x,\mathbf{y})\,\mathrm{d}x\,\mathrm{d}\pi(\mathbf{y}) \quad \text{for all } \boldsymbol{v}\in\mathbb{V}. \tag{8}$$

The existence of a unique solution $\boldsymbol{u}\in\mathbb{V}$ to (8) is guaranteed by the Riesz theorem. Throughout this work, we will refer to (8) as the *primal problem*.

Since we aim to approximate $\boldsymbol{g}(\boldsymbol{u}) \approx \boldsymbol{g}(\boldsymbol{u}_\bullet)$ by the functional value attained by an approximation $\boldsymbol{u}_\bullet \approx \boldsymbol{u}$, we assume that the goal functional $\boldsymbol{g}\colon \mathbb{V}\to\mathbb{R}$ is continuous. Further assumptions on $\boldsymbol{g}$ will be specified later.

3. Multilevel SGFEM discretization

In this section, we introduce the main ingredients of the multilevel SGFEM discretization employed in our goal-oriented adaptive algorithms. We follow the approach (and the notation) of [BPR21b, BPR21a].

3.1. Discretization in the physical domain and mesh refinement. Let $\mathcal{T}_\bullet$ be a *mesh*, i.e., a regular finite partition of $D\subset\mathbb{R}^d$ into compact nondegenerate simplices (i.e., triangles for $d=2$ and tetrahedra for $d=3$). Let $\mathcal{N}_\bullet$ denote the set of vertices of $\mathcal{T}_\bullet$. For mesh refinement, we employ newest vertex bisection (NVB) [Ste08]. We consider a (coarse) initial mesh $\mathcal{T}_0$ and denote by $\mathrm{refine}(\mathcal{T}_0)$ the set of all meshes obtained from $\mathcal{T}_0$ by performing finitely many steps of NVB refinement. Throughout this work, we assume that all meshes used for the discretization in the physical domain belong to $\mathrm{refine}(\mathcal{T}_0)$.

For each mesh $\mathcal{T}_\bullet\in\mathrm{refine}(\mathcal{T}_0)$, we denote by $\widehat{\mathcal{T}}_\bullet$ its uniform refinement. For $d=2$, $\widehat{\mathcal{T}}_\bullet$ is the mesh obtained by decomposing each element of $\mathcal{T}_\bullet$ into four triangles using three successive bisections. For $d=3$, we refer to [EGP20, Figure 3] and the associated discussion therein. Let $\widehat{\mathcal{N}}_\bullet$ be the set of vertices of $\widehat{\mathcal{T}}_\bullet$. We denote by $\mathcal{N}_\bullet^+ := (\widehat{\mathcal{N}}_\bullet\setminus\mathcal{N}_\bullet)\setminus\partial D$ the set of new interior vertices created by uniform refinement of $\mathcal{T}_\bullet$. For a set of marked vertices $\mathcal{M}_\bullet\subseteq\mathcal{N}_\bullet^+$, let $\mathcal{T}_\circ := \mathrm{refine}(\mathcal{T}_\bullet,\mathcal{M}_\bullet)$ be the coarsest mesh such that $\mathcal{M}_\bullet\subseteq\mathcal{N}_\circ$, i.e., all marked vertices of $\mathcal{T}_\bullet$ are vertices of $\mathcal{T}_\circ$. Since NVB is a binary refinement rule, it follows that $\mathcal{N}_\circ\subseteq\widehat{\mathcal{N}}_\bullet$ and $(\mathcal{N}_\circ\setminus\mathcal{N}_\bullet)\setminus\partial D = \mathcal{N}_\bullet^+\cap\mathcal{N}_\circ$. In particular, the choices $\mathcal{M}_\bullet=\emptyset$ and $\mathcal{M}_\bullet=\mathcal{N}_\bullet^+$ lead to the meshes $\mathcal{T}_\bullet = \mathrm{refine}(\mathcal{T}_\bullet,\emptyset)$ and $\widehat{\mathcal{T}}_\bullet = \mathrm{refine}(\mathcal{T}_\bullet,\mathcal{N}_\bullet^+)$, respectively.

With each mesh $\mathcal{T}_\bullet\in\mathrm{refine}(\mathcal{T}_0)$, we associate the finite element space

$$\mathbb{X}_\bullet := \mathcal{S}^1_0(\mathcal{T}_\bullet) := \{v_\bullet\in\mathbb{X} : v_\bullet|_T \text{ is affine for all } T\in\mathcal{T}_\bullet\}\subset\mathbb{X}=H^1_0(D),$$

consisting of globally continuous and $\mathcal{T}_\bullet$-piecewise affine functions. We denote by $\{\varphi_{\bullet,\xi} : \xi \in \mathcal{N}_\bullet \setminus \partial D\}$ the basis of $\mathbb{X}_\bullet$ comprising the so-called hat functions, i.e., for all $\xi \in \mathcal{N}_\bullet$, $\varphi_{\bullet,\xi} \in \mathbb{X}_\bullet$ satisfies the Kronecker property $\varphi_{\bullet,\xi}(\xi') = \delta_{\xi\xi'}$ for all $\xi' \in \mathcal{N}_\bullet$. Consistent with this notation, $\widehat{\mathbb{X}}_\bullet := \mathcal{S}^1_0(\widehat{\mathcal{T}}_\bullet)$ denotes the finite element space associated with the uniform refinement $\widehat{\mathcal{T}}_\bullet$ of $\mathcal{T}_\bullet$, and $\{\widehat{\varphi}_{\bullet,\xi} : \xi \in \widehat{\mathcal{N}}_\bullet \setminus \partial D\}$ is the corresponding set of hat functions (the basis of $\widehat{\mathbb{X}}_\bullet$). There holds the ($H^1$-stable) two-level decomposition $\widehat{\mathbb{X}}_\bullet = \mathbb{X}_\bullet \oplus \operatorname{span}\{\widehat{\varphi}_{\bullet,\xi} : \xi \in \mathcal{N}_\bullet^+\}$.

3.2. Discretization in the parameter domain and parametric enrichment. For all $m \in \mathbb{N}$, let $(P_n^m)_{n\in\mathbb{N}_0}$ be the sequence of univariate polynomials which are orthogonal to each other with respect to π_m such that P_n^m is a polynomial of degree $n \in \mathbb{N}_0$ with $\|P_n^m\|_{L^2_{\pi_m}(-1,1)} = 1$ and $P_0^m \equiv 1$. It is well-known that $\{P_n^m : n \in \mathbb{N}_0\}$ constitutes an orthonormal basis of $L^2_{\pi_m}(-1,1)$.

Let $\mathbb{N}_0^{\mathbb{N}} := \{\nu = (\nu_m)_{m\in\mathbb{N}} : \nu_m \in \mathbb{N}_0 \text{ for all } m \in \mathbb{N}\}$. We define the support of $\nu = (\nu_m)_{m\in\mathbb{N}} \in \mathbb{N}_0^{\mathbb{N}}$ as $\operatorname{supp}(\nu) := \{m \in \mathbb{N} : \nu_m \neq 0\}$. We denote by $\mathfrak{I} := \{\nu \in \mathbb{N}_0^{\mathbb{N}} : \#\operatorname{supp}(\nu) < \infty\}$ the set of all finitely supported elements of $\mathbb{N}_0^{\mathbb{N}}$. Note that $\mathfrak{I}$ is countable. With each $\nu \in \mathfrak{I}$, we associate the multivariate polynomial P_ν given by

$$P_\nu(\mathbf{y}) := \prod_{m\in\mathbb{N}} P^m_{\nu_m}(y_m) = \prod_{m\in\operatorname{supp}(\nu)} P^m_{\nu_m}(y_m) \quad \text{for all } \nu \in \mathfrak{I} \text{ and all } \mathbf{y} \in \Gamma.$$

It is well-known that the set $\{P_\nu : \nu \in \mathfrak{I}\}$ is an orthonormal basis of $L^2_\pi(\Gamma)$; see, e.g., [SG11, Theorem 2.12].

Our discretization in the parameter domain will be based on an *index set* $\mathfrak{P}_\bullet$, i.e., a finite subset of $\mathfrak{I}$. We denote by $\operatorname{supp}(\mathfrak{P}_\bullet) := \bigcup_{\nu\in\mathfrak{P}_\bullet} \operatorname{supp}(\nu)$ the set of active parameters in $\mathfrak{P}_\bullet$. We denote by $\mathbf{0} = (0, 0, \dots)$ the zero index and consider the initial index set $\mathfrak{P}_0 := \{\mathbf{0}\}$. Throughout this work, we assume that all index sets employed for the discretization in the parameter domain contain the zero index, i.e., there holds $\mathfrak{P}_0 \subseteq \mathfrak{P}_\bullet$ for each index set $\mathfrak{P}_\bullet$. Following [BS16], we introduce the *detail index set*

$$\mathfrak{Q}_\bullet := \{\mu \in \mathfrak{I} \setminus \mathfrak{P}_\bullet : \mu = \nu \pm \varepsilon_m \text{ for all } \nu \in \mathfrak{P}_\bullet \text{ and all } m = 1, \dots, M_{\mathfrak{P}_\bullet} + 1\}. \tag{9}$$

Here, $M_{\mathfrak{P}_\bullet} := \#\operatorname{supp}(\mathfrak{P}_\bullet) \in \mathbb{N}_0$ is the number of active parameters in $\mathfrak{P}_\bullet$, while, for any $m \in \mathbb{N}$, $\varepsilon_m \in \mathfrak{I}$ denotes the m-th unit sequence, i.e., $(\varepsilon_m)_i = \delta_{mi}$ for all $i \in \mathbb{N}$. A parametric enrichment of $\mathfrak{P}_\bullet$ is obtained by adding to it some marked indices $\mathfrak{M}_\bullet \subseteq \mathfrak{Q}_\bullet$, i.e., $\mathfrak{P}_\circ := \mathfrak{P}_\bullet \cup \mathfrak{M}_\bullet$. Clearly, $\mathfrak{P}_\bullet \subseteq \mathfrak{P}_\circ \subseteq \mathfrak{P}_\bullet \cup \mathfrak{Q}_\bullet$, where at least one of the inclusions is strict.

3.3. Multilevel approximation and multilevel refinement. We start by observing that the Bochner space $\mathbb{V} = L^2_\pi(\Gamma; \mathbb{X})$ is isometrically isomorphic to $\mathbb{X} \otimes L^2_\pi(\Gamma)$ and that each function $\boldsymbol{v} \in \mathbb{V}$ can be represented in the form

$$\boldsymbol{v}(x, \mathbf{y}) = \sum_{\nu\in\mathfrak{I}} v_\nu(x) P_\nu(\mathbf{y}) \quad \text{with unique coefficients } v_\nu \in \mathbb{X}. \tag{10}$$

A finite-dimensional subspace of $\mathbb{V}$ can be obtained by considering functions with a similar representation, where the infinite sum in (10) is truncated to a finite index set and the coefficients $v_\nu \in \mathbb{X}$ are approximated in suitable finite element spaces. To this end, let $\mathbb{P}_\bullet = [\mathfrak{P}_\bullet, (\mathcal{T}_{\bullet\nu})_{\nu\in\mathfrak{I}}]$ be a *multilevel structure* [BPR21a], consisting of a finite index set

$\mathfrak{P}_\bullet \subset \mathfrak{I}$ and a family of meshes $(\mathcal{T}_{\bullet\nu})_{\nu\in\mathfrak{I}}$, where $\mathcal{T}_{\bullet\nu} \in \mathrm{refine}(\mathcal{T}_0)$ for all $\nu \in \mathfrak{P}_\bullet$, while $\mathcal{T}_{\bullet\nu} = \mathcal{T}_0$ for all $\nu \in \mathfrak{I}\backslash\mathfrak{P}_\bullet$.

For two multilevel structures $\mathbb{P}_\bullet = [\mathfrak{P}_\bullet, (\mathcal{T}_{\bullet\nu})_{\nu\in\mathfrak{I}}]$ and $\mathbb{P}_\circ = [\mathfrak{P}_\circ, (\mathcal{T}_{\circ\nu})_{\nu\in\mathfrak{I}}]$, we say that $\mathbb{P}_\circ$ is obtained from $\mathbb{P}_\bullet$ using one step of *multilevel refinement*, and we write $\mathbb{P}_\circ = \texttt{REFINE}(\mathbb{P}_\bullet, \mathbb{M}_\bullet)$, if the following conditions are satisfied:

- $\mathbb{M}_\bullet = [\mathfrak{M}_\bullet, (\mathcal{M}_{\bullet\nu})_{\nu\in\mathfrak{P}_\bullet}]$ with $\mathfrak{M}_\bullet \subseteq \mathfrak{Q}_\bullet$ and $\mathcal{M}_{\bullet\nu} \subseteq \mathcal{N}^+_{\bullet\nu}$ for all $\nu \in \mathfrak{P}_\bullet$;
- $\mathfrak{P}_\circ = \mathfrak{P}_\bullet \cup \mathfrak{M}_\bullet$;
- for all $\nu \in \mathfrak{P}_\bullet$, there holds $\mathcal{T}_{\circ\nu} = \mathrm{refine}(\mathcal{T}_{\bullet\nu}, \mathcal{M}_{\bullet\nu})$;
- for all $\nu \in \mathfrak{I}\backslash\mathfrak{P}_\bullet$, there holds $\mathcal{T}_{\circ\nu} = \mathcal{T}_{\bullet\nu} = \mathcal{T}_0$.

Mimicking the notation in subsections 3.1–3.2, we consider the initial multilevel structure $\mathbb{P}_0 := [\mathfrak{P}_0, (\mathcal{T}_{0\nu})_{\nu\in\mathfrak{I}}]$ consisting of the initial index set $\mathfrak{P}_0$ and such that $\mathcal{T}_{0\nu} = \mathcal{T}_0$ for all $\nu \in \mathfrak{I}$. We denote by $\texttt{REFINE}(\mathbb{P}_0)$ the set of all multilevel structures obtained from $\mathbb{P}_0$ by performing finitely many steps of multilevel refinement. Throughout this work, we assume that all multilevel structures employed to construct a finite-dimensional subspace of $\mathbb{V}$ belong to $\texttt{REFINE}(\mathbb{P}_0)$.

Given a multilevel structure $\mathbb{P}_\bullet = [\mathfrak{P}_\bullet, (\mathcal{T}_{\bullet\nu})_{\nu\in\mathfrak{I}}]$, let $\mathbb{X}_{\bullet\nu} = \mathcal{S}^1_0(\mathcal{T}_{\bullet\nu})$ for all $\nu \in \mathfrak{P}_\bullet$. We consider the multilevel approximation space

$$\mathbb{V}_\bullet := \bigoplus_{\nu\in\mathfrak{P}_\bullet} \mathbb{V}_{\bullet\nu} \subset \mathbb{V} \quad \text{with} \quad \mathbb{V}_{\bullet\nu} := \mathbb{X}_{\bullet\nu} \otimes \mathrm{span}\{P_\nu\} = \mathrm{span}\big\{\varphi_{\bullet\nu,\xi} P_\nu \,:\, \xi \in \mathcal{N}_{\bullet\nu} \setminus \partial D\big\}. \tag{11}$$

Note that $\dim \mathbb{V}_\bullet = \sum_{\nu\in\mathfrak{P}_\bullet} \dim \mathbb{X}_{\bullet\nu}$, i.e., $\mathbb{V}_\bullet$ is a finite-dimensional subspace of $\mathbb{V}$, and that each function $\boldsymbol{v}_\bullet \in \mathbb{V}_\bullet$ can be represented in the form (cf. (10))

$$\boldsymbol{v}_\bullet(x,\mathbf{y}) = \sum_{\nu\in\mathfrak{P}_\bullet} v_{\bullet\nu}(x) P_\nu(\mathbf{y}) \quad \text{with unique coefficients } v_{\bullet\nu} \in \mathbb{X}_{\bullet\nu}.$$

Moreover, by construction, multilevel refinement implies nestedness of the associated multilevel spaces, i.e., if $\mathbb{P}_\circ \in \texttt{REFINE}(\mathbb{P}_\bullet)$ then $\mathbb{V}_\bullet \subseteq \mathbb{V}_\circ$.

For the multilevel approximation space $\mathbb{V}_\bullet$ associated with any given multilevel structure $\mathbb{P}_\bullet = [\mathfrak{P}_\bullet, (\mathcal{T}_{\bullet\nu})_{\nu\in\mathfrak{I}}]$, we consider the enriched subspace $\widehat{\mathbb{V}}_\bullet \subset \mathbb{V}$ defined as

$$\widehat{\mathbb{V}}_\bullet := \left(\bigoplus_{\nu\in\mathfrak{P}_\bullet} \big[\widehat{\mathbb{X}}_{\bullet\nu} \otimes \mathrm{span}\{P_\nu\}\big]\right) \oplus \left(\bigoplus_{\nu\in\mathfrak{Q}_\bullet} \big[\mathbb{X}_0 \otimes \mathrm{span}\{P_\nu\}\big]\right). \tag{12}$$

Note that $\mathbb{V}_\bullet \subseteq \mathbb{V}_\circ \subseteq \widehat{\mathbb{V}}_\bullet$ for any $\mathbb{P}_\circ = \texttt{REFINE}(\mathbb{P}_\bullet, \mathbb{M}_\bullet)$. Moreover, $\widehat{\mathbb{V}}_\bullet$ corresponds to the multilevel structure $\widehat{\mathbb{P}}_\bullet = \texttt{REFINE}(\mathbb{P}_\bullet, \mathbb{M}_\bullet)$ with $\mathbb{M}_\bullet = [\mathfrak{Q}_\bullet, (\mathcal{N}^+_{\bullet\nu})_{\nu\in\mathfrak{P}_\bullet}]$.

3.4. Multilevel SGFEM approximation. Given an arbitrary $\boldsymbol{w} \in \mathbb{V}$, let $\boldsymbol{w}_\bullet \in \mathbb{V}_\bullet$ and $\widehat{\boldsymbol{w}}_\bullet \in \widehat{\mathbb{V}}_\bullet$ denote the Galerkin projections of $\boldsymbol{w}$ onto $\mathbb{V}_\bullet$ and $\widehat{\mathbb{V}}_\bullet$, respectively, i.e.,

$$B(\boldsymbol{w}_\bullet, \boldsymbol{v}_\bullet) = B(\boldsymbol{w}, \boldsymbol{v}_\bullet) \quad \text{for all } \boldsymbol{v}_\bullet \in \mathbb{V}_\bullet, \tag{13a}$$

$$B(\widehat{\boldsymbol{w}}_\bullet, \widehat{\boldsymbol{v}}_\bullet) = B(\boldsymbol{w}, \widehat{\boldsymbol{v}}_\bullet) \quad \text{for all } \widehat{\boldsymbol{v}}_\bullet \in \widehat{\mathbb{V}}_\bullet. \tag{13b}$$

Existence and uniqueness of both $\boldsymbol{w}_\bullet \in \mathbb{V}_\bullet$ and $\widehat{\boldsymbol{w}}_\bullet \in \widehat{\mathbb{V}}_\bullet$ follow from the Riesz theorem. Moreover, there holds the so-called Galerkin orthogonality

$$B(\boldsymbol{w} - \boldsymbol{w}_\bullet, \boldsymbol{v}_\bullet) = 0 \quad \text{for all } \boldsymbol{v}_\bullet \in \mathbb{V}_\bullet \tag{14}$$

as well as the best approximation property

$$\| \boldsymbol{w} - \boldsymbol{w}_\bullet \| = \min_{\boldsymbol{v}_\bullet \in \mathbb{V}_\bullet} \| \boldsymbol{w} - \boldsymbol{v}_\bullet \| \tag{15}$$

(the same properties clearly hold also for $\widehat{\boldsymbol{w}}_\bullet$ with $\mathbb{V}_\bullet$ replaced by $\widehat{\mathbb{V}}_\bullet$). Furthermore, since $\mathbb{V}_\bullet \subset \widehat{\mathbb{V}}_\bullet$, there holds

$$\| \boldsymbol{w} - \boldsymbol{w}_\bullet \|^2 = \| \boldsymbol{w} - \widehat{\boldsymbol{w}}_\bullet \|^2 + \| \boldsymbol{w}_\bullet - \widehat{\boldsymbol{w}}_\bullet \|^2. \tag{16}$$

In particular,

$$\| \boldsymbol{w} - \widehat{\boldsymbol{w}}_\bullet \| \le \| \boldsymbol{w} - \boldsymbol{w}_\bullet \| \quad \text{and} \quad \| \boldsymbol{w}_\bullet - \widehat{\boldsymbol{w}}_\bullet \| \le \| \boldsymbol{w} - \boldsymbol{w}_\bullet \|. \tag{17}$$

We define the multilevel SGFEM approximation $\boldsymbol{u}_\bullet \in \mathbb{V}_\bullet$ of the solution $\boldsymbol{u} \in \mathbb{V}$ to the primal problem (8) as the Galerkin projection of $\boldsymbol{u}$ onto the multilevel approximation space $\mathbb{V}_\bullet$. Equivalently, $\boldsymbol{u}_\bullet \in \mathbb{V}_\bullet$ can be characterized as the unique solution of the following discrete variational problem: Find $\boldsymbol{u}_\bullet \in \mathbb{V}_\bullet$ such that

$$B(\boldsymbol{u}_\bullet, \boldsymbol{v}_\bullet) = F(\boldsymbol{v}_\bullet) \quad \text{for all } \boldsymbol{v}_\bullet \in \mathbb{V}_\bullet. \tag{18}$$

3.5. Saturation assumption and *a posteriori* error estimation. To obtain computable estimates of the error $\| \boldsymbol{w} - \boldsymbol{w}_\bullet \|$ of the Galerkin projection, we follow the approach proposed in [BPR21b], which is based on the separate estimation of the error components associated with discretizations in physical and parameter domains.

Here and in the sequel, for the sake of brevity, we denote the inner product on $\mathbb{X} = H^1_0(D)$ by $\langle w \,,\, v \rangle_D := \int_D a_0 \nabla w \cdot \nabla v \,\mathrm{d}x$ and the induced energy norm by $\| \cdot \|_D := \| a_0^{1/2} \nabla(\cdot) \|_{L^2(D)}$.

The parametric components of the error in the Galerkin approximation $\boldsymbol{w}_\bullet$ are estimated using the hierarchical error indicators

$$\tau_\bullet(\boldsymbol{w}|\nu) := \| e_{\boldsymbol{w}|\bullet\nu} \|_D \quad \text{for all } \nu \in \mathfrak{Q}_\bullet, \tag{19a}$$

where $e_{\boldsymbol{w}|\bullet\nu} \in \mathbb{X}_0$ is the unique solution of

$$\langle e_{\boldsymbol{w}|\bullet\nu} \,,\, v_0 \rangle_D = B(\boldsymbol{w} - \boldsymbol{w}_\bullet, v_0 P_\nu) \quad \text{for all } v_0 \in \mathbb{X}_0. \tag{19b}$$

The errors attributable to spatial discretizations are estimated using the *two-level* error indicators

$$\tau_\bullet(\boldsymbol{w}|\nu,\xi) := \frac{|B(\boldsymbol{w} - \boldsymbol{w}_\bullet, \widehat{\varphi}_{\bullet\nu,\xi} P_\nu)|}{\| \widehat{\varphi}_{\bullet\nu,\xi} \|_D} \quad \text{for all } \nu \in \mathfrak{P}_\bullet \text{ and all } \xi \in \mathcal{N}^+_{\bullet\nu}. \tag{20}$$

Overall, we thus consider the *a posteriori* error estimate

$$\tau_\bullet(\boldsymbol{w}) := \left(\sum_{\nu \in \mathfrak{P}_\bullet} \sum_{\xi \in \mathcal{N}^+_{\bullet\nu}} \tau_\bullet(\boldsymbol{w}|\nu,\xi)^2 + \sum_{\nu \in \mathfrak{Q}_\bullet} \tau_\bullet(\boldsymbol{w}|\nu)^2 \right)^{1/2}. \tag{21}$$

Remark 1. *Note that, for a general unknown $\boldsymbol{w} \in \mathbb{V}$, the error estimate $\tau_\bullet(\boldsymbol{w})$ is not computable. However, we shall employ the estimate $\tau_\bullet(\boldsymbol{w})$ only for $\boldsymbol{w} \in \{\boldsymbol{u}, \boldsymbol{z}\}$, where $\boldsymbol{u} \in \mathbb{V}$ denotes the solution to the primal problem* (8)*, while $\boldsymbol{z} \in \mathbb{V}$ denotes the solution to a so-called dual problem (see, e.g.,* (26) *below for the case of a linear goal functional). For these choices, the evaluation of $B(\boldsymbol{w}, \cdot)$ in* (19)–(20) *is known, so that $\tau_\bullet(\boldsymbol{w})$ becomes fully computable using, e.g., $B(\boldsymbol{u} - \boldsymbol{u}_\bullet, \boldsymbol{v}) = F(\boldsymbol{v}) - B(\boldsymbol{u}_\bullet, \boldsymbol{v})$ for the primal solution $\boldsymbol{w} = \boldsymbol{u}$ and $\boldsymbol{v} \in \{v_0 P_\nu, \widehat{\varphi}_{\bullet\nu,\xi} P_\nu\}$.*

It follows from the first inequality in (17) that the error of the Galerkin projection associated with the enriched multilevel space $\widehat{\mathbb{V}}_\bullet$ is not larger than the one for the space $\mathbb{V}_\bullet$. We say that the *saturation assumption* is satisfied, if considering the enriched multilevel space leads to a uniform strict reduction of the best approximation error, i.e., if there exists a constant $0 < q_{\mathrm{sat}} < 1$ such that

$$|\!|\!| \boldsymbol{w} - \widehat{\boldsymbol{w}}_\bullet |\!|\!| \leq q_{\mathrm{sat}} \, |\!|\!| \boldsymbol{w} - \boldsymbol{w}_\bullet |\!|\!|. \tag{22}$$

We now recall the following main result from [BPR21b], which shows the equivalence of the error estimate $\tau_\bullet(\boldsymbol{w})$ in (21) to the *error reduction* $|\!|\!| \boldsymbol{w}_\bullet - \widehat{\boldsymbol{w}}_\bullet |\!|\!|$ obtained by passing from $\mathbb{V}_\bullet$ to $\widehat{\mathbb{V}}_\bullet$ (cf. (16)). This implies that the proposed error estimator is *efficient*, i.e., up to a multiplicative constant, it provides a lower bound for the energy norm of the error, while its *reliability* (i.e., the upper bound for the error) is equivalent to the saturation assumption (22).

Theorem 2 ([BPR21b, Theorem 2])**.** *Let $d \in \{2, 3\}$ and $\boldsymbol{w} \in \mathbb{V}$. For the multilevel structures $\mathbb{P}_\bullet, \widehat{\mathbb{P}}_\bullet \in \mathbb{REFINE}(\mathbb{P}_0)$, consider the multilevel approximation spaces $\mathbb{V}_\bullet \subseteq \widehat{\mathbb{V}}_\bullet$ with the associated Galerkin solutions $\boldsymbol{w}_\bullet \in \mathbb{V}_\bullet$ (solving* (13a)*) and $\widehat{\boldsymbol{w}}_\bullet \in \widehat{\mathbb{V}}_\bullet$ (solving* (13b)*). Then, there holds*

$$C_{\mathrm{est}}^{-1} \, |\!|\!| \widehat{\boldsymbol{w}}_\bullet - \boldsymbol{w}_\bullet |\!|\!| \leq \tau_\bullet(\boldsymbol{w}) \leq C_{\mathrm{est}} \, |\!|\!| \widehat{\boldsymbol{w}}_\bullet - \boldsymbol{w}_\bullet |\!|\!|. \tag{23}$$

Furthermore, under the saturation assumption (22)*, the estimates* (23) *are equivalent to*

$$\frac{(1 - q_{\mathrm{sat}}^2)^{1/2}}{C_{\mathrm{est}}} \, |\!|\!| \boldsymbol{w} - \boldsymbol{w}_\bullet |\!|\!| \leq \tau_\bullet(\boldsymbol{w}) \leq C_{\mathrm{est}} \, |\!|\!| \boldsymbol{w} - \boldsymbol{w}_\bullet |\!|\!|, \tag{24}$$

The constant $C_{\mathrm{est}} \geq 1$ in (23)–(24) *depends only on $\mathcal{T}_0$, the mean field a_0, and the constants $\lambda, \Lambda > 0$ in* (7)*.* □

In 2D, it is possible to prove a more general result than that in (23); see [BPR21b, Remark 6].

Theorem 3. *Let $d = 2$ and $\boldsymbol{w} \in \mathbb{V}$. Let $\mathbb{P}_\bullet \in \mathbb{REFINE}(\mathbb{P}_0)$ and $\mathbb{P}_\circ \in \mathbb{REFINE}(\mathbb{P}_\bullet, \mathbb{M}_\bullet)$, where $\mathbb{M}_\bullet = [\mathfrak{M}_\bullet, (\mathcal{M}_{\bullet\nu})_{\nu \in \mathfrak{P}_\bullet}]$ satisfies $\mathfrak{M}_\bullet \subseteq \mathfrak{Q}_\bullet$ and $\mathcal{M}_{\bullet\nu} \subseteq \mathcal{N}_\nu^+$ for all $\nu \in \mathfrak{P}_\bullet$. Let $\mathbb{V}_\bullet \subseteq \mathbb{V}_\circ$ be the corresponding multilevel approximation spaces with the associated Galerkin solutions $\boldsymbol{w}_\bullet \in \mathbb{V}_\bullet$ (solving* (13a)*) and $\boldsymbol{w}_\circ \in \mathbb{V}_\circ$ (solving* (13a) *with $\mathbb{V}_\bullet$ replaced by $\mathbb{V}_\circ$). Then, there holds*

$$C_{\mathrm{est}}^{-1} \, |\!|\!| \boldsymbol{w}_\circ - \boldsymbol{w}_\bullet |\!|\!| \leq \left(\sum_{\nu \in \mathfrak{P}_\bullet} \sum_{\xi \in \mathcal{N}_\nu^+ \cap \mathcal{N}_{\circ\nu}} \tau_\bullet(\boldsymbol{w}|\nu, \xi)^2 + \sum_{\nu \in \mathfrak{Q}_\bullet \cap \mathfrak{P}_\circ} \tau_\bullet(\boldsymbol{w}|\nu)^2 \right)^{1/2} \leq C_{\mathrm{est}} \, |\!|\!| \boldsymbol{w}_\circ - \boldsymbol{w}_\bullet |\!|\!|. \tag{25}$$

The latter implies (23)*. The constant $C_{\mathrm{est}} \geq 1$ in* (25) *is the same as in Theorem 2.* □

The validity of estimate (25) hinges on 2D newest vertex bisection, which guarantees that the hat functions satisfy $\widehat{\varphi}_{\bullet\nu,\xi} = \varphi_{\circ\nu,\xi} \in \mathbb{X}_{\circ\nu}$ for all $\nu \in \mathfrak{P}_\bullet$ if $\mathcal{T}_{\circ\nu} = \mathrm{refine}(\mathcal{T}_{\bullet\nu}, \mathcal{M}_{\bullet\nu})$ and $\xi \in \mathcal{N}_\nu^+ \cap \mathcal{N}_{\circ\nu}$.

Remark 4. *If required for all discrete spaces $\mathbb{V}_\bullet \subset \mathbb{V}$, the saturation assumption* (22) *is a strong restriction, which may not hold in general (see* [BEK96] *for a counterexample in the deterministic setting). In the upcoming analysis, it will be required for the solution $\boldsymbol{u} \in \mathbb{V}$ to the primal problem* (8)*, for the solution to a so-called dual problem (see, e.g.,*

(26) *below in the case of a linear goal functional), and only for the sequence of nested discrete subspaces* $(\mathbb{V}_\ell)_{\ell\in\mathbb{N}_0}$ *generated by Algorithm 6 below.*

4. Goal-oriented adaptive SGFEM with linear goal functional

In this section, we assume that the goal functional $\boldsymbol{g} : \mathbb{V} \to \mathbb{R}$ is linear and bounded, i.e., $\boldsymbol{g} \in \mathbb{V}^*$. Considering this special case allows us to focus on the core arguments of the numerical analysis. An extension of our analysis to a more general class of (possibly nonlinear) goal functionals is discussed in section 5.

4.1. Dual problem and goal-oriented error estimate. Let $\boldsymbol{z} \in \mathbb{V}$ denote the solution to the so-called *dual problem*

$$B(\boldsymbol{v}, \boldsymbol{z}) = \langle \boldsymbol{g}\,,\, \boldsymbol{v}\rangle_{D\times\Gamma} \quad \text{for all } \boldsymbol{v} \in \mathbb{V}. \tag{26}$$

We approximate $\boldsymbol{z} \in \mathbb{V}$ by its Galerkin projection $\boldsymbol{z}_\bullet \in \mathbb{V}_\bullet$ satisfying

$$B(\boldsymbol{v}_\bullet, \boldsymbol{z}_\bullet) = \langle \boldsymbol{g}\,,\, \boldsymbol{v}_\bullet\rangle_{D\times\Gamma} \quad \text{for all } \boldsymbol{v}_\bullet \in \mathbb{V}_\bullet. \tag{27}$$

In (26)–(27), $\langle\cdot\,,\,\cdot\rangle_{D\times\Gamma}$ denotes the duality pairing between $\mathbb{V}$ and its dual $\mathbb{V}^*$. Existence and uniqueness of both $\boldsymbol{z} \in \mathbb{V}$ and $\boldsymbol{z}_\bullet \in \mathbb{V}_\bullet$ follow from the Riesz theorem. With the Cauchy–Schwarz inequality, we see that

$$|\boldsymbol{g}(\boldsymbol{u}) - \boldsymbol{g}(\boldsymbol{u}_\bullet)| \overset{(26)}{=} |B(\boldsymbol{u} - \boldsymbol{u}_\bullet, \boldsymbol{z})| \overset{(14)}{=} |B(\boldsymbol{u} - \boldsymbol{u}_\bullet, \boldsymbol{z} - \boldsymbol{z}_\bullet)| \le |\!|\!| \boldsymbol{u} - \boldsymbol{u}_\bullet |\!|\!|\, |\!|\!| \boldsymbol{z} - \boldsymbol{z}_\bullet |\!|\!|. \tag{28}$$

To estimate the energy errors on the right-hand side of (28), we consider the error estimation strategy introduced in subsection 3.5. In the remainder of this section, unless otherwise specified, we use the abbreviated notation

$$\mu_\bullet := \tau_\bullet(\boldsymbol{u}) \quad \text{and} \quad \zeta_\bullet := \tau_\bullet(\boldsymbol{z}). \tag{29}$$

The same notation will be used for local contributions to the error estimates as follows:

$$\mu_\bullet(\nu) := \tau_\bullet(\boldsymbol{u}|\nu),\ \mu_\bullet(\nu,\xi) := \tau_\bullet(\boldsymbol{u}|\nu,\xi) \text{ and } \zeta_\bullet(\nu) := \tau_\bullet(\boldsymbol{z}|\nu),\ \zeta_\bullet(\nu,\xi) := \tau_\bullet(\boldsymbol{z}|\nu,\xi). \tag{30}$$

Proposition 5. *Let* $d \in \{2, 3\}$. *Suppose the saturation assumption* (22) *for both the primal solution* $\boldsymbol{w} = \boldsymbol{u}$ *to* (8) *and the dual solution* $\boldsymbol{w} = \boldsymbol{z}$ *to* (26). *Then, there holds the a posteriori goal-oriented error estimate*

$$|\boldsymbol{g}(\boldsymbol{u}) - \boldsymbol{g}(\boldsymbol{u}_\bullet)| \le C_{\mathrm{rel}}\, \mu_\bullet \zeta_\bullet \quad \textit{with} \quad C_{\mathrm{rel}} = C_{\mathrm{est}}^2/(1 - q_{\mathrm{sat}}^2), \tag{31}$$

where $C_{\mathrm{est}} \ge 1$ *is the constant from Theorem 2 and* $0 < q_{\mathrm{sat}} < 1$ *from* (22).

Proof. Theorem 2 implies that

$$|\!|\!| \boldsymbol{u} - \boldsymbol{u}_\bullet |\!|\!| \le \frac{C_{\mathrm{est}}}{(1 - q_{\mathrm{sat}}^2)^{1/2}} \mu_\bullet \quad \text{as well as} \quad |\!|\!| \boldsymbol{z} - \boldsymbol{z}_\bullet |\!|\!| \le \frac{C_{\mathrm{est}}}{(1 - q_{\mathrm{sat}}^2)^{1/2}} \zeta_\bullet.$$

Combining this with (28), we conclude the proof. □

4.2. Adaptive algorithm. The main results of this section concern the following algorithm, which extends the adaptive algorithm from [BPR21b] (see Algorithm 7.C therein) to the present goal-oriented adaptive SGFEM setting. In both these algorithms, the enhancement of the approximation space $\mathbb{V}_\ell$ for each $\ell \in \mathbb{N}_0$ is steered by the Dörfler marking criterion [Dör96] performed on the joint set of all spatial and parametric error indicators (see steps (iv)–(v)).

Algorithm 6. ***Input:*** *$\mathbb{P}_0 = [\mathfrak{P}_0, (\mathcal{T}_{0\nu})_{\nu\in\mathfrak{I}}]$ with $\mathfrak{P}_0 = \{\mathbf{0}\}$ and $\mathcal{T}_{0\nu} := \mathcal{T}_0$ for all $\nu \in \mathfrak{I}$, marking parameter $0 < \theta \le 1$.*

Loop: *For all $\ell = 0, 1, 2, \dots$, iterate the following steps:*

(i) *Compute the discrete primal solution $\boldsymbol{u}_\ell \in \mathbb{V}_\ell$ and the discrete dual solution $\boldsymbol{z}_\ell \in \mathbb{V}_\ell$ associated with $\mathbb{P}_\ell = [\mathfrak{P}_\ell, (\mathcal{T}_{\ell\nu})_{\nu\in\mathfrak{I}}]$.*

(ii) *For all $\nu \in \mathfrak{Q}_\ell$, compute the parametric error indicators $\mu_\ell(\nu)$, $\zeta_\ell(\nu)$ given by* (30) *and* (19).

(iii) *For all $\nu \in \mathfrak{P}_\ell$ and all $\xi \in \mathcal{N}_{\ell\nu}^+$, compute the spatial error indicators $\mu_\ell(\nu,\xi)$, $\zeta_\ell(\nu,\xi)$ given by* (30) *and* (20).

(iv) *Determine the sets $\mathfrak{M}_\ell' \subseteq \mathfrak{Q}_\ell$ and $\mathcal{M}_{\ell\nu}' \subseteq \mathcal{N}_{\ell\nu}^+$ for all $\nu \in \mathfrak{P}_\ell$ such that*

$$\theta\,\mu_\ell^2 \le \sum_{\nu\in\mathfrak{P}_\ell}\sum_{\xi\in\mathcal{M}_{\ell\nu}'} \mu_\ell(\nu,\xi)^2 + \sum_{\nu\in\mathfrak{M}_\ell'} \mu_\ell(\nu)^2, \tag{32}$$

where the overall cardinality $M_\ell' := \#\mathfrak{M}_\ell' + \sum_{\nu\in\mathfrak{P}_\ell} \#\mathcal{M}_{\ell\nu}'$ is minimal amongst all tuples $\mathbb{M}_\ell' = [\mathfrak{M}_\ell', (\mathcal{M}_{\ell\nu}')_{\nu\in\mathfrak{P}_\ell}]$ satisfying (32).

(v) *Determine the sets $\mathfrak{M}_\ell'' \subseteq \mathfrak{Q}_\ell$ and $\mathcal{M}_{\ell\nu}'' \subseteq \mathcal{N}_{\ell\nu}^+$ for all $\nu \in \mathfrak{P}_\ell$ such that*

$$\theta\,\zeta_\ell^2 \le \sum_{\nu\in\mathfrak{P}_\ell}\sum_{\xi\in\mathcal{M}_{\ell\nu}''} \zeta_\ell(\nu,\xi)^2 + \sum_{\nu\in\mathfrak{M}_\ell''} \zeta_\ell(\nu)^2, \tag{33}$$

where the overall cardinality $M_\ell'' := \#\mathfrak{M}_\ell'' + \sum_{\nu\in\mathfrak{P}_\ell} \#\mathcal{M}_{\ell\nu}''$ is minimal amongst all tuples $\mathbb{M}_\ell'' = [\mathfrak{M}_\ell'', (\mathcal{M}_{\ell\nu}'')_{\nu\in\mathfrak{P}_\ell}]$ satisfying (33).

(vi) *If $M_\ell' \le M_\ell''$, then choose $\mathfrak{M}_\ell := \mathfrak{M}_\ell'$ and $\mathcal{M}_{\ell\nu} := \mathcal{M}_{\ell\nu}'$ for all $\nu \in \mathfrak{P}_\ell$. Otherwise choose $\mathfrak{M}_\ell := \mathfrak{M}_\ell''$ and $\mathcal{M}_{\ell\nu} := \mathcal{M}_{\ell\nu}''$ for all $\nu \in \mathfrak{P}_\ell$.*

(vii) *For all $\nu \in \mathfrak{P}_\ell$, let $\mathcal{T}_{\ell+1,\nu} := \operatorname{refine}(\mathcal{T}_{\ell\nu}, \mathcal{M}_{\ell\nu})$.*

(viii) *Define $\mathfrak{P}_{\ell+1} := \mathfrak{P}_\ell \cup \mathfrak{M}_\ell$ and $\mathcal{T}_{(\ell+1)\nu} := \mathcal{T}_0$ for all $\nu \in \mathfrak{Q}_{\ell+1}$.*

Output: *For all $\ell \in \mathbb{N}_0$, the algorithm returns the multilevel stochastic Galerkin approximations $\boldsymbol{u}_\ell, \boldsymbol{z}_\ell \in \mathbb{V}_\ell$ as well as the corresponding error estimates μ_ℓ and ζ_ℓ.* □

Remark 7. *The marking criterion in steps* (iv)–(vi) *of Algorithm 6 goes back to* [MS09] *in the deterministic setting. Below, we include two alternative marking strategies, for which all theorems of the present paper hold.*

(i) [FPv16] *proceeds as in steps* (iv)–(v)*, but modifies step* (vi)*. Specifically, with $\overline{M}_\ell := \min\{M_\ell', M_\ell''\}$, choose*

$$\overline{\mathfrak{M}}_\ell' \subseteq \mathfrak{M}_\ell' \text{ and } \overline{\mathfrak{M}}_\ell'' \subseteq \mathfrak{M}_\ell'' \text{ as well as } \overline{\mathcal{M}}_{\ell\nu}' \subseteq \mathcal{M}_{\ell\nu}' \text{ and } \overline{\mathcal{M}}_{\ell\nu}'' \subseteq \mathcal{M}_{\ell\nu}'' \text{ for all } \nu \in \mathfrak{P}_\ell$$

such that $\#\overline{\mathfrak{M}}_\ell' + \sum_{\nu\in\mathfrak{P}_\ell} \#\overline{\mathcal{M}}_{\ell\nu}' = \overline{M}_\ell = \#\overline{\mathfrak{M}}_\ell'' + \sum_{\nu\in\mathfrak{P}_\ell} \#\overline{\mathcal{M}}_{\ell\nu}''$. Finally, define

$$\mathfrak{M}_\ell := \overline{\mathfrak{M}}_\ell' \cup \overline{\mathfrak{M}}_\ell'' \text{ as well as } \mathcal{M}_{\ell\nu} := \overline{\mathcal{M}}_{\ell\nu}' \cup \overline{\mathcal{M}}_{\ell\nu}'' \text{ for all } \nu \in \mathfrak{P}_\ell.$$

While, overall, this procedure results in larger sets of marked indices and marked elements than those generated in steps (iv)–(vi) *of Algorithm 6, it still guarantees that* $\overline{M}_\ell \leq \#\mathfrak{M}_\ell + \sum_{\nu\in\mathfrak{P}_\ell} \#\mathcal{M}_{\ell\nu} \leq 2\overline{M}_\ell$.

(ii) [BET11] *defines the auxiliary estimators*

$$\rho_\ell(\nu,\xi)^2 := \mu_\ell(\nu,\xi)^2\,\zeta_\ell^2 + \mu_\ell^2\,\zeta_\ell(\nu,\xi)^2 \quad \text{for all } \nu\in\mathfrak{P}_\ell \text{ and } \xi\in\mathcal{N}_{\ell\nu}^+$$

and

$$\rho_\ell(\nu)^2 := \mu_\ell(\nu)^2\,\zeta_\ell^2 + \mu_\ell^2\,\zeta_\ell(\nu)^2 \qquad \text{for all } \nu\in\mathfrak{Q}_\ell.$$

Then, determine the sets $\mathfrak{M}_\ell\subseteq\mathfrak{Q}_\ell$ *and* $\mathcal{M}_{\ell\nu}\subseteq\mathcal{N}_{\ell\nu}^+$ *for all* $\nu\in\mathfrak{P}_\ell$ *such that*

$$\theta\bigg(\sum_{\nu\in\mathfrak{P}_\ell}\sum_{\xi\in\mathcal{N}_{\ell\nu}^+}\rho_\ell(\nu,\xi)^2 + \sum_{\nu\in\mathfrak{Q}_\ell}\rho_\ell(\nu)^2\bigg) \leq \sum_{\nu\in\mathfrak{P}_\ell}\sum_{\xi\in\mathcal{M}_{\ell\nu}}\rho_\ell(\nu,\xi)^2 + \sum_{\nu\in\mathfrak{M}_\ell}\rho_\ell(\nu)^2, \tag{34}$$

where the overall cardinality $M_\ell := \#\mathfrak{M}_\ell + \sum_{\nu\in\mathfrak{P}_\ell}\#\mathcal{M}_{\ell\nu}$ *is minimal amongst all tuples* $\mathbf{M}_\ell = [\mathfrak{M}_\ell, (\mathcal{M}_{\ell\nu})_{\nu\in\mathfrak{P}_\ell}]$ *satisfying* (34).

Finally, we note that it is not necessary to choose the respective sets with minimal overall cardinality. Instead, the overall cardinality has only to be minimal up to some fixed multiplicative constant; see the discussion in [CFPP14, PP20]. *The details on the numerical analysis of these alternative marking criteria are left to the reader; they follow by combining the present analysis with the ideas from* [FPv16], *where optimal convergence rates for either marking strategy is proved in the deterministic setting. We note that the marking strategies of* [BET11, FPv16] *are empirically superior to that of* [MS09], *since they lead to the same convergence rate, but require less adaptive steps to reach a prescribed accuracy; see the experiments in* [FPv16] *for some deterministic test problems as well as Remark 17 below.* □

4.3. Plain convergence of Algorithm 6. In the following theorem, we prove that Algorithm 6 drives the product $\mu_\ell\,\zeta_\ell$ of the error estimates to zero. The analysis exploits the ideas from our own work [BPRR19a] on the convergence of adaptive *single-level* SGFEM. In the multilevel framework considered in the present work, additional difficulties arise from the fact that, first, the finite element spaces for different active parameters might differ and, second, the structure of the goal-oriented adaptive SGFEM algorithm is inherently nonlinear (due to the error bound being the product of two error estimators). In particular, the proof of Theorem 8 below will also yield plain convergence of adaptive *multilevel* SGFEM (as considered, e.g., in [BPR21b]); see also Remark 15.

Theorem 8. *Let* $d\in\{2,3\}$. *For any choice of the marking parameter* $0<\theta\leq 1$, *Algorithm 6 yields a convergent sequence of estimator products, i.e.,*

$$\mu_\ell\zeta_\ell \xrightarrow{\ell\to\infty} 0. \tag{35}$$

Under the saturation assumption (22) *for both the primal solution* $\boldsymbol{w}=\boldsymbol{u}$ *to* (8) *and the dual solution* $\boldsymbol{w}=\boldsymbol{z}$ *to* (26), *there holds convergence of the error in the goal functional*

$$|\boldsymbol{g}(\boldsymbol{u}) - \boldsymbol{g}(\boldsymbol{u}_\ell)| \leq C_{\mathrm{rel}}\,\mu_\ell\zeta_\ell \xrightarrow{\ell\to\infty} 0. \tag{36}$$

The proof of (36) in Theorem 8 is an immediate consequence of (35) combined with the goal-oriented error estimate (31) from Proposition 5. The proof of (35) requires various

preparations. The first lemma is an early result from [BV84], which proves that adaptive algorithms (without coarsening) always lead to convergence of the discrete solutions.

Lemma 9 (*a priori* convergence; see, e.g., [BPRR19a, Lemma 13])**.** *Let V be a Hilbert space. Let $a : V \times V \to \mathbb{R}$ be an elliptic and continuous bilinear form. Let $F \in V^*$ be a bounded linear functional. For each $\ell \in \mathbb{N}_0$, let $V_\ell \subseteq V$ be a closed subspace such that $V_\ell \subseteq V_{\ell+1}$. Furthermore, define the limiting space $V_\infty := \overline{\bigcup_{\ell=0}^\infty V_\ell} \subseteq V$. Then, for all $\ell \in \mathbb{N}_0 \cup \{\infty\}$, there exists a unique Galerkin solution $u_\ell \in V_\ell$ satisfying*

$$a(u_\ell, v_\ell) = F(v_\ell) \quad \text{for all } v_\ell \in V_\ell. \tag{37}$$

Moreover, there holds $\lim_{\ell\to\infty} \|u_\infty - u_\ell\|_V = 0$. □

We will exploit Lemma 9 for the limiting multilevel space $\mathbb{V}_\infty = \overline{\bigcup_{\ell=0}^\infty \mathbb{V}_\ell}$ as well as for the limiting finite element spaces $\mathbb{X}_{\infty\nu} := \overline{\bigcup_{\ell=0}^\infty \mathbb{X}_{\ell\nu}}$, $\nu \in \mathfrak{I}$, which are well-defined with the understanding that $\mathbb{X}_{\ell\nu} = \{0\}$ for $\nu \in \mathfrak{I} \setminus \mathfrak{P}_\ell$.

Let us also recall the following result from [BPRR19a].

Lemma 10 ([BPRR19a, Lemma 15])**.** *Let $g : \mathbb{R}_{\ge 0} \to \mathbb{R}_{\ge 0}$ be a continuous function with $g(0) = 0$. Let $(x_n)_{n\in\mathbb{N}} \subset \mathbb{R}_{\ge 0}$ with $\sum_{n=1}^\infty x_n^2 < \infty$. For $k \in \mathbb{N}_0$, let $(x_n^{(k)})_{n\in\mathbb{N}} \subset \mathbb{R}_{\ge 0}$ with $\sum_{n=1}^\infty (x_n - x_n^{(k)})^2 \to 0$ as $k \to \infty$. In addition, let $(\mathcal{P}_k)_{k\in\mathbb{N}_0}$ be a sequence of nested subsets of $\mathbb{N}$ (i.e., $\mathcal{P}_k \subseteq \mathcal{P}_{k+1}$ for all $k \in \mathbb{N}_0$) satisfying the following property:*

$$x_m^{(k)} \le g\Bigg(\sum_{n\in\mathcal{P}_{k+1}\setminus\mathcal{P}_k} (x_n^{(k)})^2\Bigg) \quad \text{for all } k \in \mathbb{N}_0 \text{ and } m \in \mathbb{N} \setminus \mathcal{P}_{k+1}. \tag{38}$$

Then, $\sum_{n\in\mathbb{N}\setminus\mathcal{P}_k} x_n^2 \to 0$ as $k \to \infty$. □

Based on Lemma 10, we prove the following proposition, which is closely related to [BPRR19a, Proposition 10]. Since the result holds for the parametric error estimates related to both the primal and the dual problem, we do not use the abbreviated notation (30), but use the notation of Section 3.5 instead.

Proposition 11. *Let $\boldsymbol{w} \in \{\boldsymbol{u}, \boldsymbol{z}\}$. Let $0 < \vartheta \le 1$. Suppose that Algorithm 6 yields a subsequence $(\ell_k)_{k\in\mathbb{N}_0}$ such that*

$$\vartheta \sum_{\nu\in\mathfrak{Q}_{\ell_k}} \tau_{\ell_k}(\boldsymbol{w}|\nu)^2 \le \sum_{\nu\in\mathfrak{M}_{\ell_k}} \tau_{\ell_k}(\boldsymbol{w}|\nu)^2. \tag{39}$$

Then, there holds convergence $\sum_{\nu\in\mathfrak{Q}_\ell} \tau_\ell(\boldsymbol{w}|\nu)^2 \xrightarrow{\ell\to\infty} 0$.

Proof. Let $\boldsymbol{w}_\ell \in \mathbb{V}_\ell$ denote the Galerkin approximation of $\boldsymbol{w}$. Recall that $\tau_\ell(\boldsymbol{w}|\nu) = \|e_{\ell\nu}\|_D$ for all $\nu \in \mathfrak{Q}_\ell$, where $e_{\ell\nu} \in \mathbb{X}_0$ solves

$$\langle e_{\ell\nu}\,,\, v_0\rangle_D = B(\boldsymbol{w} - \boldsymbol{w}_\ell, v_0 P_\nu) \quad \text{for all } v_0 \in \mathbb{X}_0;$$

see (19) (here, we have slightly simplified the notation by omitting the dependence of $e_{\ell\nu}$ on $\boldsymbol{w}$). Set $e_{\ell\nu} := 0$ for all $\nu \in \mathfrak{I} \setminus \mathfrak{Q}_\ell$. Define $\boldsymbol{e}'_\ell := \sum_{\nu\in\mathfrak{I}} e_{\ell\nu} P_\nu \in \mathbb{V}'_\ell := \mathbb{X}_0 \otimes \operatorname{span}\big\{P_\nu : \nu \in \mathfrak{P}_\ell \cup \mathfrak{Q}_\ell\big\} \subseteq \widehat{\mathbb{V}}_\ell$. The remainder of the proof is split into four steps.

Step 1. In this step, we prove that there exists $\boldsymbol{e}'_\infty \in \mathbb{V}$ such that $\| \boldsymbol{e}'_\infty - \boldsymbol{e}'_\ell \| \to 0$ as $\ell \to \infty$. To this end, first note that Lemma 9 guarantees the existence of $\boldsymbol{w}_\infty \in \mathbb{V}$ such that $\| \boldsymbol{w}_\infty - \boldsymbol{w}_\ell \| \to 0$ as $\ell \to \infty$. For all $\nu \in \mathfrak{P}_\ell \cup \mathfrak{Q}_\ell$, let $\bar{e}_{\ell\nu} \in \mathbb{X}_0$ be the unique solution to

$$\langle \bar{e}_{\ell\nu} \, , \, v_0 \rangle_D = B(\boldsymbol{w} - \boldsymbol{w}_\infty, v_0 P_\nu) \quad \text{for all } v_0 \in \mathbb{X}_0.$$

While this variational formulation admits a trivial solution $\bar{e}_{\ell\nu} = 0$ for all $\nu \in \mathfrak{P}_\ell$, the role of $\mathfrak{P}_\ell$ in the above definition of $\mathbb{V}'_\ell$ is to ensure the nestedness of these finite-dimensional spaces. Now, setting $\bar{e}_{\ell\nu} := 0$ for all $\nu \in \mathfrak{I} \setminus (\mathfrak{P}_\ell \cup \mathfrak{Q}_\ell)$, we define $\bar{\boldsymbol{e}}'_\ell := \sum_{\nu \in \mathfrak{I}} \bar{e}_{\ell\nu} P_\nu \in \mathbb{V}'_\ell$. Due to the Galerkin orthogonality (14), there hold

$$B_0(\boldsymbol{e}'_\ell, \boldsymbol{v}'_\ell) = B(\boldsymbol{w} - \boldsymbol{w}_\ell, \boldsymbol{v}'_\ell) \quad \text{and} \quad B_0(\bar{\boldsymbol{e}}'_\ell, \boldsymbol{v}'_\ell) = B(\boldsymbol{w} - \boldsymbol{w}_\infty, \boldsymbol{v}'_\ell) \quad \text{for all } \boldsymbol{v}'_\ell \in \mathbb{V}'_\ell.$$

By nestedness $\mathbb{V}'_\ell \subseteq \mathbb{V}'_{\ell+1}$, Lemma 9 guarantees the existence of $\boldsymbol{e}'_\infty \in \mathbb{V}$ such that $\| \boldsymbol{e}'_\infty - \bar{\boldsymbol{e}}'_\ell \| \to 0$ as $\ell \to \infty$. Moreover, there holds

$$\begin{aligned} \| \boldsymbol{e}'_\ell - \bar{\boldsymbol{e}}'_\ell \|^2 \simeq \| \boldsymbol{e}'_\ell - \bar{\boldsymbol{e}}'_\ell \|_0^2 = B_0(\boldsymbol{e}'_\ell - \bar{\boldsymbol{e}}'_\ell, \boldsymbol{e}'_\ell - \bar{\boldsymbol{e}}'_\ell) &= B(\boldsymbol{w}_\infty - \boldsymbol{w}_\ell, \boldsymbol{e}'_\ell - \bar{\boldsymbol{e}}'_\ell) \\ &\leq \| \boldsymbol{w}_\infty - \boldsymbol{w}_\ell \| \| \boldsymbol{e}'_\ell - \bar{\boldsymbol{e}}'_\ell \|. \end{aligned}$$

This yields that

$$\| \boldsymbol{e}'_\infty - \boldsymbol{e}'_\ell \| \leq \| \boldsymbol{e}'_\infty - \bar{\boldsymbol{e}}'_\ell \| + \| \boldsymbol{e}'_\ell - \bar{\boldsymbol{e}}'_\ell \| \xrightarrow{\ell \to \infty} 0.$$

Step 2. In this step, we prove that the parametric estimator subsequence fits into the setting of Lemma 10. We represent the limit $\boldsymbol{e}'_\infty \in \mathbb{V}$ in the form $\boldsymbol{e}'_\infty = \sum_{\nu \in \mathfrak{I}} e_\nu P_\nu$. Letting $\tau_\infty(\boldsymbol{w}|\nu) := \|e_\nu\|_D$, we note that

$$\sum_{\nu \in \mathfrak{I}} \tau_\infty(\boldsymbol{w}|\nu)^2 = \sum_{\nu \in \mathfrak{I}} \|e_\nu\|_D^2 = \| \boldsymbol{e}'_\infty \|_0^2 < \infty.$$

Moreover, there holds convergence

$$\sum_{\nu \in \mathfrak{I}} |\tau_\infty(\boldsymbol{w}|\nu) - \tau_\ell(\boldsymbol{w}|\nu)|^2 \leq \sum_{\nu \in \mathfrak{I}} \|e_\nu - e_{\ell\nu}\|_D^2 = \| \boldsymbol{e}'_\infty - \boldsymbol{e}'_\ell \|_0^2 \simeq \| \boldsymbol{e}'_\infty - \boldsymbol{e}'_\ell \|^2 \xrightarrow{\ell \to \infty} 0.$$

For $\nu' \in \mathfrak{Q}_{\ell_k} \backslash \mathfrak{M}_{\ell_k}$, we obtain

$$\begin{aligned} \tau_{\ell_k}(\boldsymbol{w}|\nu')^2 \leq \sum_{\nu \in \mathfrak{Q}_{\ell_k}} \tau_{\ell_k}(\boldsymbol{w}|\nu)^2 - \sum_{\nu \in \mathfrak{M}_{\ell_k}} \tau_{\ell_k}(\boldsymbol{w}|\nu)^2 &\overset{(39)}{\leq} (1 - \vartheta) \sum_{\nu \in \mathfrak{Q}_{\ell_k}} \tau_{\ell_k}(\boldsymbol{w}|\nu)^2 \\ &\overset{(39)}{\leq} \frac{1 - \vartheta}{\vartheta} \sum_{\nu \in \mathfrak{M}_{\ell_k}} \tau_{\ell_k}(\boldsymbol{w}|\nu)^2. \end{aligned} \tag{40}$$

Step 3. To apply Lemma 10, consider the continuous function $g : \mathbb{R}_{\geq 0} \to \mathbb{R}_{\geq 0}$ defined by $g(s) := \sqrt{\vartheta^{-1}(1 - \vartheta)s}$. Setting $\tau_{\ell_k}(\boldsymbol{w}|\nu') = 0$ for $\nu' \in \mathfrak{I} \setminus \mathfrak{Q}_{\ell_k}$, we deduce from (40) that

$$\tau_{\ell_k}(\boldsymbol{w}|\nu') \leq g\Big(\sum_{\nu \in \mathfrak{M}_{\ell_k}} \tau_{\ell_k}(\boldsymbol{w}|\nu)^2 \Big) \quad \text{for all } k \in \mathbb{N}_0 \text{ and } \nu' \in \mathfrak{I} \setminus \mathfrak{M}_{\ell_k}.$$

Note that the index set $\mathfrak{I}$ is countable, since it can be understood as a countable union of countable sets, and that $\mathfrak{P}_{\ell_n} \subseteq \mathfrak{P}_{\ell_n+1} \subseteq \mathfrak{P}_{\ell_{n+1}}$, since $\ell_n + 1 \leq \ell_{n+1}$. Therefore, we can establish a one-to-one map between $\mathfrak{I}$ and $\mathbb{N}$, which allows us to identify each index set

$\mathfrak{P}_{\ell_k} \subset \mathfrak{I}$ ($k \in \mathbb{N}_0$) with a set $\mathcal{P}_k \subset \mathbb{N}$. Then $\mathcal{P}_k \subseteq \mathcal{P}_{k+1}$ and applying Lemma 10 to the sequences $(x_n)_{n\in\mathbb{N}} := (\tau_\infty(\boldsymbol{w}|\nu))_{\nu\in\mathfrak{I}}$, $(x_n^{(k)})_{n\in\mathbb{N}} := (\tau_{\ell_k}(\boldsymbol{w}|\nu))_{\nu\in\mathfrak{I}}$, we prove that

$$\sum_{\nu\in\mathfrak{I}\setminus\mathfrak{P}_{\ell_k}} \tau_\infty(\boldsymbol{w}|\nu)^2 \xrightarrow{k\to\infty} 0.$$

Step 4. Note that the sequence $\big(\sum_{\nu\in\mathfrak{I}\setminus\mathfrak{P}_\ell} \tau_\infty(\boldsymbol{w}|\nu)^2\big)_{\ell\in\mathbb{N}_0}$ is monotonic decreasing and bounded from below. Hence, it is convergent. Moreover, it has a subsequence that converges to zero. We therefore conclude that

$$\sum_{\nu\in\mathfrak{Q}_\ell} \tau_\infty(\boldsymbol{w}|\nu)^2 \le \sum_{\nu\in\mathfrak{I}\setminus\mathfrak{P}_\ell} \tau_\infty(\boldsymbol{w}|\nu)^2 \xrightarrow{\ell\to\infty} 0.$$

Overall, we derive that

$$\sum_{\nu\in\mathfrak{Q}_\ell} \tau_\ell(\boldsymbol{w}|\nu)^2 \lesssim \sum_{\nu\in\mathfrak{Q}_\ell} \tau_\infty(\boldsymbol{w}|\nu)^2 + \sum_{\nu\in\mathfrak{I}} \big(\tau_\infty(\boldsymbol{w}|\nu) - \tau_\ell(\boldsymbol{w}|\nu)\big)^2 \xrightarrow{\ell\to\infty} 0.$$

This concludes the proof. □

To prove a convergence result for the spatial contributions of $\tau_\ell(\boldsymbol{w})$, we will use the following notation: For $\omega \subset D$, we define

$$B_\omega(v,w) := \int_\Gamma \int_\omega a_0 \nabla u \cdot \nabla v \, dx \, d\pi(\mathbf{y}) + \sum_{m=1}^\infty \int_\Gamma \int_\omega y_m a_m \nabla u \cdot \nabla v \, dx \, d\pi(\mathbf{y}) \text{ for } v, w \in \mathbb{V}.$$

Note that $B_\omega(\cdot,\cdot)$ is symmetric, bilinear, and positive semidefinite. We denote by $|\!|\!| v |\!|\!|_\omega := B_\omega(v,v)^{1/2}$ the corresponding seminorm. Since the following results (Lemma 12 and Proposition 14) hold for the spatial error estimates related to both the primal and the dual problem, we do not use the abbreviated notation (30), but use the notation of Section 3.5 instead. With this remark, the following lemma is an analogue of [BPRR19a, Lemma 16]. Actually, the result formulated below is weaker than that in [BPRR19a, Lemma 16]; this is due to the fact that multilevel SGFEM employs possibly different meshes $\mathcal{T}_{\ell\nu}$ for different indices $\nu \in \mathfrak{P}_\ell$.

Lemma 12. *Let $\boldsymbol{w} \in \{\boldsymbol{u}, \boldsymbol{z}\}$. Let $\nu \in \mathfrak{P}_\ell$, $\xi \in \mathcal{N}_{\ell\nu}^+$ and denote by $\omega_{\ell\nu}(\xi) := \bigcup\{T \in \mathcal{T}_{\ell\nu} : \xi \in T\}$ the associated vertex patch. Then, the following estimate holds:*

$$\tau_\ell(\boldsymbol{w}|\nu,\xi) \le C |\!|\!| \boldsymbol{w} - \boldsymbol{w}_\ell |\!|\!|_{\omega_{\ell\nu}(\xi)}. \tag{41a}$$

Furthermore, let $\boldsymbol{w}_\infty \in \mathbb{V}$ be the limit of $(\boldsymbol{w}_\ell)_{\ell\in\mathbb{N}_0}$ guaranteed by Lemma 9. If $\widehat{\varphi}_{\ell\nu,\xi} \in \mathbb{X}_{\infty\nu}$, then there holds

$$\tau_\ell(\boldsymbol{w}|\nu,\xi) \le C |\!|\!| \boldsymbol{w}_\infty - \boldsymbol{w}_\ell |\!|\!|_{\omega_{\ell\nu}(\xi)}. \tag{41b}$$

The constant $C > 0$ in (41a) *and* (41b) *depends only on a_0 and τ.*

Proof. We recall the definition of the spatial error indicators in (20):

$$\tau_\ell(\boldsymbol{w}|\nu,\xi)^2 = \frac{|B(\widehat{\boldsymbol{w}}_\ell - \boldsymbol{w}_\ell, \widehat{\varphi}_{\ell\nu,\xi} P_\nu)|^2}{\|\widehat{\varphi}_{\ell\nu,\xi}\|_D^2} = \|\widehat{\mathbb{G}}_{\ell\nu,\xi} \widehat{e}_{\ell\nu}\|_D^2 \quad \text{for all } z \in \mathcal{N}_\ell^+, \tag{42a}$$

where $\widehat{\mathbb{G}}_{\ell\nu,\xi} : \mathbb{X} \to \operatorname{span}\{\widehat{\varphi}_{\ell\nu,\xi}\}$ is the orthogonal projection onto the one-dimensional space $\operatorname{span}\{\widehat{\varphi}_{\ell\nu,\xi}\}$ with respect to $\langle\cdot\,,\,\cdot\rangle_D$, and $\widehat{e}_{\ell\nu} \in \widehat{\mathbb{X}}_{\ell\nu}$ solves

$$\langle \widehat{e}_{\ell\nu}\,,\, \widehat{v}_{\ell\nu}\rangle_D = B(\widehat{\boldsymbol{w}}_\ell - \boldsymbol{w}_\ell, \widehat{v}_{\ell\nu} P_\nu) \quad \text{for all } \widehat{v}_{\ell\nu} \in \widehat{\mathbb{X}}_{\ell\nu}; \tag{42b}$$

see [BPR21b, Proof of Theorem 2]. This yields that

$$\tau_\ell(\boldsymbol{w}|\nu,\xi)^2 = \|\widehat{\mathbb{G}}_{\ell\nu,\xi}\widehat{e}_{\ell\nu}\|_D^2 = \langle \widehat{e}_{\ell\nu}\,,\,\widehat{\mathbb{G}}_{\ell\nu,\xi}\widehat{e}_{\ell\nu}\rangle_D = B(\widehat{\boldsymbol{w}}_\ell - \boldsymbol{w}_\ell, \widehat{\mathbb{G}}_{\ell\nu,\xi}\widehat{e}_{\ell\nu}\,P_\nu).$$

Since $\widehat{\mathbb{G}}_{\ell\nu,\xi}\widehat{e}_{\ell\nu}\,P_\nu \in \widehat{\mathbb{V}}_\ell$, we use (13b) to find that

$$B(\widehat{\boldsymbol{w}}_\ell - \boldsymbol{w}_\ell, \widehat{\mathbb{G}}_{\ell\nu,\xi}\widehat{e}_{\ell\nu}\,P_\nu) = B(\boldsymbol{w} - \boldsymbol{w}_\ell, \widehat{\mathbb{G}}_{\ell\nu,\xi}\widehat{e}_{\ell\nu}\,P_\nu).$$

Note that the support of $\widehat{\mathbb{G}}_{\ell\nu,\xi}\widehat{e}_{\ell\nu}$ lies in $\omega := \operatorname{supp}(\widehat{\varphi}_{\ell\nu,\xi})$. Therefore, the Cauchy–Schwarz inequality shows that

$$\begin{aligned}
\|\widehat{\mathbb{G}}_{\ell\nu,\xi}\widehat{e}_{\ell\nu}\|_D^2 &= \|\!|\, \mathbb{G}_{\ell\nu,\xi}\widehat{e}_{\ell\nu}P_\nu \,|\!\|_0^2 = B(\boldsymbol{w} - \boldsymbol{w}_\ell, \widehat{\mathbb{G}}_{\ell\nu,\xi}\widehat{e}_{\ell\nu}P_\nu) = B_\omega(\boldsymbol{w} - \boldsymbol{w}_\ell, \widehat{\mathbb{G}}_{\ell\nu,\xi}\widehat{e}_{\ell\nu}P_\nu) \\
&\le |\!|\!|\, \boldsymbol{w} - \boldsymbol{w}_\ell \,|\!|\!|_\omega \, |\!|\!|\, \widehat{\mathbb{G}}_{\ell\nu,\xi}\widehat{e}_{\ell\nu}P_\nu \,|\!|\!|_\omega \le |\!|\!|\, \boldsymbol{w} - \boldsymbol{w}_\ell \,|\!|\!|_\omega \, |\!|\!|\, \widehat{\mathbb{G}}_{\ell\nu,\xi}\widehat{e}_{\ell\nu}P_\nu \,|\!|\!| \\
&\overset{(7)}{\simeq} |\!|\!|\, \boldsymbol{w} - \boldsymbol{w}_\ell \,|\!|\!|_\omega \, |\!|\!|\, \widehat{\mathbb{G}}_{\ell\nu,\xi}\widehat{e}_{\ell\nu}P_\nu \,|\!|\!|_0 = |\!|\!|\, \boldsymbol{w} - \boldsymbol{w}_\ell \,|\!|\!|_\omega \, \|\widehat{\mathbb{G}}_{\ell\nu,\xi}\widehat{e}_{\ell\nu}\|_D.
\end{aligned}$$

We thus have shown that

$$\tau_\ell(\boldsymbol{w}|\nu,\xi) = \|\widehat{\mathbb{G}}_{\ell\nu,\xi}\widehat{e}_{\ell\nu}\|_D \lesssim |\!|\!|\, \boldsymbol{w} - \boldsymbol{w}_\ell \,|\!|\!|_\omega.$$

Since $\omega = \operatorname{supp}(\widehat{\varphi}_{\ell\nu,\xi}) \subseteq \omega_{\ell\nu}(\xi)$, this proves (41a). If $\widehat{\varphi}_{\ell\nu,\xi} \in \mathbb{X}_{\infty\nu}$, then $\widehat{\mathbb{G}}_{\ell\nu,\xi}\widehat{e}_{\ell\nu}P_\nu \in \mathbb{V}_\infty$ and hence

$$B(\widehat{\boldsymbol{w}}_\ell - \boldsymbol{w}_\ell, \mathbb{G}_{\ell\nu,\xi}\widehat{e}_{\ell\nu}\,P_\nu) = B(\boldsymbol{w} - \boldsymbol{w}_\ell, \widehat{\mathbb{G}}_{\ell\nu,\xi}\widehat{e}_{\ell\nu}\,P_\nu) = B(\boldsymbol{w}_\infty - \boldsymbol{w}_\ell, \widehat{\mathbb{G}}_{\ell\nu,\xi}\widehat{e}_{\ell\nu}\,P_\nu).$$

Arguing as before, we thus prove (41b). □

Note that the bounds in (41) estimate the error indicator associated with a *single* index $\nu \in \mathfrak{P}_\ell$ by the full energy norm (involving *all* indices in $\mathfrak{P}_\ell$). Hence, these bounds are less tight than their analogues in [BPRR19a, Lemma 16]. Nevertheless, they will still be useful for our purposes, thanks to the following elementary lemma, which formulates a generalized dominated convergence result for sequences. A simple proof is included for the convenience of the reader.

Lemma 13. *Let $(\alpha_n)_{n\in\mathbb{N}}, (\beta_n)_{n\in\mathbb{N}} \subset \mathbb{R}$ with $\sum_{n=1}^\infty |\beta_n| < \infty$. Let $C > 0$. For $k \in \mathbb{N}_0$, let $(\alpha_n^{(k)})_{n\in\mathbb{N}}, (\beta_n^{(k)})_{n\in\mathbb{N}} \subset \mathbb{R}$ with $|\alpha_n^{(k)}| \le C\,|\beta_n^{(k)}|$ and $\alpha_n^{(k)} \to \alpha_n$ as $k \to \infty$, for all $n \in \mathbb{N}$. Then, the convergence $\sum_{n=1}^\infty |\beta_n - \beta_n^{(k)}| \to 0$ as $k \to \infty$ implies that $\sum_{n=1}^\infty |\alpha_n| < \infty$ and $\sum_{n=1}^\infty |\alpha_n - \alpha_n^{(k)}| \to 0$ as $k \to \infty$.*

Proof. The proof is split into two steps.

Step 1. Let $\varepsilon > 0$. Due to the assumptions of the lemma, for arbitrary $N \in \mathbb{N}$ we can choose $k_0 \in \mathbb{N}$ such that

$$\sum_{n=1}^N |\alpha_n - \alpha_n^{(k)}| + C\sum_{n=1}^\infty |\beta_n - \beta_n^{(k)}| < \varepsilon \quad \text{for all } k \ge k_0.$$

Hence, by using the triangle inequality and the fact that $|\alpha_n^{(k)}| \le C\,|\beta_n^{(k)}|$ we find that

$$\begin{aligned}
\sum_{n=1}^N |\alpha_n| &\le \sum_{n=1}^N |\alpha_n^{(k)}| + \sum_{n=1}^N |\alpha_n - \alpha_n^{(k)}| \le C\sum_{n=1}^N |\beta_n^{(k)}| + \sum_{n=1}^N |\alpha_n - \alpha_n^{(k)}| \\
&\le C\sum_{n=1}^N |\beta_n| + C\sum_{n=1}^N |\beta_n - \beta_n^{(k)}| + \sum_{n=1}^N |\alpha_n - \alpha_n^{(k)}| < C\sum_{n=1}^\infty |\beta_n| + \varepsilon
\end{aligned}$$

for any $\varepsilon > 0$ and for arbitrary $N \in \mathbb{N}$. Therefore, $\sum_{n=1}^{\infty} |\alpha_n| \leq C \sum_{n=1}^{\infty} |\beta_n| < \infty$.

Step 2. Let $\varepsilon > 0$. Since $\sum_{n=1}^{\infty} |\alpha_n| + C \sum_{n=1}^{\infty} |\beta_n| < \infty$, we can choose $n_0 \in \mathbb{N}$ such that

$$\sum_{n=n_0}^{\infty} |\alpha_n| + C \sum_{n=n_0}^{\infty} |\beta_n| < \varepsilon.$$

Due to the assumed convergence, we can choose $k_0 \in \mathbb{N}$ such that

$$\sum_{n=1}^{n_0-1} |\alpha_n - \alpha_n^{(k)}| + C \sum_{n=1}^{\infty} |\beta_n - \beta_n^{(k)}| < \varepsilon \quad \text{for all } k \geq k_0.$$

Then, for all $k \geq k_0$, the triangle inequality yields that

$$\begin{aligned}
\sum_{n=1}^{\infty} |\alpha_n - \alpha_n^{(k)}| &\leq \sum_{n=1}^{n_0-1} |\alpha_n - \alpha_n^{(k)}| + \sum_{n=n_0}^{\infty} |\alpha_n| + \sum_{n=n_0}^{\infty} |\alpha_n^{(k)}| \\
&\leq \sum_{n=1}^{n_0-1} |\alpha_n - \alpha_n^{(k)}| + \sum_{n=n_0}^{\infty} |\alpha_n| + C \sum_{n=n_0}^{\infty} |\beta_n^{(k)}| \\
&\leq \sum_{n=1}^{n_0-1} |\alpha_n - \alpha_n^{(k)}| + \sum_{n=n_0}^{\infty} |\alpha_n| + C \sum_{n=n_0}^{\infty} |\beta_n| + C \sum_{n=n_0}^{\infty} |\beta_n - \beta_n^{(k)}| < 2\varepsilon.
\end{aligned}$$

This concludes the proof. □

With Lemmas 12 and 13 at hand, we can extend the result established in [BPRR19a, Proposition 11] for single-level SGFEM to multilevel SGFEM.

Proposition 14. *Let $\boldsymbol{w} \in \{\boldsymbol{u}, \boldsymbol{z}\}$. Let $0 < \vartheta \leq 1$. Suppose that Algorithm 6 yields a subsequence $(\ell_k)_{k \in \mathbb{N}_0}$ such that*

$$\vartheta \sum_{\nu \in \mathfrak{P}_{\ell_k}} \sum_{\xi \in \mathcal{N}_{\ell_k \nu}^+} \tau_{\ell_k}(\boldsymbol{w}|\nu, \xi)^2 \leq \sum_{\nu \in \mathfrak{P}_{\ell_k}} \sum_{\nu \in \mathcal{M}_{\ell_k \nu}} \tau_{\ell_k}(\boldsymbol{w}|\nu, \xi)^2. \tag{43}$$

Then, there holds convergence $\displaystyle\sum_{\nu \in \mathfrak{P}_{\ell_k}} \sum_{\xi \in \mathcal{N}_{\ell_k \nu}^+} \tau_{\ell_k}(\boldsymbol{w}|\nu, \xi)^2 \xrightarrow{k \to \infty} 0.$

Proof. The proof follows the lines of the one of [MSV08, Theorem 2.1]. Therefore, we only sketch it and highlight how the results of [MSV08] for deterministic problems can be extended to the parametric setting (see also [BPRR19a, Proposition 11] for the corresponding result in the context of single-level SGFEM). The proof is split into six steps.

Step 1. The variational problems (8) and (26), their discretizations, and the proposed adaptive algorithm satisfy the general framework described in [MSV08, section 2]:

- the variational problems (8) and (26) fit into the class of problems considered in [MSV08, section 2.1];
- the Galerkin discretizations (18) and (27) satisfy the assumptions in [MSV08, equations (2.6)–(2.8)];
- the spatial NVB refinement considered in the present paper satisfies the assumptions on the mesh refinement in [MSV08, equations (2.5) and (2.14)];
- the Dörfler marking criterion (43) implies the weak marking condition in [MSV08, equation (2.13)];

- finally, Lemma 12 proves the local discrete efficiency estimate in the parametric setting (cf. [MSV08, equation (2.9b)]). Note that the global reliability of the estimator (see the lower bound of (24) and [MSV08, equation (2.9a)]) is not exploited here (and hence, not needed for the proof of Theorem 8). In particular, the estimates (41a) and (41b) from Lemma 12 replace [MSV08, eq. (2.9b)] and [MSV08, eq. (4.11)], respectively.

Step 2. Let $\nu \in \mathfrak{P}_\infty := \bigcup_{\ell=0}^\infty \mathfrak{P}_\ell$. Let $\mathcal{T}_{\infty\nu} := \bigcup_{k\geq 0} \bigcap_{\ell\geq k} \mathcal{T}_{\ell\nu}$ be the set of all elements which remain unrefined after finitely many steps of refinement, where $\mathcal{T}_{\ell\nu} = \emptyset$ if $\nu \notin \mathfrak{P}_\ell$. In the spirit of [MSV08, eqs. (4.10)], for all $\ell \in \mathbb{N}_0$, we consider the decomposition $\mathcal{T}_{\ell\nu} = \mathcal{T}_{\ell\nu}^{\rm good} \cup \mathcal{T}_{\ell\nu}^{\rm bad} \cup \mathcal{T}_{\ell\nu}^{\rm neither}$, where

$$\begin{aligned}
\mathcal{T}_{\ell\nu}^{\rm good} &:= \{T \in \mathcal{T}_{\ell\nu} : \widehat{\varphi}_{\ell\nu,\xi} \in \mathbb{X}_{\infty\nu} \text{ for all } \xi \in \mathcal{N}_{\ell\nu}^+ \cap T\},\\
\mathcal{T}_{\ell\nu}^{\rm bad} &:= \{T \in \mathcal{T}_{\ell\nu} : T' \in \mathcal{T}_{\infty\nu} \text{ for all } T' \in \mathcal{T}_{\ell\nu} \text{ with } T \cap T' \neq \emptyset\},\\
\mathcal{T}_{\ell\nu}^{\rm neither} &:= \mathcal{T}_{\ell\nu} \setminus (\mathcal{T}_{\ell\nu}^{\rm good} \cup \mathcal{T}_{\ell\nu}^{\rm bad}).
\end{aligned}$$

The elements in $\mathcal{T}_{\ell\nu}^{\rm good}$ are refined sufficiently many times in order to guarantee (41b). The set $\mathcal{T}_{\ell\nu}^{\rm bad}$ consists of all elements such that the whole element patch remains unrefined. The remaining elements are collected in the set $\mathcal{T}_{\ell\nu}^{\rm neither}$. Note that $\mathcal{T}_{\ell\nu}^{\rm good}$ is slightly larger than the corresponding set $\mathcal{G}_{\ell\nu}^0$ in [MSV08, eq. (4.10a)], while $\mathcal{T}_{\ell\nu}^{\rm bad}$ coincides with the corresponding set $\mathcal{G}_{\ell\nu}^+$ in [MSV08, eq. (4.10b)]. As a consequence, $\mathcal{T}_{\ell\nu}^{\rm neither}$ is smaller than the corresponding set $\mathcal{G}_{\ell\nu}^*$ in [MSV08, eq. (4.10c)].

Step 3. By arguing as in the proof of Proposition 4.1 in [MSV08], we exploit the uniform shape-regularity of the mesh $\mathcal{T}_{\ell\nu}$ guaranteed by NVB and use Lemma 12 and Lemma 9 to prove that

$$\begin{aligned}
\sum_{T\in\mathcal{T}_{\ell\nu}^{\rm good}} \sum_{\xi\in\mathcal{N}_{\ell\nu}^+\cap T} \tau_\ell(\boldsymbol{w}|\nu,\xi)^2 &\overset{(41b)}{\lesssim} \sum_{T\in\mathcal{T}_{\ell\nu}^{\rm good}} \sum_{\xi\in\mathcal{N}_{\ell\nu}^+\cap T} |\!|\!| \boldsymbol{w}_\infty - \boldsymbol{w}_\ell |\!|\!|_{\omega_{\ell\nu}(\xi)}^2\\
&\lesssim |\!|\!| \boldsymbol{w}_\infty - \boldsymbol{w}_\ell |\!|\!|^2 \xrightarrow{\ell\to\infty} 0. \qquad (44)
\end{aligned}$$

Let $D_{\ell\nu}^{\rm neither} := \bigcup\{T' \in \mathcal{T}_{\ell\nu} : T \cap T' \neq \emptyset \text{ for some } T \in \mathcal{T}_{\ell\nu}^{\rm neither}\}$. Since $\mathcal{T}_{\ell\nu}^{\rm neither}$ is contained in the corresponding set $\mathcal{G}_{\ell\nu}^*$ in [MSV08, eq. (4.10c)], arguing as in Step 1 of the proof of Proposition 4.2 in [MSV08], we show that $|D_{\ell\nu}^{\rm neither}| \to 0$ as $\ell \to \infty$. Hence, Lemma 12, uniform shape regularity, and the fact that the local energy seminorm is absolutely continuous with respect to the Lebesgue measure, i.e., $|\!|\!| v |\!|\!|_\omega \to 0$ as $|\omega| \to 0$ for all $v \in \mathbb{V}$, lead to

$$\begin{aligned}
\sum_{T\in\mathcal{T}_{\ell\nu}^{\rm neither}} \sum_{\xi\in\mathcal{N}_{\ell\nu}^+\cap T} \tau_\ell(\boldsymbol{w}|\nu,\xi)^2 &\overset{(41a)}{\lesssim} \sum_{T\in\mathcal{T}_{\ell\nu}^{\rm neither}} \sum_{\xi\in\mathcal{N}_{\ell\nu}^+\cap T} |\!|\!| \boldsymbol{w} - \boldsymbol{w}_\ell |\!|\!|_{\omega_{\ell\nu}(\xi)}^2\\
&\lesssim |\!|\!| \boldsymbol{w} - \boldsymbol{w}_\ell |\!|\!|_{D_{\ell\nu}^{\rm neither}}^2 \xrightarrow{\ell\to\infty} 0. \qquad (45)
\end{aligned}$$

We note that (44) and (45) hold independently of the marking property (43), but rely only on the nestedness of the finite-dimensional subspaces $\mathbb{V}_\ell \subseteq \mathbb{V}_{\ell+1}$ for all $\ell \in \mathbb{N}_0$.

Step 4. Recall that the index set $\mathfrak{I}$ is countable so that we can identify each index $\nu \in \mathfrak{I}$ with a natural number $n \in \mathbb{N}$. For $\ell \in \mathbb{N}_0$, we consider the following sequence:

$$(\alpha_n^{(\ell)})_{n\in\mathbb{N}} = (\alpha_\nu^{(\ell)})_{\nu\in\mathfrak{I}} := \Bigg(\sum_{T\in\mathcal{T}_{\ell\nu}^{\mathrm{good}}} \sum_{\xi\in\mathcal{N}_\ell^+\cap T} \tau_\ell(\boldsymbol{w}|\nu,\xi)^2 + \sum_{T\in\mathcal{T}_{\ell\nu}^{\mathrm{neither}}} \sum_{\xi\in\mathcal{N}_{\ell\nu}^+\cap T} \tau_\ell(\boldsymbol{w}|\nu,\xi)^2 \Bigg)_{\nu\in\mathfrak{I}},$$

where $\mathcal{T}_{\ell\nu} = \emptyset$ and, consequently, $\alpha_\nu^{(\ell)} = 0$ if $\nu \in \mathfrak{I}\backslash\mathfrak{P}_\ell$. We already know from (44)–(45) that $\alpha_\nu^{(\ell)} \to 0 =: \alpha_\nu$ as $\ell \to \infty$, for all $\nu \in \mathfrak{I}$. With the notation introduced in (42), note that

$$0 \le \alpha_\nu^{(\ell)} \le \sum_{T\in\mathcal{T}_{\ell\nu}} \sum_{\xi\in\mathcal{N}_{\ell\nu}^+\cap T} \tau_\ell(\boldsymbol{w}|\nu,\xi)^2 \lesssim \sum_{\xi\in\mathcal{N}_{\ell\nu}^+} \tau_\ell(\boldsymbol{w}|\nu,\xi)^2 \overset{(42)}{=} \sum_{\xi\in\mathcal{N}_{\ell\nu}^+} \|\widehat{\mathbb{G}}_{\ell\nu,\xi}\widehat{e}_{\ell\nu}\|_D^2 \lesssim \|\widehat{e}_{\ell\nu}\|_D^2 =: \beta_\nu^{(\ell)},$$

where the final estimate is part of the proof of [BPR21b, Lemma 5, Step 2]. Defining $\mathbb{V}_\ell'' := \bigoplus_{\nu\in\mathfrak{P}_\ell} \big[\widehat{\mathbb{X}}_{\ell\nu} \otimes \mathrm{span}\{P_\nu\}\big] \subseteq \widehat{\mathbb{V}}_\ell$ and $\boldsymbol{e}_\ell'' := \sum_{\nu\in\mathfrak{P}_\ell} \widehat{e}_{\ell\nu}P_\nu$, we conclude from (42b) and (13b) that $\boldsymbol{e}_\ell'' \in \mathbb{V}_\ell''$ is the unique solution to

$$B_0(\boldsymbol{e}_\ell'', \boldsymbol{v}_\ell'') = B(\boldsymbol{w} - \boldsymbol{w}_\ell, \boldsymbol{v}_\ell'') \quad \text{for all } \boldsymbol{v}_\ell'' \in \mathbb{V}_\ell''.$$

Since $\mathbb{V}_\ell'' \subseteq \mathbb{V}_{\ell+1}''$ for all $\ell \in \mathbb{N}_0$ and since $\boldsymbol{w}_\ell \to \boldsymbol{w}_\infty$ as $\ell \to \infty$, we can argue as in Step 1 of the proof of Proposition 11 to see that Lemma 9 provides $\boldsymbol{e}_\infty'' = \sum_{\nu\in\mathfrak{I}} \widehat{e}_{\infty\nu}P_\nu \in \mathbb{V}$ such that

$$\sum_{\nu\in\mathfrak{I}} \|\widehat{e}_{\infty\nu} - \widehat{e}_{\ell\nu}\|_D^2 = |\!|\!| \boldsymbol{e}_\infty'' - \boldsymbol{e}_\ell'' |\!|\!|_0^2 \xrightarrow{\ell\to\infty} 0,$$

where $\widehat{e}_{\ell\nu} = 0$ if $\nu \in \mathfrak{I}\backslash\mathfrak{P}_\ell$. In particular, it follows that

$$\begin{aligned}
\sum_{\nu\in\mathfrak{I}} \big| \|\widehat{e}_{\infty\nu}\|_D^2 - \|\widehat{e}_{\ell\nu}\|_D^2 \big| &= \sum_{\nu\in\mathfrak{I}} \big| \|\widehat{e}_{\infty\nu}\|_D - \|\widehat{e}_{\ell\nu}\|_D \big| \big[\|\widehat{e}_{\infty\nu}\|_D + \|\widehat{e}_{\ell\nu}\|_D \big] \\
&\le \sum_{\nu\in\mathfrak{I}} \|\widehat{e}_{\infty\nu} - \widehat{e}_{\ell\nu}\|_D \big[\|\widehat{e}_{\infty\nu}\|_D + \|\widehat{e}_{\ell\nu}\|_D \big] \\
&\le 2\big[|\!|\!| \boldsymbol{e}_\infty'' |\!|\!|_0 + |\!|\!| \boldsymbol{e}_\ell'' |\!|\!|_0 \big] |\!|\!| \boldsymbol{e}_\infty'' - \boldsymbol{e}_\ell'' |\!|\!|_0 \xrightarrow{\ell\to\infty} 0.
\end{aligned}$$

With $\beta_\nu := \|\widehat{e}_{\infty\nu}\|_D^2$, we can thus apply Lemma 13 to strengthen the parameter-wise convergence to

$$\sum_{\nu\in\mathfrak{I}} \alpha_\nu^{(\ell)} = \sum_{\nu\in\mathfrak{P}_\ell} \alpha_\nu^{(\ell)} \xrightarrow{\ell\to\infty} 0.$$

In explicit terms, this proves that (44)–(45) can indeed be strengthened to

$$\sum_{\nu\in\mathfrak{P}_\ell} \Bigg(\sum_{T\in\mathcal{T}_{\ell\nu}^{\mathrm{good}}} \sum_{\xi\in\mathcal{N}_{\ell\nu}^+\cap T} \tau_\ell(\boldsymbol{w}|\nu,\xi)^2 + \sum_{T\in\mathcal{T}_{\ell\nu}^{\mathrm{neither}}} \sum_{\xi\in\mathcal{N}_{\ell\nu}^+\cap T} \tau_\ell(\boldsymbol{w}|\nu,\xi)^2 \Bigg) \xrightarrow{\ell\to\infty} 0. \tag{46}$$

Step 5. To conclude the proof, it remains to consider the sets $\mathcal{T}_{\ell\nu}^{\mathrm{bad}}$. If $\xi \in \mathcal{M}_{\ell_k\nu}$ and $T \in \mathcal{T}_{\ell_k\nu}$ with $\xi \in T$, then $T \in \mathcal{T}_{\ell_k\nu} \setminus \mathcal{T}_{\ell_k\nu}^{\mathrm{bad}} = \mathcal{T}_{\ell_k\nu}^{\mathrm{good}} \cup \mathcal{T}_{\ell_k\nu}^{\mathrm{neither}}$. Therefore, it follows from (46) that

$$\vartheta \sum_{\nu\in\mathfrak{P}_{\ell_k}} \sum_{\xi\in\mathcal{N}_{\ell_k\nu}^+} \tau_{\ell_k}(\boldsymbol{w}|\nu,\xi)^2 \overset{(43)}{\le} \sum_{\nu\in\mathfrak{P}_{\ell_k}} \sum_{\xi\in\mathcal{M}_{\ell_k\nu}} \tau_{\ell_k}(\boldsymbol{w}|\nu,\xi)^2 \xrightarrow{k\to\infty} 0.$$

In particular, we obtain (cf. [MSV08, eq. (4.17)])

$$\sum_{\xi\in\mathcal{N}^+_{\ell_k\nu}\cap T}\tau_{\ell_k}(\boldsymbol{w}|\nu,\xi)^2\xrightarrow{k\to\infty}0\quad\text{for all }\nu\in\mathfrak{P}_\ell\text{ and all }T\in\mathcal{T}^{\mathrm{bad}}_{\ell_k\nu}. \tag{47}$$

Arguing as in Steps 2–5 of the proof of Proposition 4.3 in [MSV08], we use (47) and apply the Lebesgue dominated convergence theorem to derive that

$$\sum_{T\in\mathcal{T}^{\mathrm{bad}}_{\ell_k\nu}}\sum_{\xi\in\mathcal{N}^+_{\ell_k\nu}\cap T}\tau_{\ell_k}(\boldsymbol{w}|\nu,\xi)^2\xrightarrow{k\to\infty}0\quad\text{for all }\nu\in\mathfrak{P}_\ell.$$

As in Step 4, this parameter-wise convergence can be strengthened to

$$\sum_{\nu\in\mathfrak{P}_{\ell_k}}\sum_{T\in\mathcal{T}^{\mathrm{bad}}_{\ell_k\nu}}\sum_{\xi\in\mathcal{N}^+_{\ell_k\nu}\cap T}\tau_{\ell_k}(\boldsymbol{w}|\nu,\xi)^2\xrightarrow{k\to\infty}0. \tag{48}$$

Step 6. Combining (46) and (48), we obtain

$$\begin{aligned}\sum_{\nu\in\mathfrak{P}_{\ell_k}}\sum_{\xi\in\mathcal{N}^+_{\ell_k\nu}}\tau_{\ell_k}(\boldsymbol{w}|\nu,\xi)^2\le\sum_{\nu\in\mathfrak{P}_{\ell_k}}\Bigg(&\sum_{T\in\mathcal{T}^{\mathrm{good}}_{\ell_k\nu}}\sum_{\xi\in\mathcal{N}^+_{\ell_k\nu}\cap T}\tau_{\ell_k}(\boldsymbol{w}|\nu,\xi)^2+\sum_{T\in\mathcal{T}^{\mathrm{bad}}_{\ell_k\nu}}\sum_{\xi\in\mathcal{N}^+_{\ell_k\nu}\cap T}\tau_{\ell_k}(\boldsymbol{w}|\nu,\xi)^2\\&+\sum_{T\in\mathcal{T}^{\mathrm{neither}}_{\ell_k\nu}}\sum_{\xi\in\mathcal{N}^+_{\ell_k\nu}\cap T}\tau_{\ell_k}(\boldsymbol{w}|\nu,\xi)^2\Bigg)\xrightarrow{k\to\infty}0.\end{aligned}$$

This concludes the proof. □

Proof of Theorem 8. The proof is split into five steps.

Step 1. Let $(\ell'_k)_{k\in\mathbb{N}_0}$ be the sequence of iterations, where the marking strategy of Algorithm 6 selects $\mathfrak{M}_{\ell_k}=\mathfrak{M}'_{\ell_k}$ and $\mathcal{M}_{\ell_k\nu}=\mathcal{M}'_{\ell_k\nu}$ for all $\nu\in\mathfrak{P}_{\ell_k}$ (i.e., marking with respect to the primal estimator). Let $(\ell''_k)_{k\in\mathbb{N}_0}$ be the index sequence, where the marking strategy of Algorithm 6 selects $\mathfrak{M}_{\ell_k}=\mathfrak{M}''_{\ell_k}$ and $\mathcal{M}_{\ell_k\nu}=\mathcal{M}''_{\ell_k\nu}$ for all $\nu\in\mathfrak{P}_{\ell_k}$ (i.e., marking with respect to the dual estimator). Note that this provides a partitioning of the sequence $(\mu_\ell\zeta_\ell)_{\ell\in\mathbb{N}_0}$ into two disjoint subsequences $(\mu_{\ell'_k}\zeta_{\ell'_k})_{k\in\mathbb{N}_0}$ and $(\mu_{\ell''_k}\zeta_{\ell''_k})_{k\in\mathbb{N}_0}$. Without loss of generality (as the following arguments will show), we can assume that both subsequences are countably infinite.

Step 2. In this step, we show the estimator convergence $\mu_{\ell'_k}\to0$ along the iteration sequence $(\ell'_k)_{k\in\mathbb{N}_0}$, where the primal estimator is employed for marking, i.e.,

$$\theta\mu^2_{\ell'_k}\le\sum_{\nu\in\mathfrak{P}_{\ell'_k}}\sum_{\xi\in\mathcal{M}'_{\ell'_k\nu}}\mu_{\ell'_k}(\nu,\xi)^2+\sum_{\nu\in\mathfrak{M}'_{\ell'_k}}\mu_{\ell'_k}(\nu)^2.$$

To this end, the sequence $(\ell'_k)_{k\in\mathbb{N}_0}$ is further partitioned into two disjoint subsequences $(\ell'^+_k)_{k\in\mathbb{N}_0}$ and $(\ell'^-_k)_{k\in\mathbb{N}_0}$, where

- $\displaystyle\sum_{\nu\in\mathfrak{P}_{\ell'^+_k}}\sum_{\xi\in\mathcal{M}'_{\ell'^+_k\nu}}\mu_{\ell'^+_k}(\nu,\xi)^2\ge\frac12\Bigg(\sum_{\nu\in\mathfrak{P}_{\ell'^+_k}}\sum_{\xi\in\mathcal{M}'_{\ell'^+_k\nu}}\mu_{\ell'^+_k}(\nu,\xi)^2+\sum_{\nu\in\mathfrak{M}'_{\ell'^+_k}}\mu_{\ell'^+_k}(\nu)^2\Bigg)$,
- $\displaystyle\sum_{\nu\in\mathfrak{P}_{\ell'^-_k}}\sum_{\xi\in\mathcal{M}'_{\ell'^-_k\nu}}\mu_{\ell'^-_k}(\nu,\xi)^2<\frac12\Bigg(\sum_{\nu\in\mathfrak{P}_{\ell'^-_k}}\sum_{\xi\in\mathcal{M}'_{\ell'^-_k\nu}}\mu_{\ell'^-_k}(\nu,\xi)^2+\sum_{\nu\in\mathfrak{M}'_{\ell'^-_k}}\mu_{\ell'^-_k}(\nu)^2\Bigg)$,

respectively. Again, without loss of generality (as the following arguments will show), we assume that also these two subsequences are countably infinite.

Step 2a. Along the sequence $(\ell_k'^+)_{k\in\mathbb{N}_0}$, by definition, it follows that

$$\theta \sum_{\nu\in\mathfrak{P}_{\ell_k'^+}} \sum_{\xi\in\mathcal{N}^+_{\ell_k'^+\nu}} \mu_{\ell_k'^+}(\nu,\xi)^2 \le \theta\mu^2_{\ell_k'^+} \le 2 \sum_{\nu\in\mathfrak{P}_{\ell_k'^+}} \sum_{\xi\in\mathcal{M}'_{\ell_k'^+\nu}} \mu_{\ell_k'^+}(\nu,\xi)^2,$$

i.e., there holds the Dörfler marking criterion (43) for spatial discretizations with $\vartheta = \theta/2$. Therefore, Proposition 14 proves that

$$\sum_{\nu\in\mathfrak{P}_{\ell_k'^+}} \sum_{\xi\in\mathcal{N}^+_{\ell_k'^+\nu}} \mu_{\ell_k'^+}(\nu,\xi)^2 \xrightarrow{k\to\infty} 0$$

and hence also $\mu^2_{\ell_k'^+} \to 0$ as $k\to\infty$.

Step 2b. Along the sequence $(\ell_k'^-)_{k\in\mathbb{N}_0}$, by definition, it follows that

$$\sum_{\nu\in\mathfrak{M}'_{\ell_k'^-}} \mu_{\ell_k'^-}(\nu)^2 > \frac{1}{2}\bigg(\sum_{\nu\in\mathfrak{P}_{\ell_k'^-}} \sum_{\xi\in\mathcal{M}'_{\ell_k'^-\nu}} \mu_{\ell_k'^-}(\nu,\xi)^2 + \sum_{\nu\in\mathfrak{M}'_{\ell_k'^-}} \mu_{\ell_k'^-}(\nu)^2 \bigg)$$

and hence

$$\theta \sum_{\nu\in\mathfrak{Q}_{\ell_k'^-}} \mu_{\ell_k'^-}(\nu)^2 \le \theta\mu^2_{\ell_k'^-} < 2 \sum_{\nu\in\mathfrak{M}'_{\ell_k'^-}} \mu_{\ell_k'^-}(\nu)^2,$$

i.e., there holds the Dörfler marking criterion (39) for the parametric discretization with $\vartheta = \theta/2$. Therefore, Proposition 11 implies that

$$\sum_{\nu\in\mathfrak{Q}_{\ell_k'^-}} \mu_{\ell_k'^-}(\nu)^2 \xrightarrow{k\to\infty} 0$$

and hence also $\mu^2_{\ell_k'^-} \to 0$ as $k\to\infty$.

Step 2c. From the preceding Steps 2a–2b, we prove that the sequence $(\mu_{\ell_k'})_{k\in\mathbb{N}_0}$ can be partitioned into two subsequences $(\mu_{\ell_k'^+})_{k\in\mathbb{N}_0}$ and $(\mu_{\ell_k'^-})_{k\in\mathbb{N}_0}$, which both converge to zero. According to basic calculus, this implies that $\mu_{\ell_k'} \to 0$ as $k\to\infty$.

Step 3. Note that the dual error estimator is uniformly bounded, as

$$\zeta_\ell \overset{(23)}{\lesssim} |\!|\!| \widehat{\boldsymbol{z}}_\ell - \boldsymbol{z}_\ell |\!|\!| \overset{(17)}{\le} |\!|\!| \boldsymbol{z} - \boldsymbol{z}_\ell |\!|\!| \overset{(15)}{\le} |\!|\!| \boldsymbol{z} |\!|\!| \quad \text{for all } \ell\in\mathbb{N}_0.$$

Consequently, it follows from Step 2 that

$$\mu_{\ell_k'}\zeta_{\ell_k'} \xrightarrow{k\to\infty} 0. \tag{49}$$

Step 4. Note that the roles of the primal and the dual estimators in all the preceding arguments in Steps 2–3 can be reversed. Hence, it follows that

$$\mu_{\ell_k''}\zeta_{\ell_k''} \xrightarrow{k\to\infty} 0, \tag{50}$$

where we recall that the dual estimator is employed for marking along the iteration sequence $(\ell_k'')_{k\in\mathbb{N}_0}$.

Step 5. Overall, we obtain that the sequence $(\mu_\ell \zeta_\ell)_{\ell \in \mathbb{N}_0}$ can be partitioned into two subsequences $(\mu_{\ell'_k} \zeta_{\ell'_k})_{k \in \mathbb{N}_0}$ and $(\mu_{\ell''_k} \zeta_{\ell''_k})_{k \in \mathbb{N}_0}$, which both converge to zero. According to basic calculus, this implies that $\mu_\ell \zeta_\ell \to 0$ as $\ell \to \infty$. □

Remark 15. *Note that standard adaptive SGFEM formally corresponds to the case, where the iteration sequence (ℓ''_k) in the proof of Theorem 8 is void. Therefore, the proof of Theorem 8 also establishes plain convergence of the adaptive multilevel SGFEM algorithm from* [BPR21b] *for* Marking criterion A *(separate Dörfler marking for spatial and parametric estimator parts, as employed in the present proof) as well as* Marking criterion C *(combined Dörfler marking as used in Algorithm 6). Moreover, arguing as in* [BPRR19a]*, plain convergence for* Marking criterion B *(separate Dörfler marking for spatial and parametric estimator parts based on the error reduction property) can also be proved. Since our focus in the present paper is on* Marking criterion C *that enables the proof of optimal convergence rates (see* [BPR21a] *for adaptive SGFEM or the subsequent sections of the present paper for goal-oriented adaptive SGFEM), we leave the details of the proof for* Marking criteria A and B *to the reader.*

4.4. Linear convergence for 2D. Theorem 8 proves plain convergence $\mu_\ell \zeta_\ell \to 0$ as $\ell \to \infty$. While such a convergence could in principle be arbitrarily slow, the following theorem proves geometric decay (51) for $d = 2$.

Theorem 16. *Let $d = 2$. Suppose the saturation assumption* (22) *for the primal solution $\boldsymbol{w} = \boldsymbol{u}$ to* (8) *and for the dual solution $\boldsymbol{w} = \boldsymbol{z}$ to* (26)*. Then, for any choice of the marking parameter $0 < \theta \le 1$ and with $0 < q_{\mathrm{lin}} := 1 - \frac{\theta(1-q_{\mathrm{sat}}^2)}{C_{\mathrm{est}}^4}$, Algorithm 6 yields that*

$$\| \boldsymbol{u} - \boldsymbol{u}_{\ell+1} \| \, \| \boldsymbol{z} - \boldsymbol{z}_{\ell+1} \| \le q_{\mathrm{lin}} \, \| \boldsymbol{u} - \boldsymbol{u}_\ell \| \, \| \boldsymbol{z} - \boldsymbol{z}_\ell \| \quad \text{for all } \ell \in \mathbb{N}_0. \tag{51}$$

Proof. The proof is split into two steps, where Step 1 is already accomplished in [BPR21a, Proposition 5.1], but included here for the convenience of the reader (to highlight how the restriction $d = 2$ comes into play).

Step 1. Let $\boldsymbol{w} \in \{\boldsymbol{u}, \boldsymbol{z}\}$. With the sets $\mathfrak{M}_\ell$ and $\mathcal{M}_{\ell\nu}$ for all $\nu \in \mathfrak{P}_\ell$ from Algorithm 6, suppose that

$$\theta \, \tau_\ell(\boldsymbol{w})^2 \le \sum_{\nu \in \mathfrak{P}_\ell} \sum_{\xi \in \mathcal{M}_{\ell\nu}} \tau_\ell(\boldsymbol{w}|\nu, \xi)^2 + \sum_{\nu \in \mathfrak{M}_\ell} \tau_\ell(\boldsymbol{w}|\nu)^2. \tag{52}$$

Employing estimate (25) (that has only been proved for $d = 2$), it follows that

$$\begin{aligned} \| \boldsymbol{w} - \boldsymbol{w}_\ell \|^2 &\overset{(24)}{\le} \frac{C_{\mathrm{est}}^2}{1 - q_{\mathrm{sat}}^2} \, \tau_\ell(\boldsymbol{w})^2 \le \frac{C_{\mathrm{est}}^2}{\theta(1 - q_{\mathrm{sat}}^2)} \left(\sum_{\nu \in \mathfrak{P}_\ell} \sum_{\xi \in \mathcal{M}_{\ell\nu}} \tau_\ell(\boldsymbol{w}|\nu, \xi)^2 + \sum_{\nu \in \mathfrak{M}_\ell} \tau_\ell(\boldsymbol{w}|\nu)^2 \right) \\ &\le \frac{C_{\mathrm{est}}^2}{\theta(1 - q_{\mathrm{sat}}^2)} \left(\sum_{\nu \in \mathfrak{P}_\ell} \sum_{\xi \in \mathcal{N}_{\ell\nu}^+ \cap \mathcal{N}_{\ell+1,\nu}} \tau_\ell(\boldsymbol{w}|\nu, \xi)^2 + \sum_{\nu \in \mathfrak{Q}_\ell \cap \mathfrak{P}_{\ell+1}} \tau_\ell(\boldsymbol{w}|\nu)^2 \right) \\ &\overset{(25)}{\le} \frac{C_{\mathrm{est}}^4}{\theta(1 - q_{\mathrm{sat}}^2)} \| \boldsymbol{w}_{\ell+1} - \boldsymbol{w}_\ell \|^2. \end{aligned}$$

With $0 < q_{\mathrm{lin}}^2 = 1 - \frac{\theta(1-q_{\mathrm{sat}}^2)}{C_{\mathrm{est}}^4} < 1$, the Galerkin orthogonality (14) yields

$$\| \boldsymbol{w} - \boldsymbol{w}_{\ell+1} \|^2 = \| \boldsymbol{w} - \boldsymbol{w}_\ell \|^2 - \| \boldsymbol{w}_{\ell+1} - \boldsymbol{w}_\ell \|^2 \le q_{\mathrm{lin}}^2 \, \| \boldsymbol{w} - \boldsymbol{w}_\ell \|^2. \tag{53}$$

Step 2. By nestedness of the discrete spaces $\mathbb{V}_\ell \subseteq \mathbb{V}_{\ell+1}$ and the Céa lemma (15), there holds

$$\| \boldsymbol{u} - \boldsymbol{u}_{\ell+1} \| \le \| \boldsymbol{u} - \boldsymbol{u}_\ell \| \quad \text{and} \quad \| \boldsymbol{z} - \boldsymbol{z}_{\ell+1} \| \le \| \boldsymbol{z} - \boldsymbol{z}_\ell \|.$$

According to Algorithm 6, the Dörfler marking criterion (52) holds at least for $\boldsymbol{w} = \boldsymbol{u}$ or for $\boldsymbol{w} = \boldsymbol{z}$ so that Step 1 yields

$$\| \boldsymbol{u} - \boldsymbol{u}_{\ell+1} \| \le q_{\mathrm{lin}} \| \boldsymbol{u} - \boldsymbol{u}_\ell \| \quad \text{or} \quad \| \boldsymbol{z} - \boldsymbol{z}_{\ell+1} \| \le q_{\mathrm{lin}} \| \boldsymbol{z} - \boldsymbol{z}_\ell \|.$$

In either case, this establishes linear contraction (51) for the product of energy errors. This concludes the proof. □

Remark 17. *The marking strategy from Remark 7*(ii) *leads to linear contraction* (51) *with* q_{lin} *replaced by* q_{lin}^2*; see the proof of* [BET11, (2.12)–(2.13)] *in a deterministic setting. For the marking strategy from Remark 7*(i)*, one empirically observes a similar decay; see the numerical experiments in* [FPv16] *for deterministic problems.* □

4.5. Optimal convergence rates for 2D. While linear convergence of the adaptive algorithm is proved for $d = 2$ under the above saturation assumption (22), the proof of optimal convergence rates requires a stronger property. The so-called *strong saturation assumption* has been introduced in [PRS20] in the context of adaptive boundary element methods, and the following formulation in the SGFEM setting was adopted in [BPR21a]: for $\boldsymbol{w} \in \{\boldsymbol{u}, \boldsymbol{z}\}$, there exist constants $0 < \kappa_{\mathrm{sat}} \le q_{\mathrm{sat}} < 1$ such that for all multilevel structures $\mathbb{P}_\bullet \in \mathbb{REFINE}(\mathbb{P}_0)$ and $\mathbb{P}_\star \in \mathbb{REFINE}(\mathbb{P}_\bullet)$, one step of multilevel refinement $\mathbb{P}_\circ := \mathbb{REFINE}(\mathbb{P}_\bullet, \mathbb{M}_\bullet)$ with $\mathbb{M}_\bullet := [\mathfrak{P}_\star \cap \mathfrak{Q}_\bullet, (\mathcal{N}_{\bullet\nu}^+ \cap \mathcal{N}_{\star\nu})_{\nu\in\mathfrak{P}_\bullet}]$ satisfies the implication

$$\| \boldsymbol{w} - \boldsymbol{w}_\star \| \le \kappa_{\mathrm{sat}} \| \boldsymbol{w} - \boldsymbol{w}_\bullet \| \quad \Longrightarrow \quad \| \boldsymbol{w} - \boldsymbol{w}_\circ \| \le q_{\mathrm{sat}} \| \boldsymbol{w} - \boldsymbol{w}_\bullet \|. \tag{54}$$

In other words, if using the refined multilevel structure $\mathbb{P}_\star \in \mathbb{REFINE}(\mathbb{P}_\bullet)$ results in a sufficient improvement of the error, then even one step of multilevel refinement of $\mathbb{P}_\bullet$ towards $\mathbb{P}_\star$ provides a uniform improvement of the error.

Remark 18. *It has been shown in* [BPR21a, Remark 4.2] *that the strong saturation assumption* (54) *is indeed stronger than the saturation assumption* (22)*. Furthermore, in the same way as it was pointed out in Remark 4 for the saturation assumption* (22)*, we emphasize that the proof of our main result in Theorem 19 will only exploit the strong saturation assumption for the sequence of nested discrete subspaces generated by Algorithm 6.*

Let $\mathbb{P}_\bullet = [\mathfrak{P}_\bullet, (\mathcal{T}_{\bullet\nu})_{\nu\in\mathfrak{I}}]$ be a multilevel structure, and let $\mathbb{V}_\bullet$ be the associated multilevel approximation space. Observe that

$$\dim \mathbb{V}_\bullet = \sum_{\nu\in\mathfrak{P}_\bullet} \dim \mathcal{S}_0^1(\mathcal{T}_{\bullet\nu}) \simeq \sum_{\nu\in\mathfrak{P}_\bullet} \#\mathcal{T}_{\bullet\nu} \simeq \sum_{\nu\in\mathfrak{P}_\bullet} \big[\#\mathcal{T}_{\bullet\nu} - \#\mathcal{T}_0 + 1\big] =: \#\mathbb{P}_\bullet, \tag{55}$$

where equivalence constants depend only on $\#\mathcal{T}_0$ (here, we assume that $\mathcal{T}_0$ has at least one interior vertex). Indeed, the equivalence in (55) motivates the definition of $\#\mathbb{P}_\bullet$.

To formulate optimal convergence rates, we introduce the following notion of approximability for $\boldsymbol{w} \in \{\boldsymbol{u}, \boldsymbol{z}\}$:

$$\|\boldsymbol{w}\|_{\mathbb{A}_s} := \sup_{N\in\mathbb{N}_0} (N+1)^s \min_{\substack{\mathbb{P}_{\mathrm{opt}}\in\mathbb{REFINE}(\mathbb{P}_0) \\ \#\mathbb{P}_{\mathrm{opt}} - \#\mathbb{P}_0 \le N}} \min_{\boldsymbol{v}_{\mathrm{opt}}\in\mathbb{V}_{\mathrm{opt}}} \| \boldsymbol{w} - \boldsymbol{v}_{\mathrm{opt}} \| \in \mathbb{R}_{\ge 0} \cup \{\infty\}. \tag{56}$$

In explicit terms, there holds $\|\boldsymbol{w}\|_{\mathbb{A}_s} < \infty$ if and only if there exists a sequence of multilevel structures $(\mathbb{P}_\ell^\star)_{\ell\in\mathbb{N}_0}$ with $\mathbb{P}_0^\star = \mathbb{P}_0$ (which does not necessitate the nestedness of the associated multilevel spaces $\mathbb{V}_\ell^\star$) such that the corresponding approximation errors $|\!|\!| \boldsymbol{w} - \boldsymbol{w}_\ell^\star |\!|\!| = \min_{\boldsymbol{v}_\ell\in\mathbb{V}_\ell^\star} |\!|\!| \boldsymbol{w} - \boldsymbol{v}_\ell |\!|\!|$ decay at least with an algebraic rate $s > 0$ with respect to $\#\mathbb{P}_\ell^\star$ (or, equivalently, with respect to the dimensions of $\mathbb{V}_\ell^\star$; cf (55)).

Theorem 19. *Let $d = 2$. Suppose the strong saturation assumption* (54) *for the primal solution $\boldsymbol{w} = \boldsymbol{u}$ to* (8) *as well as the dual solution $\boldsymbol{w} = \boldsymbol{z}$ to* (26)*. Then, there exists a constant $0 < \theta_{\mathrm{opt}} < 1$ depending only on q_{sat} and the constant C_{est} from Theorem 2 such that the following holds provided that $0 < \theta \le \theta_{\mathrm{opt}}$: If $s, t > 0$ with $\|\boldsymbol{u}\|_{\mathbb{A}_s} + \|\boldsymbol{z}\|_{\mathbb{A}_t} < \infty$, then*

$$\sup_{\ell\in\mathbb{N}_0} (\#\mathbb{P}_\ell - \#\mathbb{P}_0 + 1)^{s+t} |\!|\!| \boldsymbol{u} - \boldsymbol{u}_\ell |\!|\!| |\!|\!| \boldsymbol{z} - \boldsymbol{z}_\ell |\!|\!| \le C_{\mathrm{opt}} \|\boldsymbol{u}\|_{\mathbb{A}_s} \|\boldsymbol{z}\|_{\mathbb{A}_t}, \tag{57}$$

where $\boldsymbol{u}_\ell$, $\boldsymbol{z}_\ell$ ($\ell \in \mathbb{N}_0$) are generated by Algorithm 6, $C_{\mathrm{opt}} \ge 1$ depends only on s, t, $\mathcal{T}_0$, κ_{sat}, and q_{lin}.

The proof of Theorem 19 relies on two technical results for multilevel structures (Lemmas 20 and 21 below) as well as on the comparison lemma (Lemma 22). The latter result allows one to compare the multilevel structures $(\mathbb{P}_\ell)_{\ell\in\mathbb{N}_0}$ generated by Algorithm 6 with the corresponding optimal multilevel structures provided by the definition of the approximation classes $\mathbb{A}_s$ and $\mathbb{A}_t$ for $\boldsymbol{u}$ and $\boldsymbol{z}$, respectively; see (56).

Lemma 20 (overlay estimate; [BPR21a, Lemma 6.1])**.** *For any two multilevel structures $\mathbb{P}_\bullet, \mathbb{P}_\star \in \mathbb{REFINE}(\mathbb{P}_0)$, there exists a unique multilevel structure $\mathbb{P}_\bullet \oplus \mathbb{P}_\star \in \mathbb{REFINE}(\mathbb{P}_\bullet) \cap \mathbb{REFINE}(\mathbb{P}_\star) \subseteq \mathbb{REFINE}(\mathbb{P}_0)$, the so-called overlay, satisfying*

$$\#(\mathbb{P}_\bullet \oplus \mathbb{P}_\star) = \min\big\{\#\mathbb{P}_\circ : \mathbb{P}_\circ \in \mathbb{REFINE}(\mathbb{P}_\bullet) \cap \mathbb{REFINE}(\mathbb{P}_\star)\big\} \le \#\mathbb{P}_\bullet + \#\mathbb{P}_\star - \#\mathbb{P}_0. \tag{58}$$

Lemma 21 (closure estimate; [BPR21a, Lemma 6.2])**.** *Suppose that $(\mathbb{P}_\ell)_{\ell\in\mathbb{N}_0}$ is a sequence of successively refined multilevel structures, i.e., $\mathbb{P}_{\ell+1} = \mathbb{REFINE}(\mathbb{P}_\ell, \mathbb{M}_\ell)$ with $\mathbb{M}_\ell = [\mathfrak{M}_\ell, (\mathcal{M}_{\ell\nu})_{\nu\in\mathfrak{P}_\ell}]$ for all $\ell \in \mathbb{N}_0$. Then, there exists a constant $C_{\mathrm{cls}} \ge 1$ depending only on $\mathcal{T}_0$ such that*

$$\#\mathbb{P}_\ell - \#\mathbb{P}_0 \le C_{\mathrm{cls}} \sum_{k=0}^{\ell-1} \Big(\#\mathfrak{M}_k + \sum_{\nu\in\mathfrak{P}_k} \#\mathcal{M}_{k\nu} \Big) \quad \text{for all } \ell \in \mathbb{N}_0. \tag{59}$$

The following lemma generalizes [BPR21a, Lemma 6.3] from adaptive SGFEM to goal-oriented adaptive SGFEM.

Lemma 22 (comparison lemma)**.** *Let $d = 2$. Suppose the strong saturation assumption* (54) *for the primal solution $\boldsymbol{w} = \boldsymbol{u}$ to* (8) *as well as the dual solution $\boldsymbol{w} = \boldsymbol{z}$ to* (26)*. Then, with $0 < \theta_{\mathrm{opt}} := \frac{1-q_{\mathrm{sat}}^2}{C_{\mathrm{est}}^4} < 1$, there holds the following statement: Let $s, t > 0$ and $\|\boldsymbol{u}\|_{\mathbb{A}_s} + \|\boldsymbol{z}\|_{\mathbb{A}_t} < \infty$; then, for all $\mathbb{P}_\bullet \in \mathbb{REFINE}(\mathbb{P}_0)$, there exist $\mathfrak{R}_\bullet \subseteq \mathfrak{Q}_\bullet$ and $\mathcal{R}_{\bullet\nu} \subseteq \mathcal{N}_{\bullet\nu}^+$ for all $\nu \in \mathfrak{P}_\bullet$ such that*

$$\#\mathfrak{R}_\bullet + \sum_{\nu\in\mathfrak{P}_\bullet} \#\mathcal{R}_{\bullet\nu} \le 6 \big[\kappa_{\mathrm{sat}}^{-2} \|\boldsymbol{u}\|_{\mathbb{A}_s} \|\boldsymbol{z}\|_{\mathbb{A}_t}\big]^{1/(s+t)} \big[|\!|\!| \boldsymbol{u} - \boldsymbol{u}_\bullet |\!|\!| |\!|\!| \boldsymbol{z} - \boldsymbol{z}_\bullet |\!|\!|\big]^{-1/(s+t)} \tag{60}$$

as well as

$$\begin{aligned} &\theta_{\mathrm{opt}}\,\mu_\bullet^2 \le \sum_{\nu\in\mathfrak{P}_\bullet}\sum_{\xi\in\mathcal{R}_{\bullet\nu}} \mu_\bullet(\nu,\xi)^2 + \sum_{\nu\in\mathfrak{R}_\bullet}\mu_\bullet(\nu)^2 \\ &\textit{or}\qquad \theta_{\mathrm{opt}}\,\zeta_\bullet^2 \le \sum_{\nu\in\mathfrak{P}_\bullet}\sum_{\xi\in\mathcal{R}_{\bullet\nu}} \zeta_\bullet(\nu,\xi)^2 + \sum_{\nu\in\mathfrak{R}_\bullet}\zeta_\bullet(\nu)^2. \end{aligned} \tag{61}$$

Proof. If $\|\!|\, \boldsymbol{u}-\boldsymbol{u}_\bullet \,|\!\| = 0$ or $\|\!|\, \boldsymbol{z}-\boldsymbol{z}_\bullet \,|\!\| = 0$, we may simply choose $\mathfrak{R}_\bullet = \mathfrak{Q}_\bullet$ and $\mathcal{R}_{\bullet\nu} = \mathcal{N}_{\bullet\nu}^+$ for all $\nu \in \mathfrak{P}_\bullet$ so that (60)–(61) are trivially satisfied. Hence, we may suppose that $\|\!|\, \boldsymbol{u}-\boldsymbol{u}_\bullet \,|\!\| > 0$ and $\|\!|\, \boldsymbol{z}-\boldsymbol{z}_\bullet \,|\!\| > 0$.

Step 1. With $0 < \kappa_{\mathrm{sat}} < 1$ from the strong saturation assumption (54), define

$$0 < \varepsilon := \kappa_{\mathrm{sat}}^2 \|\!|\, \boldsymbol{u}-\boldsymbol{u}_\bullet \,|\!\| \|\!|\, \boldsymbol{z}-\boldsymbol{z}_\bullet \,|\!\| \overset{(15)}{<} \|\!|\, \boldsymbol{u}-\boldsymbol{u}_0 \,|\!\| \|\!|\, \boldsymbol{z}-\boldsymbol{z}_0 \,|\!\| \overset{(56)}{\le} \|\boldsymbol{u}\|_{\mathbb{A}_s}\|\boldsymbol{z}\|_{\mathbb{A}_t} < \infty. \tag{62}$$

Hence, by construction, there holds $\|\boldsymbol{u}\|_{\mathbb{A}_s}\|\boldsymbol{z}\|_{\mathbb{A}_t}\varepsilon^{-1} > 1$. Choose $N \in \mathbb{N}$ such that

$$1 \le N < \big[\|\boldsymbol{u}\|_{\mathbb{A}_s}\|\boldsymbol{z}\|_{\mathbb{A}_t}\big]^{1/(s+t)}\varepsilon^{-1/(s+t)} \le N+1. \tag{63}$$

Choose $\mathbb{P}_\varepsilon', \mathbb{P}_\varepsilon'' \in \texttt{REFINE}(\mathbb{P}_0)$ such that

$$\begin{aligned} &\#\mathbb{P}_\varepsilon' - \#\mathbb{P}_0 \le N \quad\text{and}\quad \|\!|\, \boldsymbol{u}-\boldsymbol{u}_\varepsilon' \,|\!\| = \min_{\substack{\mathbb{P}_{\mathrm{opt}}\in\texttt{REFINE}(\mathbb{P}_0)\\ \#\mathbb{P}_{\mathrm{opt}}-\#\mathbb{P}_0\le N}} \|\!|\, \boldsymbol{u}-\boldsymbol{u}_{\mathrm{opt}} \,|\!\|, \\ &\#\mathbb{P}_\varepsilon'' - \#\mathbb{P}_0 \le N \quad\text{and}\quad \|\!|\, \boldsymbol{z}-\boldsymbol{z}_\varepsilon'' \,|\!\| = \min_{\substack{\mathbb{P}_{\mathrm{opt}}\in\texttt{REFINE}(\mathbb{P}_0)\\ \#\mathbb{P}_{\mathrm{opt}}-\#\mathbb{P}_0\le N}} \|\!|\, \boldsymbol{z}-\boldsymbol{z}_{\mathrm{opt}} \,|\!\|. \end{aligned} \tag{64}$$

Define the overlays $\mathbb{P}_\varepsilon = \mathbb{P}_\varepsilon' \oplus \mathbb{P}_\varepsilon''$ and $\mathbb{P}_\star := \mathbb{P}_\varepsilon \oplus \mathbb{P}_\bullet$. Then, it follows that

$$\begin{aligned} \#\mathbb{P}_\star - \#\mathbb{P}_\bullet &\overset{(58)}{\le} \#\mathbb{P}_\varepsilon - \#\mathbb{P}_0 \overset{(58)}{\le} \#\mathbb{P}_\varepsilon' + \#\mathbb{P}_\varepsilon'' - 2\#\mathbb{P}_0 \overset{(64)}{\le} 2N \\ &\overset{(63)}{<} 2\big[\|\boldsymbol{u}\|_{\mathbb{A}_s}\|\boldsymbol{z}\|_{\mathbb{A}_t}\big]^{1/(s+t)}\varepsilon^{-1/(s+t)} \\ &\overset{(62)}{=} 2\kappa_{\mathrm{sat}}^{-2/(s+t)}\big[\|\boldsymbol{u}\|_{\mathbb{A}_s}\|\boldsymbol{z}\|_{\mathbb{A}_t}\big]^{1/(s+t)}\big[\|\!|\, \boldsymbol{u}-\boldsymbol{u}_\bullet \,|\!\| \|\!|\, \boldsymbol{z}-\boldsymbol{z}_\bullet \,|\!\|\big]^{-1/(s+t)} \end{aligned} \tag{65}$$

as well as

$$\begin{aligned} \|\!|\, \boldsymbol{u}-\boldsymbol{u}_\star \,|\!\| \|\!|\, \boldsymbol{z}-\boldsymbol{z}_\star \,|\!\| &\overset{(15)}{\le} \|\!|\, \boldsymbol{u}-\boldsymbol{u}_\varepsilon' \,|\!\| \|\!|\, \boldsymbol{z}-\boldsymbol{z}_\varepsilon'' \,|\!\| \overset{(64),(56)}{\le} (N+1)^{-(s+t)}\,\|\boldsymbol{u}\|_{\mathbb{A}_s}\|\boldsymbol{z}\|_{\mathbb{A}_t} \\ &\overset{(63)}{\le} \varepsilon \overset{(62)}{=} \kappa_{\mathrm{sat}}^2 \|\!|\, \boldsymbol{u}-\boldsymbol{u}_\bullet \,|\!\| \|\!|\, \boldsymbol{z}-\boldsymbol{z}_\bullet \,|\!\|. \end{aligned}$$

The latter implies that at least

$$\|\!|\, \boldsymbol{u}-\boldsymbol{u}_\star \,|\!\| \le \kappa_{\mathrm{sat}} \|\!|\, \boldsymbol{u}-\boldsymbol{u}_\bullet \,|\!\| \quad\text{or}\quad \|\!|\, \boldsymbol{z}-\boldsymbol{z}_\star \,|\!\| \le \kappa_{\mathrm{sat}} \|\!|\, \boldsymbol{z}-\boldsymbol{z}_\bullet \,|\!\|.$$

Therefore, defining $\mathbb{P}_\circ := \texttt{REFINE}(\mathbb{P}_\bullet, \mathbb{M}_\bullet)$ with $\mathbb{M}_\bullet := [\mathfrak{P}_\star \cap \mathfrak{Q}_\bullet, (\mathcal{N}_{\bullet\nu}^+ \cap \mathcal{N}_{\star\nu})_{\nu\in\mathfrak{P}_\bullet}]$, we obtain from the strong saturation assumption (54) that at least

$$\|\!|\, \boldsymbol{u}-\boldsymbol{u}_\circ \,|\!\| \le q_{\mathrm{sat}} \|\!|\, \boldsymbol{u}-\boldsymbol{u}_\bullet \,|\!\| \quad\text{or}\quad \|\!|\, \boldsymbol{z}-\boldsymbol{z}_\circ \,|\!\| \le q_{\mathrm{sat}} \|\!|\, \boldsymbol{z}-\boldsymbol{z}_\bullet \,|\!\|.$$

Step 2. Let $\boldsymbol{w} \in \{\boldsymbol{u}, \boldsymbol{z}\}$ with $|||\, \boldsymbol{w} - \boldsymbol{w}_\circ \,||| \le q_{\mathrm{sat}} \,|||\, \boldsymbol{w} - \boldsymbol{w}_\bullet \,|||$. Then, we find that

$$\begin{aligned}\frac{1-q_{\mathrm{sat}}^2}{C_{\mathrm{est}}^2}\,\tau_\bullet(\boldsymbol{w})^2 &\overset{(24)}{\le} (1-q_{\mathrm{sat}}^2)\,|||\, \boldsymbol{w} - \boldsymbol{w}_\bullet \,|||^2 \le |||\, \boldsymbol{w} - \boldsymbol{w}_\bullet \,|||^2 - |||\, \boldsymbol{w} - \boldsymbol{w}_\circ \,|||^2 = |||\, \boldsymbol{w}_\circ - \boldsymbol{w}_\bullet \,|||^2 \\ &\overset{(25)}{\le} C_{\mathrm{est}}^2 \Bigg(\sum_{\nu\in\mathfrak{P}_\bullet} \sum_{\xi\in\mathcal{N}_{\bullet\nu}^+\cap\mathcal{N}_{\circ\nu}} \tau_\bullet(\boldsymbol{w}|\nu,\xi)^2 + \sum_{\nu\in\mathfrak{Q}_\bullet\cap\mathfrak{P}_\circ} \tau_\bullet(\boldsymbol{w}|\nu)^2 \Bigg),\end{aligned}$$

where the final estimate is only proved for $d = 2$. Define $\mathfrak{R}_\bullet := \mathfrak{Q}_\bullet \cap \mathfrak{P}_\star$ and $\mathcal{R}_{\bullet\nu} := \mathcal{N}_{\bullet\nu}^+ \cap \mathcal{N}_{\star\nu}$ for all $\nu \in \mathfrak{P}_\bullet$. We have proved in [BPR21a, Proof of Lemma 6.3] that the above estimate yields

$$\theta_{\mathrm{opt}}\,\tau_\bullet(\boldsymbol{w})^2 \le \sum_{\nu\in\mathfrak{P}_\bullet} \sum_{\xi\in\mathcal{R}_{\bullet\nu}} \tau_\bullet(\boldsymbol{w}|\nu,\xi)^2 + \sum_{\nu\in\mathfrak{R}_\bullet} \tau_\bullet(\boldsymbol{w}|\nu)^2 \quad \text{with} \quad 0 < \theta_{\mathrm{opt}} = \frac{1-q_{\mathrm{sat}}^2}{C_{\mathrm{est}}^4} < 1 \tag{66}$$

and

$$\#\mathfrak{R}_\bullet + \sum_{\nu\in\mathfrak{P}_\bullet} \#\mathcal{R}_{\bullet\nu} \le 3\,(\#\mathbb{P}_\star - \#\mathbb{P}_\bullet). \tag{67}$$

The estimate in (66) gives (61), and the combination of (65) and (67) proves (60). This concludes the proof. □

We are now ready to prove the rate optimality property for Algorithm 6.

Proof of Theorem 19. Let $k \in \mathbb{N}_0$. Recall that according to Algorithm 6, by virtue of Lemma 22, and since $0 < \theta \le \theta_{\mathrm{opt}}$, the tuples $\mathbb{M}_k = [\mathfrak{M}_k, (\mathcal{M}_{k\nu})_{\nu\in\mathfrak{I}}]$ and $\mathbb{R}_k = [\mathfrak{R}_k, (\mathcal{R}_{k\nu})_{\nu\in\mathfrak{I}}]$ satisfy the Dörfler marking criterion either in step (iv) or in step (v) of Algorithm 6, where we define $\mathcal{M}_{k\nu} = \emptyset = \mathcal{R}_{k\nu}$ if $\nu \notin \mathfrak{P}_k$. Moreover, according to the minimal cardinality property of $\mathbb{M}_k$, it follows that

$$\begin{aligned}\#\mathfrak{M}_k + \sum_{\nu\in\mathfrak{P}_k} \#\mathcal{M}_{k\nu} \;&\le\; \#\mathfrak{R}_k + \sum_{\nu\in\mathfrak{P}_k} \#\mathcal{R}_{k\nu} \\ &\overset{(60)}{\lesssim} \big[\|\boldsymbol{u}\|_{\mathbb{A}_s}\|\boldsymbol{z}\|_{\mathbb{A}_t}\big]^{1/(s+t)} \big[|||\, \boldsymbol{u} - \boldsymbol{u}_k \,|||\,|||\, \boldsymbol{z} - \boldsymbol{z}_k \,|||\big]^{-1/(s+t)} \quad \text{for all } k \in \mathbb{N}_0.\end{aligned}$$

For any $\ell \in \mathbb{N}_0$, linear convergence (51) proves that

$$|||\, \boldsymbol{u} - \boldsymbol{u}_\ell \,|||\,|||\, \boldsymbol{z} - \boldsymbol{z}_\ell \,||| \le q_{\mathrm{lin}}^{\ell-k}\,|||\, \boldsymbol{u} - \boldsymbol{u}_k \,|||\,|||\, \boldsymbol{z} - \boldsymbol{z}_k \,||| \quad \text{for all } 0 \le k < \ell.$$

Hence, the convergence of the geometric series proves that

$$\begin{aligned}\#\mathbb{P}_\ell - \#\mathbb{P}_0 &\overset{(59)}{\lesssim} \sum_{k=0}^{\ell-1} \Bigg(\#\mathfrak{M}_k + \sum_{\nu\in\mathfrak{P}_k} \#\mathcal{M}_{k\nu}\Bigg) \\ &\lesssim \big[\|\boldsymbol{u}\|_{\mathbb{A}_s}\|\boldsymbol{z}\|_{\mathbb{A}_t}\big]^{1/(s+t)} \sum_{k=0}^{\ell-1} \big[|||\, \boldsymbol{u} - \boldsymbol{u}_k \,|||\,|||\, \boldsymbol{z} - \boldsymbol{z}_k \,|||\big]^{-1/(s+t)} \\ &\lesssim \big[\|\boldsymbol{u}\|_{\mathbb{A}_s}\|\boldsymbol{z}\|_{\mathbb{A}_t}\big]^{1/(s+t)} \big[|||\, \boldsymbol{u} - \boldsymbol{u}_\ell \,|||\,|||\, \boldsymbol{z} - \boldsymbol{z}_\ell \,|||\big]^{-1/(s+t)} \quad \text{for all } \ell \in \mathbb{N}_0.\end{aligned}$$

For $\ell \ge 1$, it follows that

$$\begin{aligned}(\#\mathbb{P}_\ell - \#\mathbb{P}_0 + 1)^{s+t}\,|||\, \boldsymbol{u} - \boldsymbol{u}_\ell \,|||\,|||\, \boldsymbol{z} - \boldsymbol{z}_\ell \,||| &\le 2^{s+t}\,(\#\mathbb{P}_\ell - \#\mathbb{P}_0)^{s+t}\,|||\, \boldsymbol{u} - \boldsymbol{u}_\ell \,|||\,|||\, \boldsymbol{z} - \boldsymbol{z}_\ell \,||| \\ &\lesssim \|\boldsymbol{u}\|_{\mathbb{A}_s}\|\boldsymbol{z}\|_{\mathbb{A}_t}.\end{aligned}$$

For $\ell = 0$, there holds

$$(\#\mathbb{P}_\ell - \#\mathbb{P}_0 + 1)^{s+t} \,|\!|\!|\, \boldsymbol{u} - \boldsymbol{u}_\ell \,|\!|\!|\, |\!|\!|\, \boldsymbol{z} - \boldsymbol{z}_\ell \,|\!|\!|\, = |\!|\!|\, \boldsymbol{u} - \boldsymbol{u}_0 \,|\!|\!|\, |\!|\!|\, \boldsymbol{z} - \boldsymbol{z}_0 \,|\!|\!|\, \le \|\boldsymbol{u}\|_{\mathbb{A}_s} \|\boldsymbol{z}\|_{\mathbb{A}_t}.$$

Combining the last two estimates, we prove (57). This concludes the proof. □

5. Goal-oriented adaptive SGFEM with nonlinear goal functional

In this section, we aim to extend the setting, the algorithm, and the analysis of section 4 to a larger class of (possibly nonlinear) goal functionals $\boldsymbol{g}\colon \mathbb{V} \to \mathbb{R}$.

5.1. Dual problem and goal-oriented error estimate. Let the goal functional $\boldsymbol{g}\colon \mathbb{V} \to \mathbb{R}$ be in C^1, in the sense that it is Gâteaux differentiable and its Gâteaux derivative $\boldsymbol{g}'\colon \mathbb{V} \to \mathbb{V}^*$ is continuous. Following the approach adopted for the case of a linear goal functional, we aim to formulate a dual problem which allows to derive a goal-oriented error estimate (cf. (26) and (28), respectively).

The fundamental theorem of calculus proves that

$$\boldsymbol{g}(\boldsymbol{u}) - \boldsymbol{g}(\boldsymbol{u}_\bullet) = \int_0^1 \langle \boldsymbol{g}'(\boldsymbol{u}_\bullet + t\,(\boldsymbol{u} - \boldsymbol{u}_\bullet))\,,\, \boldsymbol{u} - \boldsymbol{u}_\bullet\rangle_{D\times\Gamma}\,\mathrm{d}t =: \langle \boldsymbol{g}^\star_{\boldsymbol{u}}(\boldsymbol{u}_\bullet)\,,\, \boldsymbol{u} - \boldsymbol{u}_\bullet\rangle_{D\times\Gamma}. \quad (68)$$

This identity suggests to consider a dual problem with right-hand side given by $\boldsymbol{g}^\star_{\boldsymbol{u}}(\boldsymbol{u}_\bullet) \in \mathbb{V}^\star$ (cf. the derivation of the error estimate in (28) for a linear goal functional). However, $\boldsymbol{g}^\star_{\boldsymbol{u}}(\boldsymbol{u}_\bullet)$ depends also on the unknown solution $\boldsymbol{u}$ and thus cannot be used to formulate a practical dual problem. Observing that formally $\|\boldsymbol{g}^\star_{\boldsymbol{u}}(\boldsymbol{u}_\bullet) - \boldsymbol{g}'(\boldsymbol{u}_\bullet)\|_{\mathbb{V}^\star} \to 0$ as $\boldsymbol{u}_\bullet \to \boldsymbol{u}$, for a given $\boldsymbol{w} \in \mathbb{V}$ (in what follows, $\boldsymbol{w} \in \{\boldsymbol{u}, \boldsymbol{u}_\bullet\}$), we consider the following (practical, if $\boldsymbol{w}$ is known) dual problem: Find $\boldsymbol{z}[\boldsymbol{w}] \in \mathbb{V}$ such that

$$B(\boldsymbol{v}, \boldsymbol{z}[\boldsymbol{w}]) = \langle \boldsymbol{g}'(\boldsymbol{w})\,,\, \boldsymbol{v}\rangle_{D\times\Gamma} \quad \text{for all } \boldsymbol{v} \in \mathbb{V}. \quad (69)$$

Later, we will approximate $\boldsymbol{z}[\boldsymbol{w}] \in \mathbb{V}$ by its Galerkin projection $\boldsymbol{z}_\bullet[\boldsymbol{w}] \in \mathbb{V}_\bullet$, i.e.,

$$B(\boldsymbol{v}_\bullet, \boldsymbol{z}_\bullet[\boldsymbol{w}]) = \langle \boldsymbol{g}'(\boldsymbol{w})\,,\, \boldsymbol{v}_\bullet\rangle_{D\times\Gamma} \quad \text{for all } \boldsymbol{v}_\bullet \in \mathbb{V}_\bullet. \quad (70)$$

Existence and uniqueness of both $\boldsymbol{z}[\boldsymbol{w}] \in \mathbb{V}$ and $\boldsymbol{z}_\bullet[\boldsymbol{w}] \in \mathbb{V}_\bullet$ follow from the Riesz theorem. Note that

$$\begin{aligned}
\boldsymbol{g}(\boldsymbol{u}) - \boldsymbol{g}(\boldsymbol{u}_\bullet) &\overset{(68)}{=} \langle \boldsymbol{g}^\star_{\boldsymbol{u}}(\boldsymbol{u}_\bullet) - \boldsymbol{g}'(\boldsymbol{u}_\bullet)\,,\, \boldsymbol{u} - \boldsymbol{u}_\bullet\rangle_{D\times\Gamma} + \langle \boldsymbol{g}'(\boldsymbol{u}_\bullet)\,,\, \boldsymbol{u} - \boldsymbol{u}_\bullet\rangle_{D\times\Gamma} \\
&\overset{(69)}{=} \langle \boldsymbol{g}^\star_{\boldsymbol{u}}(\boldsymbol{u}_\bullet) - \boldsymbol{g}'(\boldsymbol{u}_\bullet)\,,\, \boldsymbol{u} - \boldsymbol{u}_\bullet\rangle_{D\times\Gamma} + B(\boldsymbol{u} - \boldsymbol{u}_\bullet, \boldsymbol{z}[\boldsymbol{u}_\bullet]) \\
&\overset{(14)}{=} \langle \boldsymbol{g}^\star_{\boldsymbol{u}}(\boldsymbol{u}_\bullet) - \boldsymbol{g}'(\boldsymbol{u}_\bullet)\,,\, \boldsymbol{u} - \boldsymbol{u}_\bullet\rangle_{D\times\Gamma} + B(\boldsymbol{u} - \boldsymbol{u}_\bullet, \boldsymbol{z}[\boldsymbol{u}_\bullet] - \boldsymbol{z}_\bullet[\boldsymbol{u}_\bullet]).
\end{aligned}$$

We suppose that there exists $C_{\mathrm{goal}} \ge 0$ such that

$$|\langle \boldsymbol{g}'(\boldsymbol{v}) - \boldsymbol{g}'(\boldsymbol{w})\,,\, \boldsymbol{z}\rangle_{D\times\Gamma}| \le C_{\mathrm{goal}} \,|\!|\!|\, \boldsymbol{v} - \boldsymbol{w} \,|\!|\!|\, |\!|\!|\, \boldsymbol{z} \,|\!|\!|\, \quad \text{for all } \boldsymbol{v}, \boldsymbol{w}, \boldsymbol{z} \in \mathbb{V}. \quad (71)$$

This leads to

$$\begin{aligned}
\langle \boldsymbol{g}^\star_{\boldsymbol{u}}(\boldsymbol{u}_\bullet) - \boldsymbol{g}'(\boldsymbol{u}_\bullet)\,,\, \boldsymbol{u} - \boldsymbol{u}_\bullet\rangle_{D\times\Gamma} &\overset{(68)}{=} \int_0^1 \langle [\boldsymbol{g}'(\boldsymbol{u}_\bullet + t(\boldsymbol{u} - \boldsymbol{u}_\bullet)) - \boldsymbol{g}'(\boldsymbol{u}_\bullet)]\,,\, \boldsymbol{u} - \boldsymbol{u}_\bullet\rangle_{D\times\Gamma}\,\mathrm{d}t \\
&\overset{(71)}{\le} C_{\mathrm{goal}} \int_0^1 t \,|\!|\!|\, \boldsymbol{u} - \boldsymbol{u}_\bullet \,|\!|\!|\,^2\,\mathrm{d}t = \frac{1}{2}\, C_{\mathrm{goal}} \,|\!|\!|\, \boldsymbol{u} - \boldsymbol{u}_\bullet \,|\!|\!|\,^2.
\end{aligned}$$

In particular, we derive the following estimate of the error in the nonlinear goal functional:

$$|\boldsymbol{g}(\boldsymbol{u}) - \boldsymbol{g}(\boldsymbol{u}_\bullet)| \leq |\!|\!| \boldsymbol{u} - \boldsymbol{u}_\bullet |\!|\!| \, |\!|\!| \boldsymbol{z}[\boldsymbol{u}_\bullet] - \boldsymbol{z}_\bullet[\boldsymbol{u}_\bullet] |\!|\!| + \frac{1}{2} C_{\mathrm{goal}} |\!|\!| \boldsymbol{u} - \boldsymbol{u}_\bullet |\!|\!|^2. \tag{72}$$

Remark 23. *The key assumption* (71)*, and hence the error estimate* (72)*, is valid at least for linear and quadratic goal functionals. First, for a bounded linear goal functional* $\boldsymbol{g} \in \mathbb{V}^*$*, one has* $\langle \boldsymbol{g}'(\boldsymbol{v}) \, , \, \boldsymbol{z} \rangle_{D\times\Gamma} = \langle \boldsymbol{g} \, , \, \boldsymbol{z} \rangle_{D\times\Gamma}$ *for all* $\boldsymbol{v}, \boldsymbol{z} \in \mathbb{V}$*, and, hence,* (71) *is satisfied with* $C_{\mathrm{goal}} = 0$ *(in particular, in this case,* (72) *reduces to* (28)*). Second, consider the quadratic goal functional* $\boldsymbol{g}(\boldsymbol{u}) = b(\boldsymbol{u}, \boldsymbol{u})$*, where* $b\colon \mathbb{V} \times \mathbb{V} \to \mathbb{R}$ *is a continuous bilinear form. Then,* $\langle \boldsymbol{g}'(\boldsymbol{v}) \, , \, \boldsymbol{z} \rangle_{D\times\Gamma} = b(\boldsymbol{v}, \boldsymbol{z}) + b(\boldsymbol{z}, \boldsymbol{v})$*, and it follows that*

$$\langle \boldsymbol{g}'(\boldsymbol{v}) - \boldsymbol{g}'(\boldsymbol{w}) \, , \, \boldsymbol{z} \rangle_{D\times\Gamma} = b(\boldsymbol{v} - \boldsymbol{w}, \boldsymbol{z}) + b(\boldsymbol{z}, \boldsymbol{v} - \boldsymbol{w}) \quad \forall \, \boldsymbol{v}, \boldsymbol{w}, \boldsymbol{z} \in \mathbb{V}.$$

Hence, (71) *is satisfied and* $C_{\mathrm{goal}} > 0$ *depends only on the continuity constant for* $b(\cdot, \cdot)$*.*

The following lemma will later turn out to be a crucial argument.

Lemma 24. *For any* $\boldsymbol{w} \in \mathbb{V}$*, there holds*

$$|\!|\!| \boldsymbol{z}_\bullet[\boldsymbol{w}] - \boldsymbol{z}_\bullet[\boldsymbol{u}_\bullet] |\!|\!| \leq |\!|\!| \boldsymbol{z}[\boldsymbol{w}] - \boldsymbol{z}[\boldsymbol{u}_\bullet] |\!|\!| \leq C_{\mathrm{goal}} |\!|\!| \boldsymbol{w} - \boldsymbol{u}_\bullet |\!|\!|. \tag{73}$$

Proof. First, it follows from (69)–(70) that

$$\begin{aligned}
|\!|\!| \boldsymbol{z}_\bullet[\boldsymbol{w}] - \boldsymbol{z}_\bullet[\boldsymbol{u}_\bullet] |\!|\!|^2 &= B(\boldsymbol{z}_\bullet[\boldsymbol{w}] - \boldsymbol{z}_\bullet[\boldsymbol{u}_\bullet], \boldsymbol{z}_\bullet[\boldsymbol{w}]) - B(\boldsymbol{z}_\bullet[\boldsymbol{w}] - \boldsymbol{z}_\bullet[\boldsymbol{u}_\bullet], \boldsymbol{z}_\bullet[\boldsymbol{u}_\bullet]) \\
&= B(\boldsymbol{z}_\bullet[\boldsymbol{w}] - \boldsymbol{z}_\bullet[\boldsymbol{u}_\bullet], \boldsymbol{z}[\boldsymbol{w}]) - B(\boldsymbol{z}_\bullet[\boldsymbol{w}] - \boldsymbol{z}_\bullet[\boldsymbol{u}_\bullet], \boldsymbol{z}[\boldsymbol{u}_\bullet]) \\
&= B(\boldsymbol{z}_\bullet[\boldsymbol{w}] - \boldsymbol{z}_\bullet[\boldsymbol{u}_\bullet], \boldsymbol{z}[\boldsymbol{w}] - \boldsymbol{z}[\boldsymbol{u}_\bullet]) \leq |\!|\!| \boldsymbol{z}_\bullet[\boldsymbol{w}] - \boldsymbol{z}_\bullet[\boldsymbol{u}_\bullet] |\!|\!| \, |\!|\!| \boldsymbol{z}[\boldsymbol{w}] - \boldsymbol{z}[\boldsymbol{u}_\bullet] |\!|\!|,
\end{aligned}$$

which proves the first estimate. The second estimate follows from (69) and (71), namely

$$\begin{aligned}
|\!|\!| \boldsymbol{z}[\boldsymbol{w}] - \boldsymbol{z}[\boldsymbol{u}_\bullet] |\!|\!|^2 &= B(\boldsymbol{z}[\boldsymbol{w}] - \boldsymbol{z}[\boldsymbol{u}_\bullet], \boldsymbol{z}[\boldsymbol{w}]) - B(\boldsymbol{z}[\boldsymbol{w}] - \boldsymbol{z}[\boldsymbol{u}_\bullet], \boldsymbol{z}[\boldsymbol{u}_\bullet]) \\
&\overset{(69)}{=} \langle \boldsymbol{g}'(\boldsymbol{w}) \, , \, \boldsymbol{z}[\boldsymbol{w}] - \boldsymbol{z}[\boldsymbol{u}_\bullet] \rangle_{D\times\Gamma} - \langle \boldsymbol{g}'(\boldsymbol{u}_\bullet) \, , \, \boldsymbol{z}[\boldsymbol{w}] - \boldsymbol{z}[\boldsymbol{u}_\bullet] \rangle_{D\times\Gamma} \\
&= \langle \boldsymbol{g}'(\boldsymbol{w}) - \boldsymbol{g}'(\boldsymbol{u}_\bullet) \, , \, \boldsymbol{z}[\boldsymbol{w}] - \boldsymbol{z}[\boldsymbol{u}_\bullet] \rangle_{D\times\Gamma} \overset{(71)}{\leq} C_{\mathrm{goal}} |\!|\!| \boldsymbol{w} - \boldsymbol{u}_\bullet |\!|\!| \, |\!|\!| \boldsymbol{z}[\boldsymbol{w}] - \boldsymbol{z}[\boldsymbol{u}_\bullet] |\!|\!|.
\end{aligned}$$

This concludes the proof. □

As done in section 4, to estimate the energy errors appearing on the right-hand side of (72), we consider the error estimation strategy introduced in subsection 3.5. In the remainder of this section, unless otherwise specified, we use the abbreviated notation

$$\mu_\bullet := \tau_\bullet(\boldsymbol{u}) \quad \text{and} \quad \zeta_\bullet := \tau_\bullet(\boldsymbol{z}[\boldsymbol{u}_\bullet]). \tag{74}$$

The same notation is used for the local contributions, e.g., $\mu_\bullet(\nu) := \tau_\bullet(\boldsymbol{u}|\nu)$ or $\zeta_\bullet(\nu, \xi) := \tau_\bullet(\boldsymbol{z}[\boldsymbol{u}_\bullet]|\nu, \xi)$. We stress that indeed both estimators in (74) are computable.

Combining the error estimate (72) with the results of Theorem 2 and Lemma 24, we obtain a reliable a *posteriori* error estimator of the error in the nonlinear goal functional. We stress that the constant C_{rel} in the following estimate (75) depends only on the saturation assumption (22) for $\boldsymbol{w} = \boldsymbol{u}$ and $\boldsymbol{w} = \boldsymbol{z}[\boldsymbol{u}]$, while any dependence on $\boldsymbol{z}[\boldsymbol{u}_\bullet]$ as used in the definition of $\zeta_\bullet$ is avoided.

Proposition 25. *Let $d \in \{2,3\}$. Suppose the saturation assumption* (22) *for both the primal solution $\boldsymbol{w} = \boldsymbol{u}$ to* (8) *and the (theoretical) dual solution $\boldsymbol{w} = \boldsymbol{z}[\boldsymbol{u}]$. Then, there holds the a posteriori goal-oriented error estimate*

$$|\boldsymbol{g}(\boldsymbol{u}) - \boldsymbol{g}(\boldsymbol{u}_\bullet)| \le C_{\mathrm{rel}}\, \mu_\bullet \big[\mu_\bullet^2 + \zeta_\bullet^2\big]^{1/2}, \tag{75}$$

where $C_{\mathrm{rel}} > 0$ depends only on the constants $C_{\mathrm{goal}} \ge 0$ in (71)*, $C_{\mathrm{est}} \ge 1$ in* (23)*, and $0 < q_{\mathrm{sat}} < 1$ in* (22)*.*

Proof. Under the saturation assumption (22) for $\boldsymbol{w} = \boldsymbol{u}$, Theorem 2 proves that

$$\|\!| \boldsymbol{u} - \boldsymbol{u}_\bullet |\!\| \le \frac{C_{\mathrm{est}}}{(1-q_{\mathrm{sat}}^2)^{1/2}}\, \mu_\bullet. \tag{76}$$

Under the saturation assumption (22) for $\boldsymbol{w} = \boldsymbol{z}[\boldsymbol{u}]$, Theorem 2 proves that

$$\begin{aligned}
\|\!| \boldsymbol{z}[\boldsymbol{u}_\bullet] - \boldsymbol{z}_\bullet[\boldsymbol{u}_\bullet] |\!\| &\le \|\!| \boldsymbol{z}[\boldsymbol{u}] - \boldsymbol{z}[\boldsymbol{u}_\bullet] |\!\| + \|\!| \boldsymbol{z}[\boldsymbol{u}] - \boldsymbol{z}_\bullet[\boldsymbol{u}] |\!\| + \|\!| \boldsymbol{z}_\bullet[\boldsymbol{u}] - \boldsymbol{z}_\bullet[\boldsymbol{u}_\bullet] |\!\| \\
&\overset{(73)}{\le} 2C_{\mathrm{goal}} \|\!| \boldsymbol{u} - \boldsymbol{u}_\bullet |\!\| + \|\!| \boldsymbol{z}[\boldsymbol{u}] - \boldsymbol{z}_\bullet[\boldsymbol{u}] |\!\| \\
&\overset{(24)}{\le} 2C_{\mathrm{goal}} \|\!| \boldsymbol{u} - \boldsymbol{u}_\bullet |\!\| + \frac{C_{\mathrm{est}}}{(1-q_{\mathrm{sat}}^2)^{1/2}}\, \tau_\bullet(\boldsymbol{z}[\boldsymbol{u}]).
\end{aligned}$$

Note that the *a posteriori* error estimate has a seminorm structure and hence

$$\begin{aligned}
|\tau_\bullet(\boldsymbol{z}[\boldsymbol{u}]) - \zeta_\bullet| \le \tau_\bullet(\boldsymbol{z}[\boldsymbol{u}] - \boldsymbol{z}[\boldsymbol{u}_\bullet]) &\overset{(23)}{\le} C_{\mathrm{est}} \|\!| (\widehat{\boldsymbol{z}}_\bullet[\boldsymbol{u}] - \widehat{\boldsymbol{z}}_\bullet[\boldsymbol{u}_\bullet]) - (\boldsymbol{z}_\bullet[\boldsymbol{u}] - \boldsymbol{z}_\bullet[\boldsymbol{u}_\bullet]) |\!\| \\
&\le C_{\mathrm{est}} \big(\|\!| \widehat{\boldsymbol{z}}_\bullet[\boldsymbol{u}] - \widehat{\boldsymbol{z}}_\bullet[\boldsymbol{u}_\bullet] |\!\| + \|\!| \boldsymbol{z}_\bullet[\boldsymbol{u}] - \boldsymbol{z}_\bullet[\boldsymbol{u}_\bullet] |\!\| \big) \overset{(73)}{\le} 2C_{\mathrm{est}} C_{\mathrm{goal}} \|\!| \boldsymbol{u} - \boldsymbol{u}_\bullet |\!\|.
\end{aligned}$$

Combining the last two estimates, we derive that

$$\begin{aligned}
\|\!| \boldsymbol{z}[\boldsymbol{u}_\bullet] - \boldsymbol{z}_\bullet[\boldsymbol{u}_\bullet] |\!\| &\le 2C_{\mathrm{goal}} \Big(1 + \frac{C_{\mathrm{est}}^2}{(1-q_{\mathrm{sat}}^2)^{1/2}}\Big) \|\!| \boldsymbol{u} - \boldsymbol{u}_\bullet |\!\| + \frac{C_{\mathrm{est}}}{(1-q_{\mathrm{sat}}^2)^{1/2}}\, \zeta_\bullet \\
&\overset{(76)}{\le} \frac{C_{\mathrm{est}}}{(1-q_{\mathrm{sat}}^2)^{1/2}} \left[2C_{\mathrm{goal}} \Big(1 + \frac{C_{\mathrm{est}}^2}{(1-q_{\mathrm{sat}}^2)^{1/2}}\Big) \mu_\bullet + \zeta_\bullet \right].
\end{aligned} \tag{77}$$

Overall, we thus see that

$$\begin{aligned}
|\boldsymbol{g}(\boldsymbol{u}) - \boldsymbol{g}(\boldsymbol{u}_\bullet)| &\overset{(72)}{\le} \|\!| \boldsymbol{u} - \boldsymbol{u}_\bullet |\!\| \|\!| \boldsymbol{z}[\boldsymbol{u}_\bullet] - \boldsymbol{z}_\bullet[\boldsymbol{u}_\bullet] |\!\| + \frac{3}{2} C_{\mathrm{goal}} \|\!| \boldsymbol{u} - \boldsymbol{u}_\bullet |\!\|^2 \\
&\lesssim \mu_\bullet \big[\mu_\bullet + \zeta_\bullet\big] + \mu_\bullet^2 \simeq \mu_\bullet \big[\mu_\bullet^2 + \zeta_\bullet^2\big]^{1/2}.
\end{aligned}$$

This concludes the proof of (75). □

5.2. Adaptive algorithm. In view of the *a posteriori* error estimate (75), the adaptive algorithm must ensure that either the primal estimator μ_ℓ or the combined primal-dual estimator $(\mu_\ell^2 + \zeta_\ell^2)^{1/2}$ tends to zero as $\ell \to \infty$. To this end, we employ Algorithm 6, but replace the marking criterion (33) in step (v) by

$$\theta \big[\mu_\ell^2 + \zeta_\ell^2\big] \le \sum_{\nu \in \mathfrak{P}_\ell} \sum_{\xi \in \mathcal{M}_{\ell\nu}''} \big[\mu_\ell(\nu,\xi)^2 + \zeta_\ell(\nu,\xi)^2\big] + \sum_{\nu \in \mathfrak{M}_\ell''} \big[\mu_\ell(\nu)^2 + \zeta_\ell(\nu)^2\big]. \tag{78}$$

We also note that, while the computation of the discrete primal and dual solutions in step (i) of Algorithm 6 can be carried out in parallel in the case of a linear goal functional

$\boldsymbol{g} \in \mathbb{V}^*$ (problems (18) and (27) are independent of each other), in the nonlinear case they must be performed sequentially (first the primal problem, then the dual problem), because the right-hand side of the discrete dual problem, i.e., (70) with $\boldsymbol{w} = \boldsymbol{u}_\bullet$, depends on the discrete primal solution.

5.3. Plain convergence. The following theorem is the analogue to Theorem 8 and proves plain convergence of the modified adaptive algorithm for goal-oriented adaptive SGFEM with nonlinear goal functionals.

Theorem 26. *Let $d \in \{2, 3\}$. For any choice of the marking parameter $0 < \theta \le 1$, Algorithm 6 with the modified marking criterion* (78) *in step* (v) *yields a convergent sequence of estimator products, i.e.,*

$$\mu_\ell \big[\mu_\ell^2 + \zeta_\ell^2\big]^{1/2} \xrightarrow{\ell\to\infty} 0. \tag{79}$$

Under the saturation assumption (22) *for both the primal solution $\boldsymbol{w} = \boldsymbol{u}$ and the (theoretical) dual solution $\boldsymbol{w} = \boldsymbol{z}[\boldsymbol{u}]$, there holds convergence of the error in the goal functional*

$$|\boldsymbol{g}(\boldsymbol{u}) - \boldsymbol{g}(\boldsymbol{u}_\ell)| \le C_{\rm rel}\, \mu_\ell \big[\mu_\ell^2 + \zeta_\ell^2\big]^{1/2} \xrightarrow{\ell\to\infty} 0. \tag{80}$$

Remark 27. *We stress that, while Theorem 26 requires the saturation assumption* (22) *for $\boldsymbol{w} \in \{\boldsymbol{u}, \boldsymbol{z}[\boldsymbol{u}]\}$, the modified Algorithm 6 (employing the marking criterion* (78)*) evaluates the error estimate* (21) *for $\boldsymbol{w} \in \{\boldsymbol{u}, \boldsymbol{z}[\boldsymbol{u}_\bullet]\}$ (since $\boldsymbol{z}_\bullet[\boldsymbol{u}_\bullet] \in \mathbb{V}_\bullet$ is computable, while $\boldsymbol{z}_\bullet[\boldsymbol{u}] \in \mathbb{V}_\bullet$ depends on the unknown $\boldsymbol{u}$ and thus is not computable).*

Sketch of proof of Theorem 26. We follow the lines of the proof of Theorem 8, where we must now consider the estimators $\mu_\ell = \tau_\ell(\boldsymbol{u})$ and $\rho_\ell = \big[\tau_\ell(\boldsymbol{u})^2 + \tau_\ell(\boldsymbol{z}[\boldsymbol{u}_\ell])^2\big]^{1/2}$. Consequently, we must show that Proposition 11 and Proposition 14 remain valid for the combined primal-dual error estimator ρ_ℓ.

We first note the *a priori* convergence results $|||\, \boldsymbol{u}_\infty - \boldsymbol{u}_\ell \,||| \to 0$ and $|||\, \boldsymbol{z}_\infty[\boldsymbol{u}_\infty] - \boldsymbol{z}_\ell[\boldsymbol{u}_\infty] \,||| + |||\, \boldsymbol{z}_\ell[\boldsymbol{u}_\infty] - \boldsymbol{z}_\ell[\boldsymbol{u}_\ell] \,||| \to 0$ as $\ell \to \infty$, where the limiting functions $\boldsymbol{u}_\infty, \boldsymbol{z}_\infty[\boldsymbol{u}_\infty] \in \mathbb{V}$ are provided by Lemma 9.

Inspecting the proof of Proposition 11, we see that Proposition 11 remains valid with $\tau_\ell(\boldsymbol{w}|\nu)^2$ being replaced by $\rho_\ell(\nu)^2 = \tau_\ell(\boldsymbol{u}|\nu)^2 + \tau_\ell(\boldsymbol{z}[\boldsymbol{u}_\ell]|\nu)^2$.

Inspecting the proof of Proposition 14, we see that only Step 3 of the proof must be checked. To verify the analogue of (44), let $k \in \mathbb{N}_0$ and note that

$$\sum_{T\in\mathcal{T}_{\ell\nu}^{\rm good}} \sum_{\xi\in\mathcal{N}_{\ell\nu}^+\cap T} \big[\tau_\ell(\boldsymbol{u}|\nu,\xi)^2 + \tau_\ell(\boldsymbol{z}[\boldsymbol{u}_k]|\nu,\xi)^2\big] \lesssim |||\, \boldsymbol{u}_\infty - \boldsymbol{u}_\ell \,|||^2 + |||\, \boldsymbol{z}_\infty[\boldsymbol{u}_k] - \boldsymbol{z}_\ell[\boldsymbol{u}_k] \,|||^2$$

For $k = \ell$, the triangle inequality and Lemma 24 prove that

$$\begin{aligned} |||\, \boldsymbol{z}_\infty[\boldsymbol{u}_\ell] - \boldsymbol{z}_\ell[\boldsymbol{u}_\ell] \,||| &\le |||\, \boldsymbol{z}_\infty[\boldsymbol{u}_\ell] - \boldsymbol{z}_\infty[\boldsymbol{u}_\infty] \,||| + |||\, \boldsymbol{z}_\infty[\boldsymbol{u}_\infty] - \boldsymbol{z}_\ell[\boldsymbol{u}_\infty] \,||| + |||\, \boldsymbol{z}_\ell[\boldsymbol{u}_\infty] - \boldsymbol{z}_\ell[\boldsymbol{u}_\ell] \,||| \\ &\lesssim |||\, \boldsymbol{u}_\infty - \boldsymbol{u}_\ell \,||| + |||\, \boldsymbol{z}_\infty[\boldsymbol{u}_\infty] - \boldsymbol{z}_\ell[\boldsymbol{u}_\infty] \,||| \xrightarrow{\ell\to\infty} 0. \end{aligned}$$

Hence, we are led to

$$\sum_{T\in\mathcal{T}_{\ell\nu}^{\rm good}} \sum_{\xi\in\mathcal{N}_{\ell\nu}^+\cap T} \rho_\ell(\nu,\xi)^2 \xrightarrow{\ell\to\infty} 0. \tag{44$'$}$$

Similar observations verify the analogue of (45). Indeed,

$$\sum_{T\in\mathcal{T}_{\ell\nu}^{\mathrm{neither}}}\sum_{\xi\in\mathcal{N}_{\ell\nu}^{+}\cap T}\big[\tau_\ell(\boldsymbol{u}|\nu,\xi)^2+\tau_\ell(\boldsymbol{z}[\boldsymbol{u}_\ell]|\nu,\xi)^2\big]\lesssim |\!|\!|\,\boldsymbol{u}-\boldsymbol{u}_\ell\,|\!|\!|^2_{D_{\ell\nu}^{\mathrm{neither}}}+|\!|\!|\,\boldsymbol{z}[\boldsymbol{u}_\ell]-\boldsymbol{z}_\ell[\boldsymbol{u}_\ell]\,|\!|\!|^2_{D_{\ell\nu}^{\mathrm{neither}}}.$$

Since $|\!|\!|\,\boldsymbol{z}[\boldsymbol{u}_\ell]-\boldsymbol{z}_\ell[\boldsymbol{u}_\ell]\,|\!|\!| \to |\!|\!|\,\boldsymbol{z}[\boldsymbol{u}_\infty]-\boldsymbol{z}_\infty[\boldsymbol{u}_\infty]\,|\!|\!|$ and $|D_{\ell\nu}^{\mathrm{neither}}|\to 0$ as $\ell\to\infty$, we derive that

$$\sum_{T\in\mathcal{T}_{\ell\nu}^{\mathrm{neither}}}\sum_{\xi\in\mathcal{N}_{\ell\nu}^{+}\cap T}\rho_\ell(\nu,\xi)^2\xrightarrow{\ell\to\infty}0. \tag{45$'$}$$

Arguing as above, we then see that also Proposition 14 remains valid with $\rho_\ell=\tau_\ell(\boldsymbol{u})+\tau_\ell(\boldsymbol{z}[\boldsymbol{u}_\ell])$ replacing $\tau_\ell(\boldsymbol{w})$.

Altogether, we can follow the lines of the proof of Theorem 8 to verify that

$$\mu_\ell\big[\mu_\ell^2+\zeta_\ell^2\big]^{1/2}=\mu_\ell\rho_\ell\xrightarrow{\ell\to\infty}0.$$

This concludes the proof. □

6. Numerical results

In this section, to illustrate the performance of Algorithm 6 (including its modification for the case of nonlinear goal functionals as discussed in section 5.2) and to underpin our theoretical findings, we present a collection of numerical experiments in 2D. All computations have been performed using the MATLAB toolbox Stochastic T-IFISS [BRS20, BR22]. Throughout this section, we consider the parametric model problem (1) introduced in section 2 and assume that each parameter in $\mathbf{y}=(y_m)_{m\in\mathbb{N}}\in\Gamma$ is the image of a uniformly distributed independent mean-zero random variable, so that $\mathrm{d}\pi_m(y_m)=\mathrm{d}y_m/2$.

6.1. Linear goal functional. In our first experiment, we consider problem (1) posed on the L-shaped (physical) domain $D=(-1,1)^2\setminus(-1,0]^2$. The diffusion coefficient is given by (2) with $a_0=4$ and $a_m=4\,(99/199)^m\,\chi_C$ for all $m\in\mathbb{N}$, where $\chi_C: D\to\{0,1\}$ denotes the characteristic function of the disk $C\subset D$ of center $(1/2,1/2)$ and radius $1/4$. The inequalities in (3)–(4) are satisfied with $a_0^{\min}=a_0^{\max}=4$ and $\tau=0.99$. The right-hand side function $\boldsymbol{f}$ in (1) is given by $\boldsymbol{f}=f_0+\nabla\cdot(f_1,f_2)$, where $f_0=1$, $f_1=\chi_S/4$, and $f_2=0$. Here, $\chi_S: D\to\{0,1\}$ denotes the characteristic function of the square $S=(-1,-1/2)\times(1/2,1)\subset D$. This choice leads to the expression

$$F(\boldsymbol{v})=\int_\Gamma\int_D\boldsymbol{v}(x,\mathbf{y})\,\mathrm{d}x\,\mathrm{d}\pi(\mathbf{y})-\frac{1}{4}\int_\Gamma\int_S\frac{\partial\boldsymbol{v}}{\partial x_1}(x,\mathbf{y})\,\mathrm{d}x\,\mathrm{d}\pi(\mathbf{y})\quad\text{for all }\boldsymbol{v}\in\mathbb{V} \tag{81}$$

for the linear form on the right-hand side of (8). A similar form is considered for the linear goal functional $\boldsymbol{g}\in\mathbb{V}^\star$, which is given by

$$\boldsymbol{g}(\boldsymbol{v})=\int_\Gamma\int_D\boldsymbol{v}(x,\mathbf{y})\,\mathrm{d}x\,\mathrm{d}\pi(\mathbf{y})-\frac{1}{4}\int_\Gamma\int_T\frac{\partial\boldsymbol{v}}{\partial x_1}(x,\mathbf{y})\,\mathrm{d}x\,\mathrm{d}\pi(\mathbf{y})\quad\text{for all }\boldsymbol{v}\in\mathbb{V}, \tag{82}$$

where $T\subset D$ denotes the triangle with vertices $(1,-1)$, $(1,-1/2)$, $(1/2,-1)$. The motivation behind these representations for $\boldsymbol{f}$ and $\boldsymbol{g}$ is to introduce different singularities in the solutions to the primal and dual problems. The physical domain D and the subdomains C, S, T involved in the definition of the problem data are depicted in Figure 1 (top-left).

We run Algorithm 6 with $\theta=0.5$ in (32)–(33) and compare its performance with Algorithm 4.2 in [BPRR19b]. The latter is based on the single-level SGFEM and employs

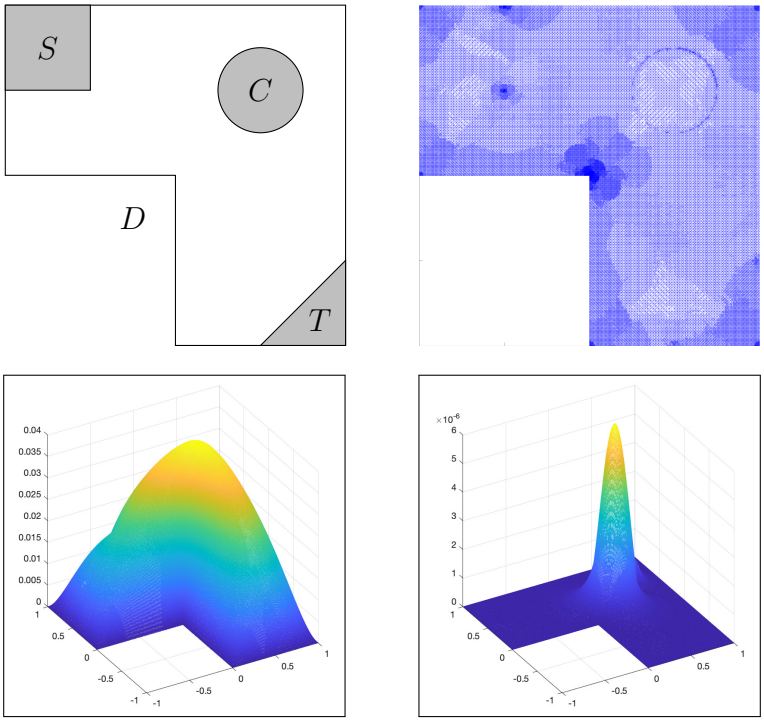

FIGURE 1. Experiment in section 6.1: computational domain (top-left); adaptively refined mesh $\mathcal{T}_{15,\mathbf{0}}$ associated with the the zero index at an intermediate step of Algorithm 6 (top-right); expectation (bottom-left) and variance (bottom-right) of the final multilevel SGFEM approximation to the primal solution.

a different marking criterion from the one in Algorithm 6. Specifically, at each iteration of the adaptive loop, Algorithm 4.2 in [BPRR19b] performs *separate* Dörfler marking of spatial and parametric error indicators (in the experiment below, we use the parameters $\theta_{\mathbb{X}} = \theta_{\mathfrak{P}} = 0.5$) and, depending on which component of the error estimate is larger, carries out either mesh refinement or parametric enrichment. In contrast, Algorithm 6 performs a *combined* Dörfler marking followed by simultaneous spatial and parametric enrichments at each iteration. For a comparison between separate and combined marking/enrichment strategies in the context of standard adaptivity for multilevel SGFEM, we refer to [BPR21b]. Note that performing a combined enrichment of spatial and parametric components of single-level SGFEM approximations is prohibitively expensive, due to the multiplicative increase of the dimension of the resulting approximation space.

For both algorithms, we start from the same initial discretization (based on the singleton $\mathfrak{P}_0 = \{\mathbf{0}\}$ as initial index set and a uniform initial mesh $\mathcal{T}_0$ made of 384 right-angled triangles) and we stop the computation when $\mu_\ell \zeta_\ell \leq \mathsf{tol} := 1 \cdot 10^{-6}$.

In Figure 1 (bottom), we show the plots of the expectation (bottom-left) and the variance (bottom-right) of the final multilevel SGFEM approximation to the primal solution. We omit the corresponding plots for the final approximation to the dual solution, as they look very similar. In Figure 1 (top-right), we show the adaptively refined mesh associated with the zero index at an intermediate step ($\ell = 15$) of Algorithm 6. We observe that this mesh captures the spatial features of both the primal and the dual solutions. Indeed, both solutions exhibit a geometric singularity at the reentrant corner, which is effectively

captured by the mesh. Moreover, the mesh clearly identifies the boundary of C, which is the support of the coefficients a_m in (2) ($m \in \mathbb{N}$) as well as the support of the variance; cf. Figure 1 (bottom-right). The primal solution exhibits a singularity along the line connecting the points $(-1/2, 1/2)$ and $(-1/2, 1)$ (i.e., the right vertical edge of S) due to the low regularity of the linear form in (81). The dual solution exhibits a singularity along the line connecting the points $(1/2, -1)$ and $(1, -1/2)$ (i.e., the longest edge of T) due to the low regularity of the goal functional in (82). Thanks to the marking criterion of Algorithm 6, these features are also captured by the mesh, which indeed is refined in the vicinity of the points $(-1/2, 1/2)$, $(-1/2, 1)$, $(1/2, -1)$, and $(1, -1/2)$.

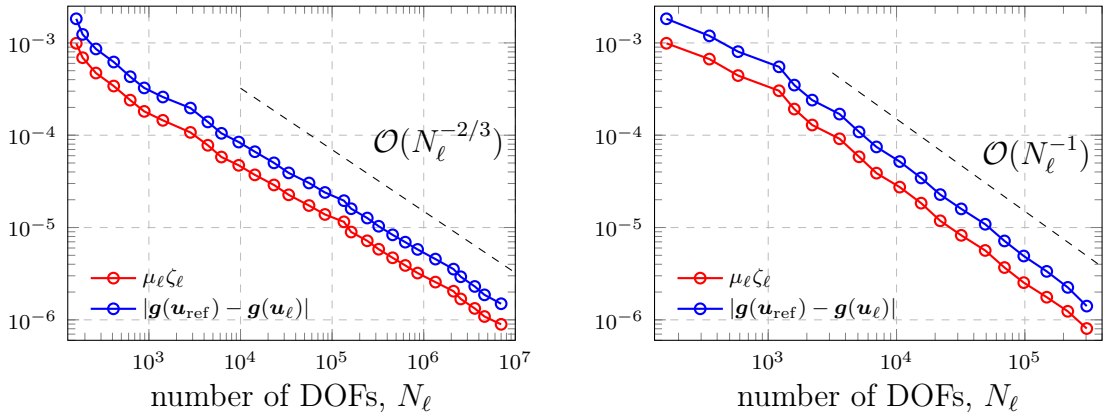

FIGURE 2. Experiment in section 6.1: decay of the error estimates $\mu_\ell \zeta_\ell$ and the reference errors $|g(u_{\mathrm{ref}}) - g(u_\ell)|$ at each iteration of the goal-oriented single-level (left) and multilevel (right) adaptive algorithms.

In Figure 2, we plot the error estimate $\mu_\ell \zeta_\ell$ and the reference error $|g(u_{\mathrm{ref}}) - g(u_\ell)|$ in the goal functional against the number of degrees of freedom (DOFs), $N_\ell := \dim \mathbb{V}_\ell$, at each iteration of the two goal-oriented adaptive algorithms. Here, u_{ref} denotes a reference solution computed by running Algorithm 6 to a lower tolerance ($\mathsf{tol}_{\mathrm{ref}} := 1 \cdot 10^{-7}$). The results of the single-level algorithm ([BPRR19b, Algorithm 4.2]) are displayed in the left plot, whereas those of the multilevel algorithm (Algorithm 6) are shown in the right plot.

It is clear from this figure that Algorithm 6 outperforms its single-level counterpart. Indeed, for the single-level algorithm, both the error estimates and the reference errors decay with the suboptimal rate $\mathcal{O}(N_\ell^{-2/3})$, whereas for the multilevel algorithm we observe the rate $\mathcal{O}(N_\ell^{-1})$. For Algorithm 6 this is in agreement with our theoretical result in Theorem 19, since $\mathcal{O}(N_\ell^{-1})$ is the best possible decay rate for the product $\mu_\ell \zeta_\ell$ that is achievable by conforming first-order finite elements. As a consequence, in order to reach the prescribed tolerance, Algorithm 6 requires a significantly smaller number of DOFs than Algorithm 4.2 in [BPRR19b] ($N_\ell \approx 3 \cdot 10^5$ vs. $N_\ell \approx 7 \cdot 10^6$). We conclude by observing that for both approaches the error estimates and the reference errors decay with the same rate and that, in this example, the error in the goal functional is underestimated by the estimator product.

6.2. Nonlinear goal functional. Let us now demonstrate the performance and effectiveness of Algorithm 6 in the case of nonlinear goal functionals.

6.2.1. *Test problems.* We consider four different setups for model problem (1) by varying the physical domain $D \subset \mathbb{R}^2$ (square, L-shaped, and slit domains), the right-hand side function $\boldsymbol{f}$, and the goal functional $\boldsymbol{g}$. The diffusion coefficient is the same for all four setups and is the one introduced in [EGSZ14, Section 11.1] (and considered in many other works, e.g., [EGSZ15, BS16, EM16, BR18, BPRR19b, BPR21b]). Specifically, for every $x = (x_1, x_2) \in D$, we set $a_0(x) := 1$ and choose the coefficients $a_m(x)$ in (2) to represent planar Fourier modes of increasing total order, i.e.,

$$a_m(x) := Am^{-2} \cos(2\pi\beta_1(m)\, x_1) \cos(2\pi\beta_2(m)\, x_2) \quad \text{for all } m \in \mathbb{N},$$

where $0 < A < 1/\zeta(2)$ (here $\zeta(\cdot)$ denotes the Riemann zeta function), β_1 and β_2 are defined as $\beta_1(m) := m - k(m)(k(m)+1)/2$ and $\beta_2(m) := k(m) - \beta_1(m)$, respectively, with $k(m) := \lfloor -1/2 + \sqrt{1/4 + 2m} \rfloor$ for all $m \in \mathbb{N}$. Assumption (3) is satisfied with $a_0^{\min} = a_0^{\max} = 1$. Since $\tau = A\,\zeta(2)$, assumption (4) is fulfilled for any choice of $0 < A < 1/\zeta(2)$. We set $A := 0.9/\zeta(2) \approx 0.547$, which yields $\tau = 0.9$.

In each setup, the goal functional features a weight function $w \in L^\infty(D)$ that we use to introduce local spatial features in the corresponding QoI. For the sake of reproducibility, we specify the tolerance $\mathsf{tol} > 0$ that we use to stop the algorithm (i.e., we stop the computation when the goal-oriented error estimate $\mu_\ell \sqrt{\mu_\ell^2 + \zeta_\ell^2}$ is less than tol) as well as the (lower) tolerance $\mathsf{tol}_{\mathrm{ref}} > 0$ that is used for computing the reference solution $\boldsymbol{u}_{\mathrm{ref}}$. In all experiments presented below, we use $\theta = 1/2$ in (78). Let us now describe the problem specifications for each setup.

• *Setup 1: expectation of a weighted L^2-norm.* The physical domain is the unit square $D = (0,1)^2$. The right-hand side function is constant: $\boldsymbol{f} \equiv 1$ in D. The goal functional is the expectation of the (squared) weighted L^2-norm:

$$\boldsymbol{g}(\boldsymbol{u}) = \int_\Gamma \int_D w(x)\, \boldsymbol{u}(x, \mathbf{y})^2 \,\mathrm{d}x \,\mathrm{d}\pi(\mathbf{y});$$

cf. [BIP21, Section 3.1]. In this experiment, we choose $w = \chi_S/|S|$, where $\chi_S : D \to \{0,1\}$ is the characteristic function of the square $S = (5/8, 7/8) \times (9/16, 13/16) \subset D$. The initial mesh $\mathcal{T}_0$ is a uniform mesh of 512 right-angled triangles. The tolerances are set to $\mathsf{tol} = 3 \cdot 10^{-7}$ and $\mathsf{tol}_{\mathrm{ref}} = 1 \cdot 10^{-7}$.

• *Setup 2: expectation of a nonlinear convection term.* The physical domain is the L-shaped domain $D = (-1,1)^2 \setminus (-1,0]^2$. The right-hand side function is constant: $\boldsymbol{f} \equiv 1$ in D. The goal functional is the expectation of a nonlinear convection term, i.e.,

$$\boldsymbol{g}(\boldsymbol{u}) = \int_\Gamma \int_D w(x)\, \boldsymbol{u}(x, \mathbf{y}) \left(\frac{\partial \boldsymbol{u}}{\partial x_1}(x, \mathbf{y}) + \frac{\partial \boldsymbol{u}}{\partial x_2}(x, \mathbf{y}) \right) \mathrm{d}x \,\mathrm{d}\pi(\mathbf{y})$$

(see [BIP21, Section 3.2]), where $w = \chi_T/|T|$ and $\chi_T : D \to \{0,1\}$ is the characteristic function of the triangle $T = \mathrm{conv}\{(1,0),(1,1),(0,1)\} \cap D \subset D$. The initial mesh $\mathcal{T}_0$ is a uniform mesh of 384 right-angled triangles. The tolerances are set to $\mathsf{tol} = 5 \cdot 10^{-6}$ and $\mathsf{tol}_{\mathrm{ref}} = 1 \cdot 10^{-6}$.

• *Setup 3: second moment of a linear goal functional.* The physical domain is the unit square domain $D = (0,1)^2$. Inspired by [MS09, Example 7.3], we choose the right-hand side function $\boldsymbol{f}$ such that

$$F(\boldsymbol{v}) = -\int_\Gamma \int_{T_f} \frac{\partial \boldsymbol{v}}{\partial x_1}(x, \mathbf{y}) \,\mathrm{d}x \,\mathrm{d}\pi(\mathbf{y}) \quad \text{for all } \boldsymbol{v} \in \mathbb{V},$$

where $T_f = \operatorname{conv}\{(0,0),(1/2,0),(0,1/2)\} \cap D \subset D$. In the spirit of [TSGU13, Section 3.4(b)], the goal functional is given by the (rescaled) second moment of a linear functional. Specifically, we consider the following goal functional:

$$\boldsymbol{g}(\boldsymbol{u}) = 100 \int_\Gamma \left(\int_D w(x)\, \boldsymbol{u}(x,\mathbf{y})\, \mathrm{d}x \right)^2 \mathrm{d}\pi(\mathbf{y}),$$

where $w = \chi_{T_g}/|T_g|$. Here, $\chi_{T_g} : D \to \{0,1\}$ is the characteristic function of the triangle $T_g = \operatorname{conv}\{(1,1/2),(1,1),(1/2,1)\} \cap D \subset D$. The initial mesh $\mathcal{T}_0$ is a uniform mesh of 512 right-angled triangles, and the tolerances are set to $\mathsf{tol} = 6 \cdot 10^{-7}$ and $\mathsf{tol}_{\mathrm{ref}} = 2 \cdot 10^{-7}$.

• *Setup 4: variance of a linear goal functional.* Let $D_\delta = (-1,1)^2 \setminus \overline{T}_\delta$, where $T_\delta = \operatorname{conv}\{(0,0),(-1,\delta),(-1,-\delta)\}$. In this test case, we aim at performing computations on the (physical) slit domain $(-1,1)^2 \setminus ([-1,0] \times \{0\})$. The slit domain is not Lipschitz, however, it is well known that an elliptic problem on this domain can be seen as the limit of the problems posed on the Lipschitz domain D_δ as $\delta \to 0$. Therefore, we set $D = D_\delta$ with $\delta = 0.005$. The right-hand side function is constant: $\boldsymbol{f} \equiv 1$ in D. The goal functional is given by the (rescaled) variance of a linear functional. Specifically, we consider the following goal functional:

$$\boldsymbol{g}(\boldsymbol{u}) = 100 \operatorname{Var}_{\mathbf{y}} \left[\int_D w(x)\, \boldsymbol{u}(x,\mathbf{y})\, \mathrm{d}x \right], \tag{83}$$

where the weight function $w \in L^\infty(D)$ is a mollifier centered at $x_0 = (2/5, -1/2)$ with radius $r = 3/20$ (we refer to [BPRR19b, equation (58)] for the specific expression). Thus, the integral over D in (83) approximates the function value $\boldsymbol{u}(x_0,\mathbf{y})$ for each $\mathbf{y} \in \Gamma$. The initial mesh $\mathcal{T}_0$ is a uniform mesh of 512 right-angled triangles, and the tolerances are set to $\mathsf{tol} = 4 \cdot 10^{-5}$ and $\mathsf{tol}_{\mathrm{ref}} = 1 \cdot 10^{-5}$.

We note that the four nonlinear goal functionals considered in this section satisfy inequality (71) with $C_{\mathrm{goal}} > 0$ depending only on $\|w\|_{L^\infty(D)}$ and the Poincaré constant of the physical domain D.

6.2.2. *Results.* In Figure 3, for all setups, we show the adaptively refined mesh associated with the zero index at an intermediate step of Algorithm 6. We observe that, in all cases, the meshes capture the spatial features of the primal and dual solutions; these features are induced by the geometry of the physical domain as well as by the local features of the chosen right-hand side function $\boldsymbol{f}$ and goal functional $\boldsymbol{g}$. The intensity of local mesh refinement reflects the strength of the singularity; e.g., in the plot for Setup 2 (top-right), the local mesh refinement at the reentrant corner of the L-shaped domain is stronger than the one due to the local support of the weight function w.

In Figure 4, for all setups, we plot the error estimates $\mu_\ell \sqrt{\mu_\ell^2 + \zeta_\ell^2}$ (in red) and the reference errors $|\boldsymbol{g}(\boldsymbol{u}_{\mathrm{ref}}) - \boldsymbol{g}(\boldsymbol{u}_\ell)|$ (in blue) against the number of DOFs at each iteration of the goal-oriented adaptive algorithm. We observe that, for all setups, the goal-oriented adaptive algorithm drives the error estimate to zero, thus confirming the result of Theorem 26. Furthermore, we see that in each setup, the error estimate provides an upper bound for the reference error, and both quantities converge to zero with the same rate. Finally, in the same way as observed in the experiment of section 6.1 for Algorithm 6 with a linear goal functional, all plots in Figure 4 show that the decay of both the error estimates and the reference errors with respect to the number of DOFs is of order N_ℓ^{-1},

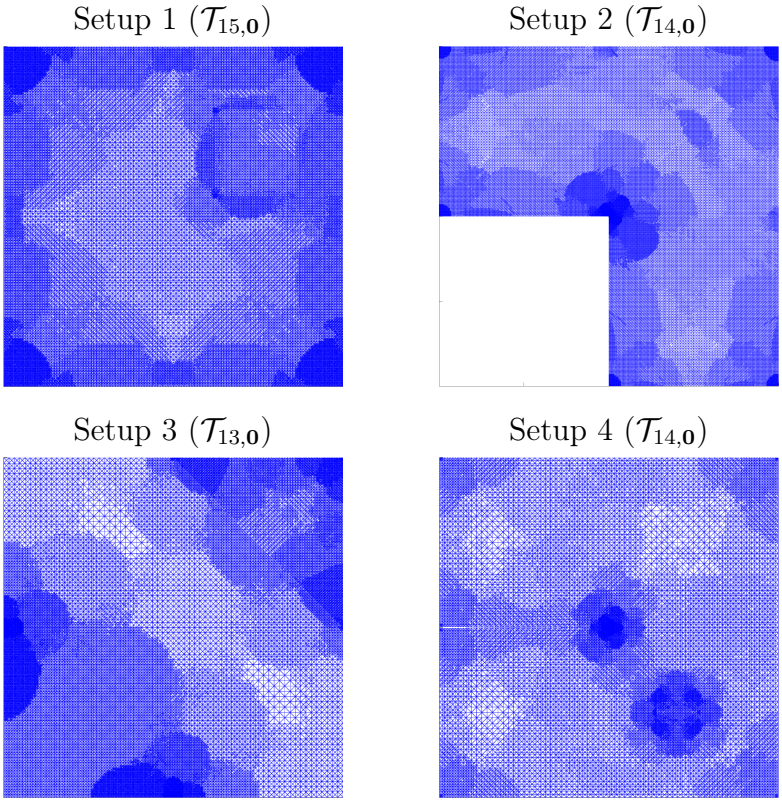

FIGURE 3. Experiment in section 6.2: adaptively refined meshes associated with the zero index at an intermediate step of Algorithm 6 for all four setups.

i.e., the best possible decay rate achievable by conforming first-order finite elements. Although the rate optimality property of Algorithm 6 for nonlinear goal functionals is not currently covered by our theoretical analysis, the results presented in Figure 4 seem to suggest that this property does hold at least for certain types of nonlinear functionals; see [BIP21] for first results in the parameter-free setting for the case of a quadratic goal functional.

7. Concluding remarks

The design of provably efficient solution strategies for high-dimensional parametric PDEs is important for reliable uncertainty quantification. Adaptive algorithms are indispensable in this context, as they provide computationally cost-effective mechanisms for generating accurate approximations and accelerating convergence. In this paper, we have designed a goal-oriented SGFEM-based adaptive algorithm for accurate approximation of quantities of interest—linear or nonlinear functionals of solutions to elliptic PDEs with inputs depending on infinitely many parameters. We have also analyzed the convergence and rate optimality of the approximations generated by the proposed algorithm.

The adaptive algorithm and theoretical results presented in this paper extend the existing body of works on adaptive SGFEM algorithms in two directions. Firstly, for *linear* goal functionals, we have combined the algorithmic developments in [EGSZ14, BPR21b] and [BPRR19b] to design a goal-oriented adaptive algorithm that generates *multilevel*

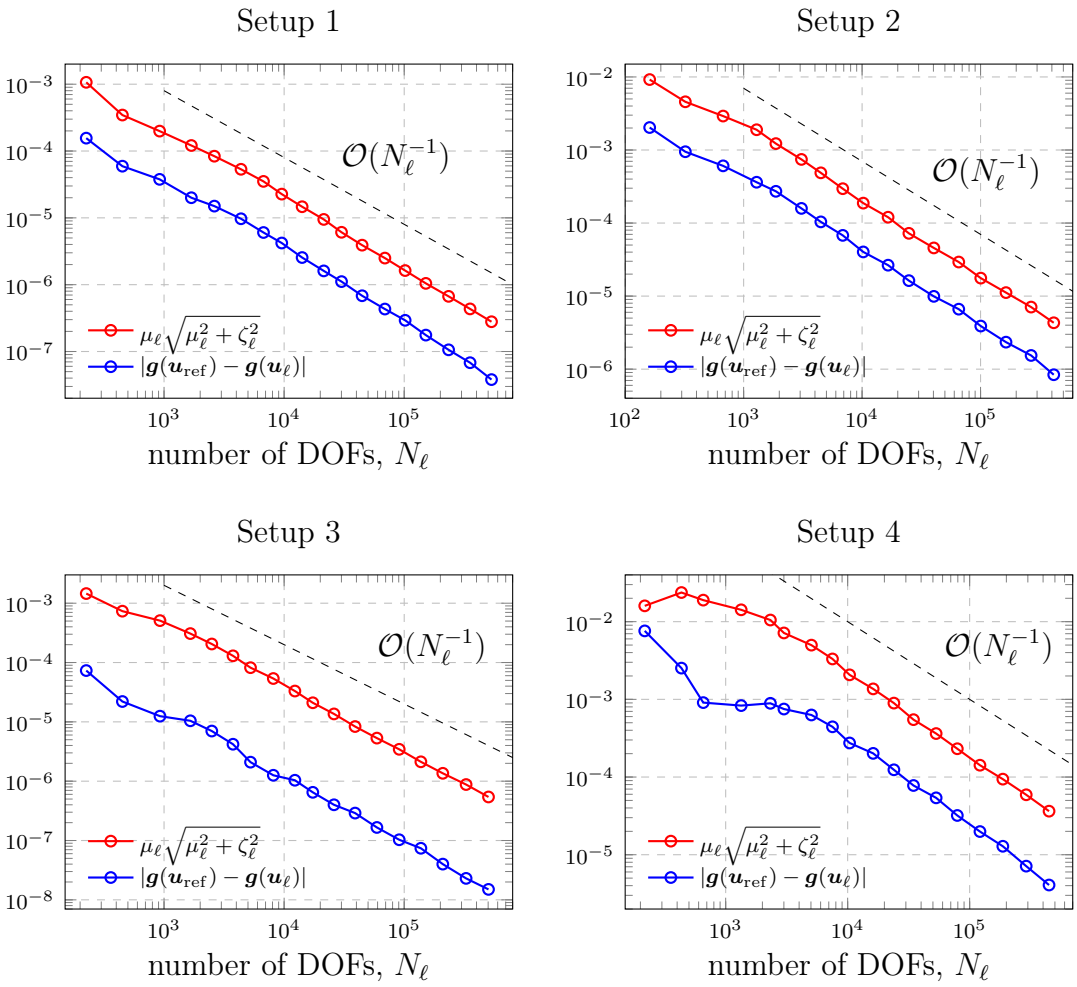

FIGURE 4. Experiments in section 6.2: decay of the error estimates $\mu_\ell\sqrt{\mu_\ell^2+\zeta_\ell^2}$ and the reference errors $|g(u_{\mathrm{ref}})-g(u_\ell)|$ at each iteration of the goal-oriented multilevel adaptive algorithms for all four setups.

SGFEM approximations by independently refining the finite element spaces associated with different gPC-coefficients. Furthermore, we have extended the underlying goal-oriented error estimation strategy to the case of *nonlinear* goal functionals and modified the adaptive algorithm accordingly. Secondly, we have extended the convergence analysis in [BPRR19a] and, for linear goal functionals, the rate optimality analysis in [BPR21a] to the proposed goal-oriented adaptive algorithm. We note that our error estimation strategy (cf. Propositions 5 and 25), algorithmic developments, and convergence results (cf. Theorems 8 and 26) hold for linear and nonlinear goal functionals as well as for spatial domains in $\mathbb{R}^2$ and $\mathbb{R}^3$. The rate optimality analysis, however, is restricted to linear goal functionals and to two-dimensional spatial domains (cf. Theorem 19). The extension of this analysis to nonlinear goal functionals and three-dimensional domains is non-trivial and will be the subject of future research.

References

[AO10] R. C. Almeida and J. T. Oden. Solution verification, goal-oriented adaptive methods for stochastic advection–diffusion problems. *Comput. Methods Appl. Mech. and Engrg.*, 199(37-40):2472–2486, 2010.

[BDW11] T. Butler, C. Dawson, and T. Wildey. A posteriori error analysis of stochastic differential equations using polynomial chaos expansions. *SIAM J. Sci. Comput.*, 33(3):1267–1291, 2011.

[BEK96] F. A. Bornemann, B. Erdmann, and R. Kornhuber. A posteriori error estimates for elliptic problems in two and three space dimensions. *SIAM J. Numer. Anal.*, 33(3):1188–1204, 1996.

[BET11] R. Becker, E. Estecahandy, and D. Trujillo. Weighted marking for goal-oriented adaptive finite element methods. *SIAM J. Numer. Anal.*, 49(6):2451–2469, 2011.

[BIP21] R. Becker, M. Innerberger, and D. Praetorius. Optimal convergence rates for goal-oriented FEM with quadratic goal functional. *Comp. Meth. Appl. Math.*, 21:267–288, 2021.

[BPR21a] A. Bespalov, D. Praetorius, and M. Ruggeri. Convergence and rate optimality of adaptive multilevel stochastic Galerkin FEM. *IMA J. Numer. Anal.*, 2021. (appeared online; https://doi.org/10.1093/imanum/drab036).

[BPR21b] A. Bespalov, D. Praetorius, and M. Ruggeri. Two-level a posteriori error estimation for adaptive multilevel stochastic Galerkin FEM. *SIAM/ASA J. Uncertain. Quantif.*, 9(3):1184–1216, 2021.

[BPRR19a] A. Bespalov, D. Praetorius, L. Rocchi, and M. Ruggeri. Convergence of adaptive stochastic Galerkin FEM. *SIAM J. Numer. Anal.*, 57(5):2359–2382, 2019.

[BPRR19b] A. Bespalov, D. Praetorius, L. Rocchi, and M. Ruggeri. Goal-oriented error estimation and adaptivity for elliptic PDEs with parametric or uncertain inputs. *Comput. Methods Appl. Mech. Engrg.*, 345:951–982, 2019.

[BPW15] C. Bryant, S. Prudhomme, and T. Wildey. Error decomposition and adaptivity for response surface approximations from PDEs with parametric uncertainty. *SIAM/ASA J. Uncertain. Quantif.*, 3(1):1020–1045, 2015.

[BR18] A. Bespalov and L. Rocchi. Efficient adaptive algorithms for elliptic PDEs with random data. *SIAM/ASA J. Uncertain. Quantif.*, 6(1):243–272, 2018.

[BR22] A. Bespalov and L. Rocchi. Stochastic T-IFISS, January 2022. Available online at `https://web.mat.bham.ac.uk/A.Bespalov/software/index.html#stoch_tifiss`.

[BRS20] A. Bespalov, L. Rocchi, and D. Silvester. T-IFISS: a toolbox for adaptive FEM computation. *Comput. Math. Appl.*, 2020. In press.

[BS16] A. Bespalov and D. Silvester. Efficient adaptive stochastic Galerkin methods for parametric operator equations. *SIAM J. Sci. Comput.*, 38(4):A2118–A2140, 2016.

[BV84] I. Babuška and M. Vogelius. Feedback and adaptive finite element solution of one-dimensional boundary value problems. *Numer. Math.*, 44:75–102, 1984.

[CD15] A. Cohen and R. DeVore. Approximation of high-dimensional parametric PDEs. *Acta Numer.*, 24:1–159, 2015.

[CFPP14] C. Carstensen, M. Feischl, M. Page, and D. Praetorius. Axioms of adaptivity. *Comput. Math. Appl.*, 67(6):1195–1253, 2014.

[CPB19] A. J. Crowder, C. E. Powell, and A. Bespalov. Efficient adaptive multilevel stochastic Galerkin approximation using implicit a posteriori error estimation. *SIAM J. Sci. Comput.*, 41(3):A1681–A1705, 2019.

[CST13] J. Charrier, R. Scheichl, and A. L. Teckentrup. Finite element error analysis of elliptic PDEs with random coefficients and its application to multilevel Monte Carlo methods. *SIAM J. Numer. Anal.*, 51(1):322–352, 2013.

[Dör96] W. Dörfler. A convergent adaptive algorithm for Poisson's equation. *SIAM J. Numer. Anal.*, 33(3):1106–1124, 1996.

[EGP20] C. Erath, G. Gantner, and D. Praetorius. Optimal convergence behavior of adaptive FEM driven by simple $(h-h/2)$-type error estimators. *Comput. Math. Appl.*, 79(3):623–642, 2020.

[EGSZ14] M. Eigel, C. J. Gittelson, C. Schwab, and E. Zander. Adaptive stochastic Galerkin FEM. *Comput. Methods Appl. Mech. Engrg.*, 270:247–269, 2014.

[EGSZ15] M. Eigel, C. J. Gittelson, C. Schwab, and E. Zander. A convergent adaptive stochastic Galerkin finite element method with quasi-optimal spatial meshes. *ESAIM Math. Model. Numer. Anal.*, 49(5):1367–1398, 2015.

[EM16] M. Eigel and C. Merdon. Local equilibration error estimators for guaranteed error control in adaptive stochastic higher-order Galerkin finite element methods. *SIAM/ASA J. Uncertain. Quantif.*, 4(1):1372–1397, 2016.

[EMN16] M. Eigel, C. Merdon, and J. Neumann. An adaptive multilevel Monte Carlo method with stochastic bounds for quantities of interest with uncertain data. *SIAM/ASA J. Uncertain. Quantif.*, 4(1):1219–1245, 2016.

[FPv16] M. Feischl, D. Praetorius, and K. van der Zee. An abstract analysis of optimal goal-oriented adaptivity. *SIAM J. Numer. Anal.*, 54:1423–1448, 2016.

[GS02] M. B. Giles and E. Süli. Adjoint methods for PDEs: a posteriori error analysis and postprocessing by duality. *Acta Numer.*, 11:145–236, 2002.

[GWZ14] M. D. Gunzburger, C. G. Webster, and G. Zhang. Stochastic finite element methods for partial differential equations with random input data. *Acta Numer.*, 23:521–650, 5 2014.

[MLM07] L. Mathelin and O. Le Maître. Dual-based a posteriori error estimate for stochastic finite element methods. *Comm. App. Math. Com. Sc.*, 2(1):83–115, 2007.

[MS09] M. S. Mommer and R. Stevenson. A goal-oriented adaptive finite element method with convergence rates. *SIAM J. Numer. Anal.*, 47:861–886, 2009.

[MSV08] P. Morin, K. G. Siebert, and A. Veeser. A basic convergence result for conforming adaptive finite elements. *Math. Models Methods Appl. Sci.*, 18(5):707–737, 2008.

[PP20] C.-M. Pfeiler and D. Praetorius. Dörfler marking with minimal cardinality is a linear complexity problem. *Math. Comp.*, 89:2735–2752, 2020.

[PRS20] D. Praetorius, M. Ruggeri, and E. P. Stephan. The saturation assumption yields optimal convergence of two-level adaptive BEM. *Appl. Numer. Math.*, 152:105–124, 2020.

[SG11] C. Schwab and C. J. Gittelson. Sparse tensor discretizations of high-dimensional parametric and stochastic PDEs. *Acta Numer.*, 20:291–467, 2011.

[Ste08] R. Stevenson. The completion of locally refined simplicial partitions created by bisection. *Math. Comp.*, 77(261):227–241, 2008.

[TSGU13] A. L. Teckentrup, R. Scheichl, M. B. Giles, and E. Ullmann. Further analysis of multilevel Monte Carlo methods for elliptic PDEs with random coefficients. *Numer. Math.*, 125(3):569–600, 2013.

School of Mathematics, University of Birmingham, Edgbaston, Birmingham B15 2TT, United Kingdom

Email address: a.bespalov@bham.ac.uk

Institute of Analysis and Scientific Computing, TU Wien, Wiedner Hauptstrasse 8–10, 1040 Vienna, Austria

Email address: dirk.praetorius@asc.tuwien.ac.at

Department of Mathematics and Statistics, University of Strathclyde, 26 Richmond Street, Glasgow G1 1XH, United Kingdom

Email address: michele.ruggeri@strath.ac.uk